INVESTIGATION OF ENRICHMENT OF RARE EARTH ORE IN ESKIŞEHIR-BEYLIKOVA REGION BY FLOTATION

ESKİŞEHİR-BEYLİKOVA BÖLGESİNDEKİ NADİR TOPRAK CEVHERİNİN FLOTASYON İLE ZENGİNLEŞTİRİLMESİNİN ARAŞTIRILMASI

KARINA PATRICIA MOYA LASCANO

ASST.PROF.DR. Ergin GÜLCAN

Supervisor

Submitted to
Graduate School of Science and Engineering of Hacettepe University
as a Partial Fulfillment to the Requirements
for the Award of the Degree of Master of Science in
Mining Engineering.

2023

ABSTRACT

INVESTIGATION OF THE ENRICHMENT OF RARE EARTH ORE IN ESKIŞEHIR-BEYLIKOVA REGION BY FLOTATION

Karina Patricia MOYA LASCANO

Master of Mining, Department of MINING ENGINEERING

Supervisor: Asst.Prof.Dr. Ergin Gülcan

June 2023, 88 pages

Rare earth minerals have great importance in advanced technology products and defense industry. Rare earth mineral deposits in the Eskişehir - Beylikova region, which is one of the most important deposits in Turkey, is known as a "Complex Ore" since it consists of a wide variety of minerals. Bastnaesite, fluorite, barite, and calcite minerals are reported to be found in the ore within a complex mineralization. Lanthanum (La), cerium (Ce) and neodymium (Nd) are primary rare earth elements found in the deposit. Many technological studies have been carried out in previous years for the separation and enrichment of both thorium and rare earth oxides from Beylikova complex REE ore. However, R&D studies up to now could not be able to present convincing data for a comprehensive process for economically enriching the ore components such as bastnaesite, fluorite and barite all along.

The aim of the thesis is to investigate flotation behavior of the Eskişehir- Beylikova ore primarily focusing on the valuable gangue minerals of fluorite and barite, along with the rare earth oxides. Removing and separating fluorite and barite from this ore as separate sellable products are key to operate the field economically. Within this aim, zeta potential measurements of fluorite and barite within ore were conducted as a function of pH, under

different collectors and under different depressants. Following, flotation behavior of related contents was investigated under varying collector dosages and different pH values.

For this purpose, experimental studies were started with the characterization of the minerals to determine the mineralogy of the Beylikova deposit. Following, pure barite, and fluorite minerals were obtained. All the mineral samples were subjected to the measurement of the zeta potential by means of the electrophoresis technique under all the quoted variants. Within these measurements, the effects of the solution on the mineral surface of interest being evaluated under different conditions. In addition, IEP values are presented which could be useful as a database for future research. Following, a series of flotation tests under different conditions were performed for validation. During flotation tests, different collector types, depressants, collector mixtures and activators were used, and results were evaluated.

The zeta potential results for pure barite with the instrumentation used (optical and laser) showed results so close that the IEP variation is ZN=5.25 and ZS=5.27. The addition of collecting agents had an effect on the zeta potential, especially in the case of positive electrical charges and the implementation of an upright absorption. In contrast, the zeta potential of fluorite with ZN and ZS showed a similar trend and the IEP variation was ZN=8.8 and ZS=8.1. The zeta potential was also significantly reduced by the addition of a collector. For the flotation process that was carried out sequentially, starting with the barite rougher and counting with the fluorite rougher. In the flotation of barite, the best results are shown with the mixture of A825 (300 g/t) and A845 (100 g/t) with 77.51% $BaSO_4$ grade and 95.93% recovery. The rougher tail of the barite flotation was transferred to the fluorite rougher flotation. Where the recovery and grade were 35.68% and 79.80% respectively with A726, being the higher results obtained under the two different collectors used (A704 and A726).

Keywords: Rare Earth Elements, Bastnaesite, Zeta Potential, Flotation, Barite, Fluorite

ÖZET

ESKIŞEHIR-BEYLIKOVA BÖLGESINDEKI NADIR TOPRAK CEVHERININ FLOTASYON ILE ZENGINLEŞTIRILMESININ ARAŞTIRILMASI

Karina Patricia MOYA LASCANO

Yüksek Lisans, Maden Bölümü

Tez Danışmanı: Dr.Öğr.Üyesi Ergin Gülcan

Haziran 2023, 88 sayfa

Nadir toprak mineralleri ileri teknoloji ürünlerinde ve savunma sanayinde büyük öneme sahiptir. Türkiye'nin en önemli yataklarından biri olan Eskişehir - Beylikova bölgesindeki nadir toprak minerali yatakları, çok çeşitli minerallerden oluştuğu için "Kompleks Cevher" olarak bilinmektedir. Cevherde kompleks bir cevherleşme içerisinde bastnaesit, florit, barit ve kalsit minerallerinin bulunduğu bildirilmektedir. Lantan (La), seryum (Ce) ve neodim (Nd) yatakta bulunan başlıca nadir toprak elementleridir. Beylikova kompleks NTE cevherinden hem toryum hem de nadir toprak oksitlerin ayrıştırılması ve zenginleştirilmesi için önceki yıllarda birçok teknolojik çalışma yapılmıştır. Ancak bugüne kadar yapılan Ar-Ge çalışmaları, bastnaesit, florit ve barit gibi cevher bileşenlerinin ekonomik olarak zenginleştirilmesine yönelik kapsamlı bir süreç için ikna edici veriler sunamamıştır.

Bu tezin amacı, Eskişehir-Beylikova cevherinin flotasyon davranışını, öncelikle değerli gang mineralleri olan florit ve barit ile nadir toprak oksitlerine odaklanarak incelemektir. Florit ve baritin bu cevherden ayrı satılabilir ürünler olarak çıkarılması ve ayrılması,

sahanın ekonomik olarak işletilmesi için kilit öneme sahiptir. Bu amaçla, cevher içindeki florit ve baritin zeta potansiyel ölçümleri pH'ın bir fonksiyonu olarak, yağ asitleri ve hidroksamat gibi farklı toplayıcı konsantrasyonları altında ve farklı bastırıcılar altında gerçekleştirilmiştir. Ardından, ilgili içeriklerin flotasyon davranışları farklı toplayıcı dozajları ve farklı pH değerleri altında incelenmiştir.

Bu amaçla, deneysel çalışmalara Beylikova yatağının mineralojisini belirlemek için minerallerin karakterizasyonu ile başlanmıştır. Ardından, saf barit ve florit mineralleri elde edilmiştir. Tüm mineral numuneleri, elektroforez tekniği ile tüm alıntılanan varyantlar altında potansiyel zeta ölçümüne tabi tutulmuştur. Bu ölçümlerde, çözeltinin ilgili mineral yüzeyi üzerindeki etkileri farklı koşullar altında değerlendirilmiştir. Ayrıca, gelecekteki araştırmalar için bir veri tabanı olarak faydalı olabilecek IEP değerleri de sunulmuştur. Ardından, zeta potansiyel ölçüm testleri temelinde elde edilen bilgilerle, doğrulama için farklı koşullar altında bir dizi flotasyon testi gerçekleştirilmiştir. Flotasyon testleri sırasında farklı toplayıcı tipleri, bastiricilar, toplayıcı karışımları ve canlandırıcı kullanılmış ve sonuçlar değerlendirilmiştir.

Kullanılan cihazlarla (optik ve lazer) saf barit için elde edilen zeta potansiyeli sonuçları, IEP varyasyonu ZN=5.25 ve ZS=5.27 olacak kadar yakın sonuçlar göstermiştir. Toplayıcı eklenmesi, özellikle pozitif elektrik yükleri ve dolayısıyla zeta potansiyeli üzerinde etkili olmuştur. Buna karşılık, floritin ZN ve ZS ile zeta potansiyeli benzer bir eğilim göstermiş ve IEP değişimi sırasıyla ZN=8.8 ve ZS=8.1 olmuştur. Zeta potansiyelinin bir toplayıcının eklenmesiyle önemli ölçüde azaldığı görülmektedir. Sırayla gerçekleştirilen flotasyon işlemi barit kava flotasyonu ile başlanmış ve fluorit kava flotasyonu ile devam edilmiştir. Barit flotasyonunda en iyi sonuçlara %77.51 $BaSO_4$ tenörü ve %95.93 verimi ile A825 (300 g/t) ve A845 (100 g/t) toplayıcılarının karışımı ile ulaşılmıştır. Barit kaba flotasyonunun atığı florit kaba flotasyonuna aktarılmıştır. Burada, kullanılan iki farklı toplayıcı (A704 ve A726) altında elde edilen en iyi sonuçlar A726 ile %35.68 verim ve %79.80 tenör şeklinde elde edilmiştir.

Anahtar Kelimeler: Nadir Toprak Elementleri, Bastnasit, Zeta Potansiyeli, Flotasyon, Barit, Florit

ACKNOWLEDGEMENTS

I would like to express my deepest gratitude to my thesis advisor, Assist. Prof. Dr. Ergin GÜLCAN, for his guidance, support, and encouragement throughout my research. His insights and feedback were invaluable in shaping and improving the quality of this thesis.

I would also like to thank YTB-Turkiye Scholarships for believing in my potential and giving me the opportunity to continue my education and pursue one of my professional goals.

I am grateful to Rare Earth Elements Research Institute (NATEN) of Turkey for providing the necessary material for my research. This support allowed me to carry out the experiments and collect the data necessary for this study.

Finally, I want to express my heartfelt thanks to my family for their unwavering support and inspiration. Their love and understanding helped me persevere during the drawn-out and occasionally challenging process of completing this thesis.

CONTENTS

LIST OF FIGURES

LIST OF TABLES

SYMBOLS AND ABBREVIATIONS

SYMBOLS

E_s	Streaming Potential (volt)
D	Dielectric Constant
E	Potential Gradient (volt /cm)
M	Metal
pH	Potential of Hydrogen
V	Particle Velocity (cm / sec)
Δp	Pressure Drop (cmHg)
ζ	Zeta Potential (volts)
μ	Solution Viscosity (poise)
σ	Conductivity (mho /cm)

ABREVIATIONS

d	Depressant Agent
DLS	Dynamic Light Scattering
HREE	Heavies Rare Earth Elements
IEP	Isoelectric point
LREE	Lights Rare Earth Elements
MLA	Mineralogical Liberation Analysis
RE	Rare Elements
REE	Rare Earth Elements
REM	Rare Earth Minerals
REO	Rare Earth Oxides
SOP	Standard Operating Procedure
UV	Ultraviolet
Mt	million metric ton

1. INTRODUCTION

Rare earth elements (REE) are used to name a group of fifteen lanthanide metallic elements. Later, scandium and yttrium were added to this group which have almost identical physical and chemical properties. These elements are not found in pure metal form and are considered lithophilic having affinity to the association or reaction with silicates. Due to these reasons, they are mostly found in a variety of compounds such as carbonates, oxides, silicates, and phosphates [1].

Moreover, REEs are not in a predictable dispersion in an ore. Since different rare elements and different abundances can be observed in a deposit in very low concentrations, their processing presents economical and technical challenges. Despite these challenges, their increasing demand in recent years due to the use of these specific rare earth elements in a wide variety of advanced technological applications still encourages industry endure these challenges [2]. Within this group of rare earths (RE's): monazite ((RE, Th) (PO_4) and bastnaesite (RE (CO_3) F) are the main minerals with economic-commercial interest which also represent the main resource of REE in nature [3][4].

The flotation behavior of fluorite and barite in relation with RE minerals in Beylikova ore are the minerals of focus for this thesis study. Due to previous reports, the deposit of rare earth elements of Beylikova located in Eskişehir - Turkey presents a content of fluorite, barite and bastnaesite as main minerals of interest. Later, minerals such as monazite and parisite were also reported [5][6]. On the other hand, the noteworthy amounts of the barite and fluorite that are present in the ore also commonly cause problems in the ore in terms of obtaining economically processible RE minerals within the ore.

Flotation process is expected to play the most crucial role in enriching Rare Earth Minerals (REMs) (bastnaesite, monazite, etc.), fluorite, and barite in Beylikova REE ore. Unfortunately, studies up to now could not presented convincing results in obtaining sellable fluorite and barite products from the ore along with the targeted REE minerals [7][8][9]. Additionally, bastnaesite type ores containing REE can show great differences in ore mineralogy which can even fluctuate through veins in an ore body. There are examples where the REE mineral beneficiation process flowsheets are changed

periodically in some very large-scale REE operations as Baiyun-Obo Mine – Mongolia [10].

Experimental studies of the thesis focused on the rare earth deposit of Beylikova region of Turkey. As mentioned earlier, Beylikova deposit is known to be composed of three major contents, namely fluorite, barite, and REMs. When these major species are considered as predominant individual ionic species (such as cerium (Ce^{+3}), fluorite (F^{-}) and carbon (CO_3^{-2}) (as carbonate), etc., they effect the resulting generated electrochemical characteristic behavior of the bulk solution. They become crucial in terms of developing an effective and applicable enrichment strategy. Therefore, understanding how these individual ionic species react in solution is a basic and important parameter for promoting a solution for analysis and the investigation of the process options [11]. Experimental studies were started with detailed mineralogical analyses. With the Beylikova deposit, it is evident that the only way to produce a further processable and high-grade REO concentrate was by efficiently eliminating the fluorite and barite components (of which the overall percentage in the ore is around 75%). Additionally, in order to implement an economically feasible processing plant, fluorite and barite must be obtained as separate and sellable products. Hence, within this thesis, effects of different methodologies and sample preparation methods based on the measurements of the zeta potential of fluorite and barite to improve the enrichment of the fluorite and barite along with REMs were studied. For this purpose, zeta potential measurement studies for fluorite and barite were performed with different collector and depressant regimes. Through the following second stage, the previous findings were tested via extensive flotation experiments and results were evaluated.

1.1. Rare Earth Minerals

The rare earth elements are typically found in deposits of hard rocks or minerals including carbonates, oxides, phosphates, and silicates. In addition, the occurrence of these elements is rare as the name indicates, and they are not found in nature individually. They have the most typical occurrence as oxides of rare elements (REO), which reach 60% of all REMs. A list of common REMs and their contents are summarized in Table 1.1. However, it can be considered that 95% of rare earth resources occur in only three main minerals which are bastnaesite, monazite and xenotime [12].

Table 1.1: The common REMs [10].

Mineral	Formula	Rare earth content, %
Aeschynite	$(Ce,Ca,Th)(Ti,Nb)_2O_6$	Ce_2O_3 = 15.5–19.5 $(Y,Er)_2O_3$ = 0.9–4.5
Bastnaesite	$(Ce,La,Pr)(CO_3)F$	Ce_2O_3=36.9–40.5 $(La,Pr,\ldots)_2O_3$ = 36.3–36.6
Euxenite	$(Y,Ce,Ca,U,Th)(Ti, Nb,Ta)_2O_6$	$(Y,Er)_2O_3$=18.2–27.7 $(Ce,La,\ldots)_2O_3$ =16–30
Fergusonite	$(Y,Sr,Ce,U)(Nb,Ta, Ti)O_4$	Y_2O_3=31–42 $(Ce,La,\ldots)_2O_3$=0.9–6 Er_2O_3 = 0–14
Gadolinite	$(Y,Ce)_2FeBe_2Si_2O_{10}$	Y_2O_3=30.7–46.5 $(Ce,La,\ldots)_2O_3$=5.23
Loparite	$(Na,Ca,Ce,Sr)_2(Ti,Ta, Nb)_2O_6$	$(Ce,La,\ldots)_2O_3$=32–34
Monazite	$(Ce,La\ldots)PO_4$	$(Ce,La,\ldots)_2O_3$= 50–68
Orthite	$(Ca,Ce)2(Al,Fe)_3Si_3O_{12}$ [O,OH]	Ce_2O_3= 0–6 La_2O_3= 0–7 Y_2O_3= 0–8
Parisite	$Ca\ (Ce,La\ldots)_2(CO_3)F_2$	Ce_2O_3=26–31 $(La,Nd,\ldots)_2O_3$=27.3–30.4 Y=8
Priorite	$(Y,Er,Ca,Th)(Ti,Nb)_2O_6$	$(Y,Er)_2O_3$=21. 1–28.7 Ce_2O_3= 3.7–4.3
Samarskite	$(Y,Er,U,Ce,Th)_4\ (Nb, Ta)_6O_2$	Y_2O_3=6.4- 14.5 Er_2O_3=2.7–13.4 Ce_2O_3=0.25–3.2 La_2O_3=0.37–1 $(Pr,Nd)_2O_3$ = 0.74 – 4.2
Xenotime	YPO_4	Y_2O_3=52–62
Yttrocerite	$(Ca,Y,Ce,Er)F_{2\text{-}3}H_2O$	Ce = 8.5–11.5 Y=14.3–37.7

1.1.1. Bastnaesite

The bastnaesite is a fluorocarbonate mineral typically in complex form of carbonate-silicate rocks and found within alkaline intrusive, which consists of rare earth elements (RE), fluoride (F^-) and carbonate (CO_3^{-2}) ions, mostly denoted as RE (CO^3) F. Bastnaesite is considered as the first light RE resource with a presence of approx. 70% of rare earth oxide (REO) [36]. This mineral can be subclassified based on the content of rare elements (RE) such as bastnaesite–(Ce), bastnaesite–(La), bastnaesite–(Nd), bastnaesite-(Y), hydroxyl-bastnaesite-(Nd), hydroxy bastnaesite-(Ce) and thorium-bastnaesite. Bastnaesite–Ce (Figure 1.1) is one of the most commonly found REM in Earth's crust. Characteristic properties of bastnasite are given in the Table 1.2 [13].

Figure 1.1: Ce Bastnaesite – REM.

Table 1.2: Bastnaesite properties [13].

Properties	
Color	pale white, tan, gray, brown, yellow and pink
Luster	pearly, vitreous, greasy to dull
Transparency	translucent to opaque
Crystal system	Hexagonal
Hardness	4 to 4.5
Specific gravity	4.7 to 5.0
Streak	White

The Bastnaesite is also considered as a complex ore due to chemical susceptibility. High presence of rare earth oxides (REO) within bastnasite tend to dissolve and/or easily combine with mineral gangue, especially with phosphates [14]. The bastnaesite is characterized by the content of light element lanthanides, especially lanthanum, cerium, and neodymium [10] [6]. The deposit of rare earth elements of Beylikova located in Eskişehir – Turkey region presents a content of fluorite, barite and bastnaesite (Ce, La, Nd) as main minerals of interest. The reserve is anticipated to be large enough to produce 12,000 tons of REO annually.

1.1.2. Monazite

Monazite is a complex phosphate mineral, commonly designated as light rare earth (LREE)PO_4. It is considered to contain approx. 55-60% REO (Figure 1.2). Monazite is generally found with heavy minerals or with other contents of ore bodies, thus, it is considered a by-product. This occurrence tendency is a result of its own characteristics such as resistance to chemical attack and its high specific gravity. It has a natural

characteristic of associating with magnetite (Fe_3O_4), ilmenite (Fe_2TiO_3) and zircon ($ZrSiO_4$) [1] [15].

Figure 1.2: Monazite – REM [16].

The start of the exploitation of this mineral was given by its being the main LREE source, especially in the recovery of cerium, lanthanum, and molybdenum. Its production decreased with the start of the exploitation of the bastnasite which replaced it as the main source of REE, thus decreasing to 5% in the year 2022. Currently, deposits containing monazite are found mainly in Australia, Brazil, China, India, Malaysia, South Africa, and the United States [17].

Table 1.3: Monazite properties [16].

Properties	
Color	Brown, reddish brown, yellowish brown, yellow, orange, pink
Luster	Resinous, waxy, vitreous
Transparency	Transparent to translucent
Crystal system	Monoclinic
Hardness	5 – 5.5
Specific gravity	4.6 to 5.4 (varies greatly depending on the type and concentration of rare earths)
Special Characteristic	Radioactivity, heavy weight and mode of occurrence.

1.1.3. Cerianite

Cerium oxide (CeO_2) form of cerianite mineral is known to be the simplest mineral containing cerium. It has a high presence probability with thorium and uranium. This condition attributes similar characteristics to cerianite minerals just as monazite. Cerianite also has high LREE content in various combinations [18]. Figure 1.3 shows the compositional variations of cerianite. Its concentration is considered mainly related to a secondary phase. Its formation occurs at relatively low temperatures and pH values. Its

occurrence is found in rock encrustations along with a large amount of carbon and silicates. It is also common to find it as an oxidation product, especially under hydrothermal oxidative conditions [19]. This mineral has characteristics such as a high oxygen storage capacity, noble metal dispersion capacity and thermal stabilization that makes it highly attractive at industry level applications, as shown Table 1.4 [16].

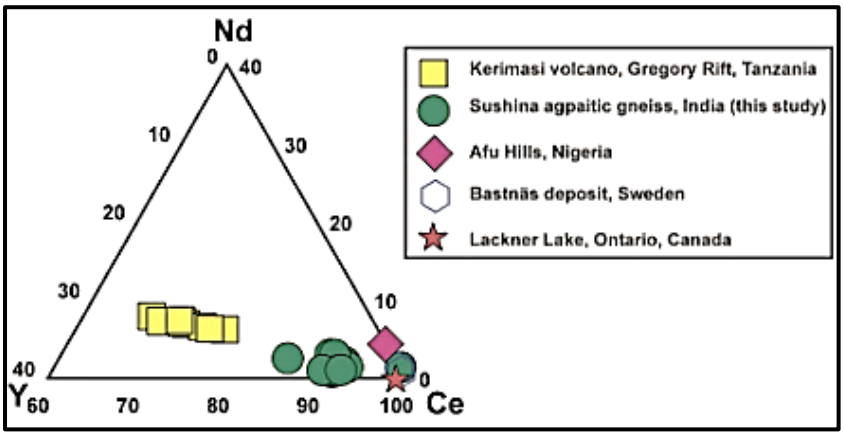

Figure 1.3: Cerianite compositional variation in terms of LREE [20]

Table 1.4: The cerianite properties [16]

Properties	
Color	Greenish yellow, Resin brown, Dark greenish brown
Transparency	Translucent
Density	7.216

1.1.4. Lateritic Rare Earth Minerals

The main source of heavy rare earth elements are laterite deposits, which are formed by ion absorption. These deposits are linked with a wide range of lithologies containing REE, having a predominance of bastnaesite, monazite, xenotime, and parasite. The deposits were likely generated under relatively similar climatic conditions but most likely came from various host rocks. On the other hand, in comparison to the primary deposits of HREEs, they are easier to enrich. Some deposits that are considered as lateritic are listed in the Table 1.5 [21].

Table 1.5: Lateritic REM deposits [22]

Lateritic Deposits		
Deposit	**Source**	**Tonnage, (Mt)**
Ngulla, Tanzania	Carbonatite	170
Mt. Weld, Australia	Carbonatite	23.94
Tantalus, Madagascar	Granite	14.4
Dong Pao, Vietnam	Granite	7.4
Araxá, Brazil	Carbonite	6.34
Jianghua, China	Granite	0.012
Mabounie, Gabon	Carbonite	-
Madeira, Brazil	Carbonite	-
Pitinga, Brazil	Apogranite	-
Stromberg, Australia	Altered tuffaceous sandstone	-

1.1.5. Rare Earth Elements and Their Applications

Rare earth elements are used to designate a family group of fifteen lanthanide metallic elements. Subsequently, scandium and yttrium were added to this group. REEs have almost identical physical and chemical properties to one another, generally occurring together in minerals, and behaving as a single chemical entity. The group consists of elements of lanthanum, cerium, praseodymium, neodymium, promethium, samarium, europium, gadolinium, terbium, dysprosium, holmium, erbium, thulium, ytterbium, lutetium, scandium and yttrium shown in the Figure 1.4. They can be divided into two groups; the first named as 'lights' or 'LREEs' that include from lanthanum^{57} to europium^{63}, while the second group called 'heavies' or 'HREEs' from gadolinium^{64} to lutetium^{71} [1][10][23].

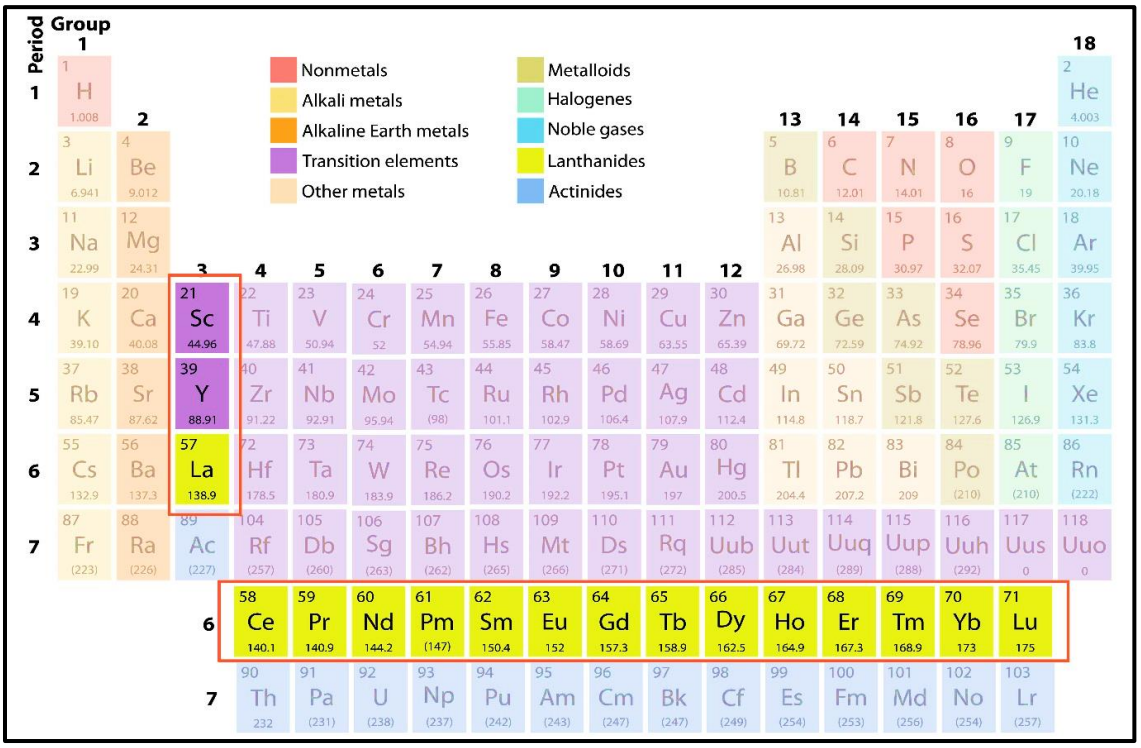

Figure 1.4: The rare earth elements on the periodic table

The chemical similarity among rare earth elements shows the viability of occurrence altogether in nature. This phenomenon is assumed as a consequence of highly similar electron configurations, which has an ionic dominance, mainly determined by M^{3+} ions. The exception of that is cerium $^{4+}$ and europium $^{2+}$ [24]. REEs are characterized by being generally soft, malleable, ductile, and typically reactive.

$$La^{3+} > Ce^{3+} > Pr^{3+} > Nd^{3+} > Pm^{3+} > Sm^{3+} > Eu^{3+} > Gd^{3+} > Tb^{3+} > Dy^{3+} > Ho^{3+} > Y^{3+} > Er^{3+} > Tm^{3+} > Yb^{3+} > Lu^{3+} > Sc^{3+}.$$

Figure 1.5: Decreasing basicity of rare earth elements

Basicity is a property that determines the degree to which cations are hydrolyzed in an aqueous solution and is considered one to the important properties of REE. In turn, this characteristic is related to the concentration of the lanthanides. They can be organized as shown in Figure 1.5, according to decreasing basicity. Along with basicity, **resistivity** (REEs are characteristic for having poor electrical conduction), **magneticity** (most of REEs are highly paramagnetic except for scandium, yttrium, lanthanum, ytterbium, and lutetium), and r**eactivity (**REEs have this characteristic especially at high temperatures and when they are finely divided) are other important properties of REEs [10].

The REE has a wide range application in modern life. Currently, demand for REEs are increasing exponentially which can be seen in figures proposed by Goodenugh et al. [24] given in Figure 1.6. Since, it is considered a crucial material in the development of various industries such as nuclear technology, metallurgy, magnets, ceramics, electronics, optics, and medical applications (Table 1.6) [1][25].

Table 1.6: Uses of the rare earths [1][25].

Element	Application
Lanthanum	NiMH batteries, petroleum cracking catalysts, green phosphors, and optics
Cerium	Catalysts, UV light absorption in glass, polishing media
Praseodymium	Yellow pigment, additive to Nd-Fe-B magnets
Neodymium	Lasers, glass coloring, Nd-Fe-B magnets
Samarium	Sm-Co permanent magnets, laser applications
Europium	Phosphors (red) for TV, computer screens, and fluorescent lamps
Gadolinium	Host for phosphors, X-Ray screens, MRI contrast agents
Terbium	Phosphors (green) for TV, computer screens, fluorescent lamps
Dysprosium	Added to Nd-Fe-B magnets for increased high temperature performance
Holmium	Additive in Y-Fe-B (YIG) and Y-La-F (YLF) lasers
Erbium	Glass coloring, fiber optic amplifier, and medical lasers
Ytterbium	Fiber amplification, fiber optics
Lutetium	Dopant in garnet crystals such as indium-gallium-garnet (IGG)
Yttrium	Ceramic crucibles, fluorescent phosphors, computer displays, automotive fuel consumption sensors
Scandium	Ceramics, lasers, phosphors, high performance alloys

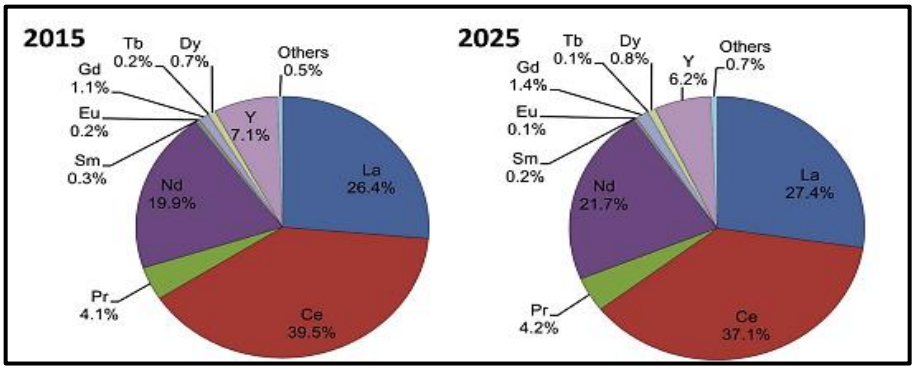

Figure 1.6: Proximate REE demand per element between 2015-2025 [24]

1.2.Gangue Minerals of Rare Earth Minerals

The REEs are not found in pure metal forms, and are considered lithophilic having affinity to the association or reaction with silicates. Due to these reasons, they are mostly found within a variety of compounds such as carbonates, oxides, silicates, and phosphates. However, the composition and quantity of mineral gangue vary with the type of deposit [23].

As noted earlier, the primary gangue minerals in Beylikova-Eskişehir deposit are fluorite, barite, calcite, and silicate, which also represent a major problem during the enrichment of the REMs due to following important points [8]:

- **Calcite:** It is a carbonate mineral which has a semi-soluble characteristic. It makes the process quite difficult to separate calcite from rare earth carbonates due to their similar surface qualifications. Bastnaesite mineral is particularly affected during the flotation process [1].
- **Fluorite:** Fluorite has been identified as one of the most common gangue minerals occurring in REM bodies. It should be handled and analyzed carefully. It is a semi-soluble alkaline mineral that frequently co-occurs with REE and presents processing challenges. It also shares similar surface issues with the mineral of interest. Natural fluorite tends to exhibit normal hydrophobicity, although it is a mineral which could be considered as hydrophilic and hydrophobic. Additionally, the hydrophobic characteristics tend to vary according to the physical characteristics such as color and crystal structure (Figure 1.7) [26]. Also, it has two predominant ionic species, the calcium ion (Ca^{+2}) and the fluoride ion (F^{-2}), ions primarily responsible for electrokinetic behavior [2][27].

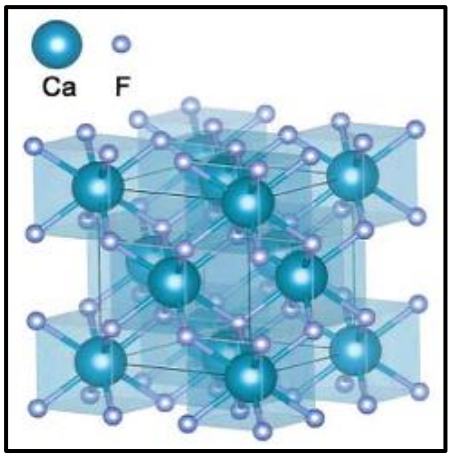

Figure 1.7: The structure of Fluorite [26].

- **Barite:** It is a heavy sulfate mineral that is recognized as a prominent gangue mineral representing an alkaline part by Ba^{2+} and the part ion sulfate SO_4^{2-}. The largest influence on electrokinetic behavior comes from the charges of these ions. [26]. The barite deposits commonly contain the mineral in coarse crystalline form. They have an intercalated growth. For these reasons, they are considered as highly structured symmetrical crystals. Moreover, crystallographic restrictions and complexity in the precipitation media might be responsible for the dispersion and interaction of barite with REE [28].

2. FLOTATION OF FLUORITE, BARITE, AND RARE EARTH MINERALS

The froth flotation process (Figure 2.1) is based on the variation of the surface properties between the mineral of interest and the gangue minerals involved. These differences in surface properties can be altered by the addition of chemical agents to generate major surface differences. In the case of REMs, due to the presence of mineral gangue with similar surface characteristics, the separation process is considered complex [29].

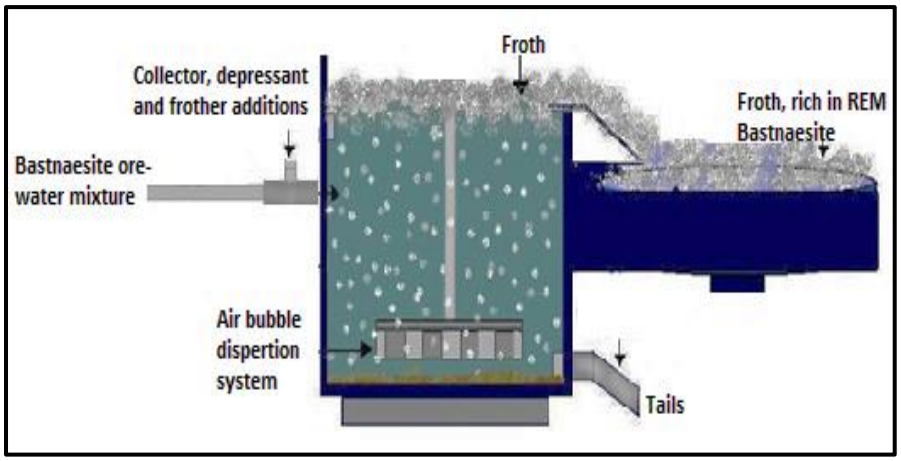

Figure 2.1: Flotation scheme [30].

Understanding the behavior of all minerals present in ore and how the absorption phenomenon occurs under different chemical agents could help to generate optimal conditions for the flotation process. Consequently, the measurement of electrokinetic potential/zeta potential is considered the main contribution to the flotation process design. Electrokinetic potential/zeta potential investigations allow both characterizing and monitoring the real interactions between phases (mineral-bulk solution) and the changes that take place.

2.1.Zeta Potential

The behavior of the mineral particles when submerged in a solution exhibits a wide range of phenomes. One of them is the generation of a positive or negative charge on the surface layers of the mineral particles. The developed charge has a great deal of dependence on the ion liberation process. Hence, the following cases can be discussed as highly relevant and common when discussing the surface charge [31]:

- **Specific chemical interactions:** Chemical reactions occur in a solution, depending on the nature of the mineral. The typical case that is encountered with oxides, which are highly present in REMs, is the formation of surface acid groups. They react strongly to changes in the pH of the system [3].
- **Preferential dissolution of ions:** The term is commonly used for simple univalent ionic solids of the mineral within which there must be equal numbers of positive and negative ions on a surface plane. Depending on the hydration energies relative to each ion present, they can be hydrated to a greater or lesser extent, generating preferential dissolution in the bulk solution. As a result of this phenomenon, there remains an increase in the concentration of opposite ions on the mineral surface, establishing an electrical charge. These ions are the potential determining ions [29].
- **Lattice substitution**: Atoms in the surface can substitute enabling a surface potential. This substitution may be responsible for the differences in the electrical properties at the surfaces and the edges of the mineral. The structure of the mineral could affect the electrokinetic behavior [32].

As a result of these points, when the minerals are immersed in the solution, an inhomogeneous electrical region between the involved mineral and the bulk solution is generated [3].

The electrical double layer model is a scheme developed based on the electrical nature of the mineral surface when a mineral is immersed in a solution. Hence, a non-homogeneous electrical region between the solid (mineral) and solution (generally water) interactions is produced due to ion release processes such as dissolution and/or hydration in the mineral-solution interaction. These free ions with both negative and positive charges will be attracted or repelled according to the charge of the mineral surface. The charged surface acquires an electrical potential, generating a counter layer or diffuse layer when it is balanced by these charges (Figure 2.2) [33][31][34].

The diffuse layer is concentrated close to the surface of the particle. With distance, it gradually gets smaller. The distinctive feature of the diffuse layer is its capacity to control, to a greater or lesser extent, the absorption action of reagents in solution such as collectors, depressants, activators, etc. The method for characterization of this phenomenon is the measurement of the zeta potential [1][11].

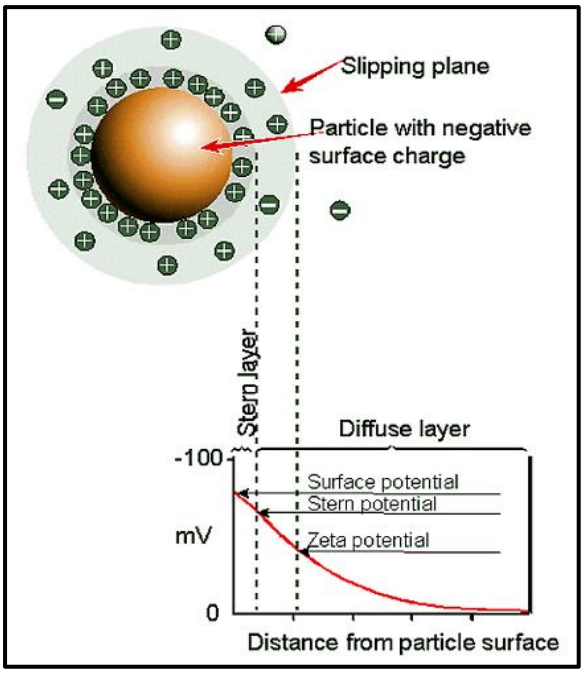

Figure 2.2: Schematic of the zeta potential [33].

2.1.1. Zeta Potential Measurement and Affecting Factors

Since the double layer potential is difficult to measure, zeta potential resulted by the electrokinetic effect can be measured. Zeta potential generally is the measured charge in mini volts at the boundary plane formed by the electrical double layer. It is measured directly and related with the charge of the particle and the thickness of the double layer [35]. Therefore, the magnitude of the zeta potential gives a general foresight of stability of potential of the system. pH value is considered as the primary and the most important factor in investigating the zeta potential. The common curve is usually plotted as zeta potential (mV) vs. pH value (Figure 2.3). In terms of this curve, the particles tend to acquire a negative charge in the alkaline zone, while they acquire a positive charge in the acidic zone [4].

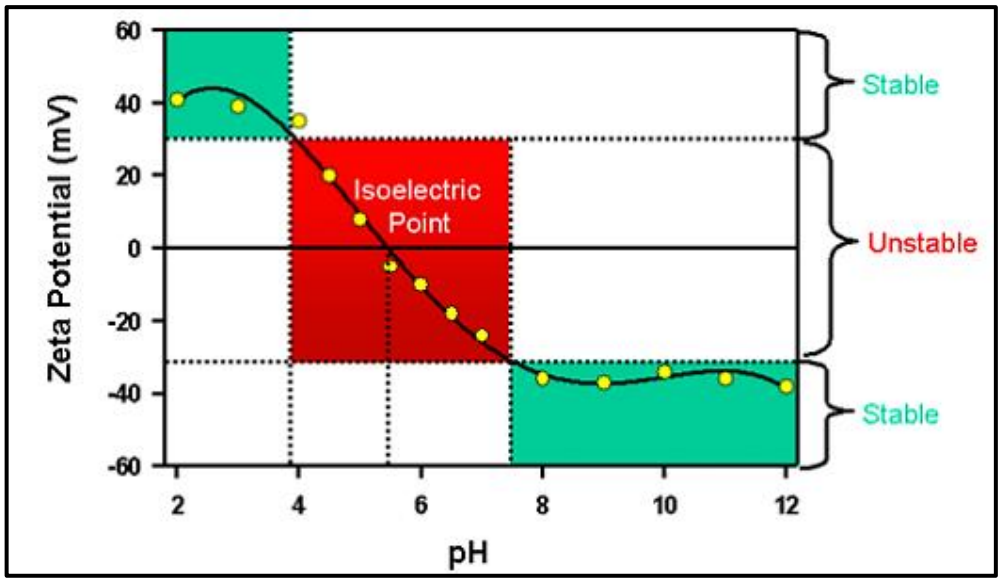

Figure 2.3: Zeta potential versus pH showing the position of the isoelectric point [33].

Another significant aspect of this system is the neutralization point, typically called the isoelectric point (IEP). IEP is considered an important characteristic specific to each mineral in the system, when observed. IEP helps determine effective conditions for separating a valuable mineral from the gangue. Hence, it is expected to understand how the absorption and selection mechanisms of the reagents occur in the flotation [36][37][38].

Different methods can be used to measure the zeta potential, such as electrophoretic, electroacoustic, and streaming potential:

- **Electrophoresis:** It is generated when fine particles are dispersed in some dielectric material within the electrolytic solution, creating the effect of an electric field in which the particles move through the fluid. It is the most common method due to its relative simplicity. In this technique, an electric field is applied. Nevertheless, it has limitations associated with optical measurements. To determine the migration velocity of the particles in a potential gradient, the following equation (Equation 1) is used [31][39].

$$\zeta = 4\,\pi\,\left(\frac{\mu}{D}\right)\left(\frac{V}{E}\right) * 9x10^4 \qquad \text{Equation 1}$$

Where:

$\zeta = zeta\ potential, (\ volts)$

$\mu = solution\ viscosity, (poise)$

$D = dielectric\ constant$

$V = particle\ velocity, (cm/sec)$

$E = potential\ gradient, (\ volt/cm)$

- **Electroacoustic:** It is an application of high frequency, alternating electric fields to the suspension of particles. The charged particles oscillate and produce a sound wave of the same frequency. The zeta potential of the sample can be calculated from the phase and magnitude of the resulting sound wave. However, the technique is poorly suited for cases where only very small quantities of pure mineral samples are available, which is generally the case with REMs [12].
- **Streaming**: It is the application of a pressure difference in such a way that the liquid flows through a bed of particles generating the electric field. The aqueous section and the mineral must be measured in both mechanically and chemically stable forms, which generates significant problems for the application. Then, the potential generated when the bulk solution is forced through a packed bed of the particles could be calculated by the following equation (Equation 2) [3][22].

$$\zeta = 84.85\ x10^4\ \left(\frac{\mu\ \sigma\ E_s}{D\ \Delta p}\right)$$ Equation 2

Where:

$\zeta = zeta\ potential, (\ volts)$

$\mu = solution\ viscosity, (poise)$

$D = dielectric\ constant$

$\sigma = conductivity, (mho/\ cm)$

$E_s = streaming\ potential, (volt)$

$\Delta p =\ \ pressure\ drop, cm\ Hg$

2.1.2. Determining Ions of Bastnasite

Surface charges developed by bastnasite mineral are quite complicated. The process involves solution chemistry based on individual ions as well as dissolution, precipitation, and/or determining ions with high variability of change with various parameters within the bulk solution [12]. When the bastnasite mineral is dissolved, a portion of it forms new

solid species, while another portion turns into an active component of an electrocharged solution. For example, the following are some of the most significant findings regarding Ce-Bastnasite mineral behavior in solutions:

- The individual ions belonging to bastnaesite mineral have a high hydrolysis characteristic in water.
- Cerium ions (Ce^{+3}) belonging to bastnaesite mineral tend to form hydroxy complexes which react in a same but more complex way with both fluorite and carbonate. They precipitate as cerium fluorite or cerium hydroxide, depending on the pH of the system [40][41].

When a neutral reference pH is considered, a new precipitate of cerium hydroxide forms when the concentration value is increased to or exceeds a limit. Similarly, cerium fluoride precipitate is anticipated to form when the pH value decreases and exceeds the limit [42].

Herrera et al. [36] present the possible formation of precipitates in an aqueous solution. Figure 2.4, Tables 2.1, and Table 2.2 show the distribution of the possible free ions as well as the solid particles in relation to the pH of the system. Considering the predominance of the generated solid phases, this phenomenon depends on the dissolution-precipitation that takes place at the different pH values. This is because the pH value is affecting the electrochemical nature of the solid-solution through regulation of the solubility and the chemistry.

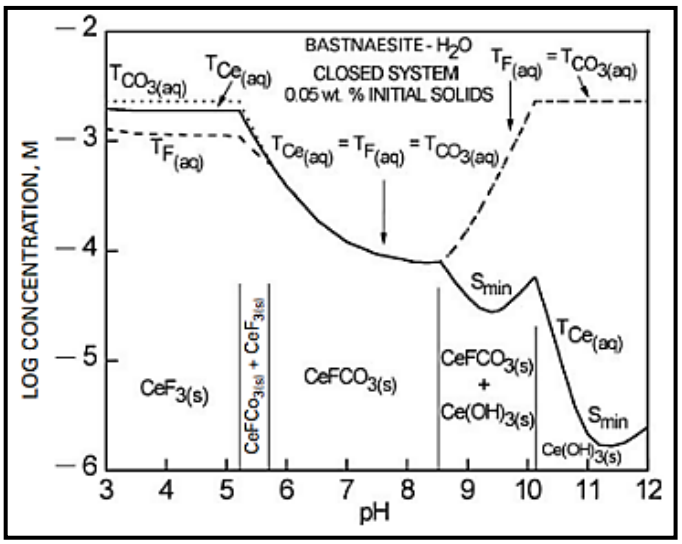

Figure 2.4: Equilibrium distribution of bastnaesite in a solution as a pH function

Table 2.1: Ions of bastnaesite in a solution as a pH function

pH range	Solid Phases Present
< 5.2	Ce F
5.22 -5.74	$CeFCO_3 – CeF_3$
5.74 - 8.55	$CeFCO_3$
8.56 – 10.12	$CeFCO_3$ - $Ce(OH)_3$
>10.2	$Ce(OH)_3$

Table 2.2: Fluoride speciation of bastnaesite in a solution as a pH function

pH range	Ions present
3- 8.7	free fluoride, free cerium
8.7 – 12	free fluoride, free carbonate

Additional characteristic effects regarding the pH variability are [1][29][35][11][36]:

- Theoretically, under the restrictions of the pH value shown in vertical lines in Figure 2.4, a complete first dilution could be regarded as either cerium fluoride or, on the other hand, cerium hydroxide.
- Exceeding these limits is also considered representative since the dissolution of both fluoride and cerium hydroxide increases. These options leave the bulk solution more acidic or more basic, respectively.
- Significant impact on electrophoretic mobility can be observed, showing a positive response at low pH values and a negative response at high pH levels.
- The charged surface, electrophoretic mobility, new solid particles, and derived ions generate a highly active solution.

These findings address probable formations such as precipitates and the free ions in the bulk solution. They can be considered factors in the alkaline and acidic characteristics of the solution and their dependence on the pH value. Furthermore, it is known that fluorocarbonate minerals, in the case of Ce-Bastnasite, often show irregular crystalline structures such as syntaxial intergrowth and stacking faults. It causes high alterations in its chemical structure, adding difficulty in the form of dissolution-precipitation behavior [2].

One of the most relevant value measurements of the zeta potential is the isoelectric point (IEP) at which charges are balanced, which means a measurement equal to zero is obtained (Figure 2.5) [29].

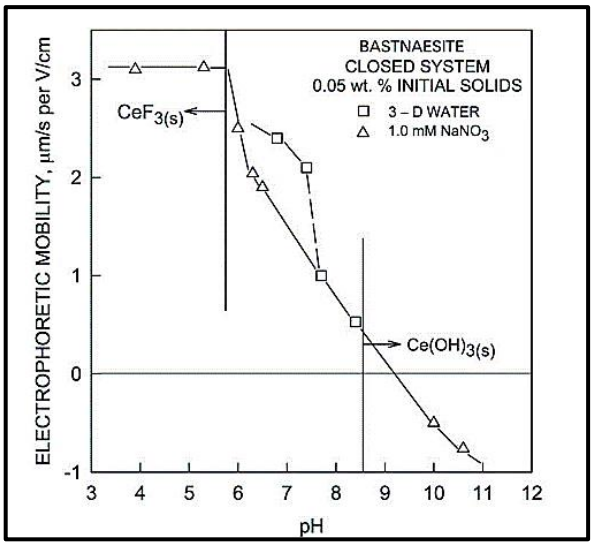

Figure 2.5: Isoelectric point (IEP) of the bastnaesite [25].

The IEP values of bastnaesite reported on previous research pool tends to vary in between pHs 4.6 reported by Smith and Shomard [38] and 9.5 reported by Pradip [34]. Both Figure 2.6 and Table 2.3 show this variation of IEP values, where different researchers measured different values even for the same REO deposit such as the Mountain Pass case, Bastnaesite deposit in California - United States [2].

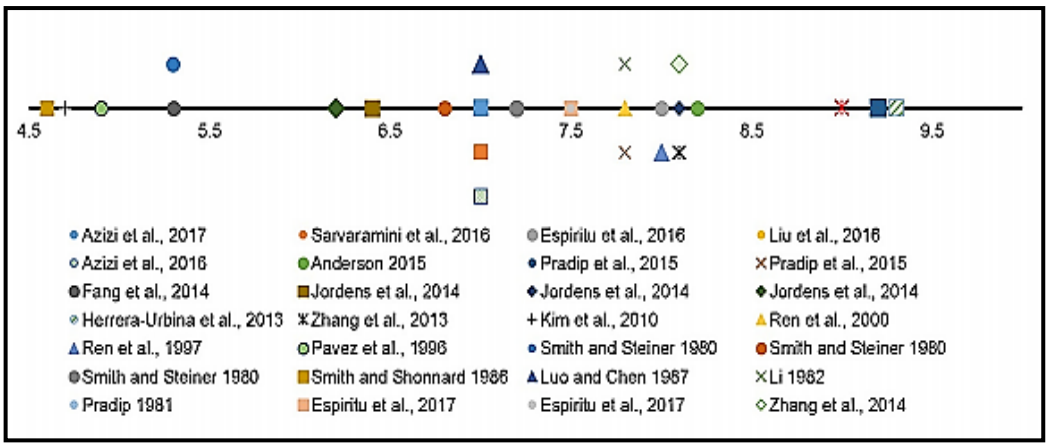

Figure 2.6: IEP of the studies developed on the bastnaesite mineral [29].

According to the research presented by Espiritu et al. [43], results varied between pH 7 and 8. Measurements of the electrical potential of bastnasite were carried out in the presence of NaCl as a background electrolyte, and under different conditioning times. These values of the zeta potential are attributed to a supernatant effect and are almost insignificant for the variation of the conditioning time. Regarding the presence of supernatants, it is considered that they would be affected by the presence of OH^- ions on

the mineral surface. Therefore, this is considered a determining ion of the potential, which acts favorably with the Ce atoms on the surface of the bastnasite mineral, charging more negatively to the mineral surface.

The findings established by Zhang et al.(2014) [44] and Zhang et al. (2013) [2] (Table 2.3) show a PZC with a tendency close to a pH of 8, attributing the variation to the properties of the anions of the mineral. Furthermore, ratifying CO_3^{-2} ion derived from bastnaesite acts as a weak acid with a strong tendency to adsorb hydrogen ions from solution. Since, in search of equilibrium, the mineral tends to go to the alkaline side.

Similarly, Ren et al. [45] present a pH result of approx. 8 for the IEP; the research was conducted in pure water, supporting the recent findings presented by Herrera et al. [36]. The results indicate that the electronegative region is most likely caused by the adsorption of OH^- and $Ce(OH)^{4-}$ to the surface in the high pH region. Whereas H^+ and Ce^{3+} ions are most probable to be responsible for the electropositive region at low pH.

On the other hand, Jordens et al. [11] analyzed the IEP of bastnaesite mineral via two different types of techniques: electrophoretic and acoustic. The resulting values were 6.3 and 8.1, respectively, suggesting a great difference in results even with the identical mineral samples analyzed.

Table 2.3: Reported IEP values for bastnaesite [2].

IEP (pH)	Reference	Source
4.6	Smith and Shonnard, 1986	Synthesis
4.9	Pavez et al., 1996	-
5.3	Houot, 1991	Mountain Pass
6.8	Houot, 1991	Mountain Pass
7.2	Houot, 1991	Mountain Pass
7.0	Luo and Chen, 1984	Bayan Obo
7.8	Ren et al., 2000	
8.0	Ren et al., 1997	
9.5	Pradip, 1981	

The variation of these cited results is concerning and confusing in terms of determining a beneficiation route based on flotation. Especially, the reaction of bastnaesite surfaces according to the variation in the pH of the system shows complexities and does not only depend on (H^-) and (OH^+) ions [32]. These discrepancies in the results in the different research are attributed to variations in the ion determinants, mineral composition, and

structure of mineral surfaces, as well as the technique, and even the procedure involved in the sample preparation for zeta determination [46]. According to researchers such as Anderson and Taylor [1], Fuerstenau et al. (1992) (1999) (2005) [39][40][41]] and Pradip and Fuerstenau.(1984) (1985) (1991) [47][48][49], the background electrolyte solution also affects the results of the magnitude and value of the potential. This background electrolytic solution, such as KCl and KNO_3 has been used in much of the research due to the potassium, chloride, and nitrogen ions that are described as ions indifferent to the potential of the bastnasite mineral. Since they are expected to show a slight or no effect on the IEP measurements.

2.1.3. Determinant Ions of Fluorite

According to the previous findings on the measurements of the zeta potential of fluorite, fluorite ions have strongly marked their characteristics through the alkaline and acidic part (Figure 2.7). These findings suggest that the surface potential responses should, in theory, be very little affected by pH values [32].

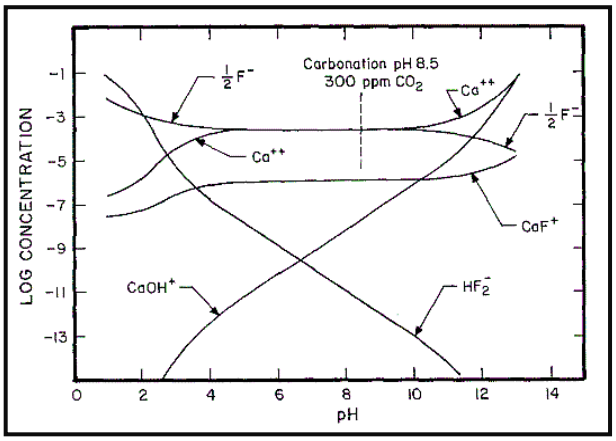

Figure 2.7: Ions distribution of fluorite - aqueous system [32].

The electropositive effect on the zeta potential is justified by the fluorine ions. They tend to hydrate more than calcium ions. The responses of the zeta potential are typically not affected by the amount of these ions present. As a result, it should be assumed that fluorine ions do not have the ability to act as a determining ion [50].

On the other hand, it is observed that the potential tends to decrease with an increase in the pH value. According to the results presented by Miller and Hiskey [32] and Miller et al. [50], this variation in behavior is mainly due to carbonation on the mineral surface. Depending on the concentration of hydrogen ions, the characteristics of fluorite are

expected to change those of calcite ($CaCO^3$), which behaves as a weak acid. When this happens, the zeta potential tends to rapidly fall, having a negative character. Additionally, it is known that fluorite tends to be widely affected by CO_2, generating carbonation on the mineral surface, which eventually causes zeta potential measurements to be affected. Due to these characteristics, both calcium and carbonate ions are considered the determining potential ions for fluorite mineral. Therefore, their concentrations have a high effect on the zeta potential values, which in turn, justifies the dependence of the change on the variation of pH. Additional and important findings to take into consideration are [50][32][51][52]:

- The influence of the conditioning time is important. Because if it is too long, the system tends to exhibit a reduction in the zeta potential values due to the carbonation effect.
- The system is affected by lattice, structure, and cleavage planes that will generate an effect on the variation of the energy.
- The solid concentrations influence the chemical equilibrium, which is dictated by surface charge and by the release of ions, particularly calcium ions. Hence, a high concentration indicates a quick chemical equilibrium, whereas a low concentration indicates a slow chemical equilibrium, a large ion release, and a sluggish dissolution.

The reported isoelectric points for fluorite mineral can be seen in Table 2.4.

Table 2.4: The reported IEP values for flourite mineral [2].

IEP (pH)	Reference	Technique
7	Choi	Electrophoresis
10.6	Fuerstenau	Electrophoresis
8.5	Dobias	
9.5 (Synthetic)	Rao	Electrophoresis
6.2 - 8.8 (Natural)	Rao	Electrophoresis

For the background of electrolytes such as NaCl, a low or almost null effect on the zeta potential is attributed. This is due to the high natural ionic strength of the system, which means a highly structured electric double layer with little variation in the measurements [2].

2.1.4. Determining Ions of Barite

The measurements of the zeta potential of barite present a positive charge response with low pH, while with a high pH, it exhibits a negative charge (Figure 2.8). In the acidic region, there is a predominance of barium species such as cations of Ba^{+} and Ba OH^{+}. In the alkaline region, predominant sulfate anion species are HSO_4^{-} and SO_4^{2-}. In this sense, it is expected that the determining ions will fluctuate with the change in pH along these zones [26].

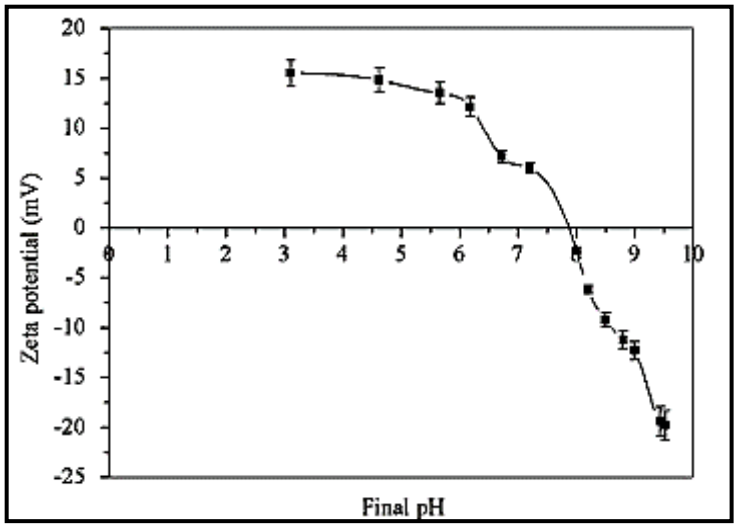

Figure 2.8: Zeta potential of barite in absence of back electrolytes [26].

Some additional highly relevant findings presented by researchers are [53][54][55][26]:

- The pH can be lowered by the formation of metal hydroxides as a result of the reaction of OH^{-} with dissolved cations.
- The decrease in pH shows a decrease in negative charge due to H^{+} absorption to the negatively charged particles.
- The zeta potential is greatly affected by the heterogeneity of the surface and by the presence of some impurities generating varied responses of IEP.
- The concentration of barite in the solution has a significant impact on the zeta potential, altering its responsiveness.
- The absorption of H^{+} and OH^{-} ions as well as their interactions with the dissolved ion lattice should both get special consideration.

Table 2.5 presents some values of the IEP for the barite mineral. If the IEP tends to be in the alkaline region, it could be due to an increase in barium concentration. On the other

hand, when the IEP tends to be in an acidic region due to the predominance of ionic sulfate species (HSO^{4-} and SO_4^{2-}). The results reaffirm that these species are the determining ions of potential when barite is considered [1][40][28].

Table 2.5: The reported IEP values for barite mineral [2].

IEP (pH)	**Research (**as presented in [83])	**Technique**
7	Orthgiess and Dobias, 1994	-
10	Pradip and Fuerstenau, 1984	-
4.5	Rao et al, 1990 and Marinakis and Shergold, 1985	Electrophoresis

According to the study carried out by Hang et al. [26], the effect of simple electrolyte systems such as NaCl or $NaNO^3$ as the background electrolytes on the measurements of the zeta potential are not significant. Therefore, the IEP measurements can be performed with little disruption. Theoretically, the resulting minimum alterations could be due to the monovalent ions compressing the electrical double layer (EDL) presenting a reduction effect in the measured IEP values. Since they are not capable of causing a charge inversion, these can be considered non-determining ions for the barite mineral.

2.2. Flotation of Rare Earth Minerals (REMs)

REMs, particularly bastnaesite, are classified as semi-soluble salt minerals and are typically associated with gangue minerals such as fluorite and barite. These minerals act similarly within the flotation system due to their common physical, chemical, and dissolving properties [44]. Furthermore, the dissolved species from the gangues and semisoluble salts are particularly absorbed on the valuable mineral surface in the system. The separation of REMs from gangue minerals can be accomplished using diverse techniques, such as gravity and magnetic separation techniques. Nevertheless, the most important technique due to the complexity of REM ores (especially for bastnaesite) is flotation [40][34].

During flotation, crucial reactions could be produced by minerals when the pH of the system changes [43][56][57]. Due to this, selective agents are required to carry out a successful flotation. These agents include collectors, depressants, pH controllers, etc. [45][58]. Gangue minerals have a significant impact on the choice of chemical agents used in the flotation of REMs, especially bastnaesite. There are numerous researches on bastnaesite flotation, and some interesting findings can be listed as follows [48][49][29]:

- Bastnaesite found in a carbonatite ore can be recovered using fatty acid type collectors with or without heat pretreatment. Improved results could be obtained with oleic acid modified with phosphate ester.
- Bastnaesite found in barite–fluorite ores usually respond either fatty acid agent or sodium oleate. Bastnaesite floatability could be improved significantly after barite pre-flotation.
- Bastnaesite found pegmatitic deposits can be successfully recovered with various types of collectors such as tall oil modified with secondary amine or petroleum sulphurated group.

For REM flotation, a variety of chemical agents have been investigated. Collectors (such as fatty acids, various hydroxamates, dicarboxylic acids, and phosphoric acids) and depressants according to the gangue mineral type leave interest findings [12][11]. An in-depth list of collectors and depressants of interest are summarized in Table 2.6 and Table 2.7, respectively.

Table 2.6: Collector agents with bastnaesite [2].

Classification of Collector		**Components**
Hydroxamate	$C_{5\text{-}9}$ Alkyl hydroxamate	RCONHOH
	$C_{7\text{-}9}$ Alkyl hydroxamate	RCONHOH
	Aromatic hydroxamate	$C_6H_5CONHOH$
	Salicylic hydroxamic acid	$C_6H_4OHCONHOH$ (ScH)
	H2O5	$C_8H_5NO_3$
	Naphthalenic hydroxamate	LF-P_{81}
	2-hydroxyl3-naphthoylhydroxamate	H_2O_5
	Cyclohexylhydroxamate	CHH
	Benzylhydroxamate	BzH
	Octylhydroxamate	OtH – OHA
	Potassium Octylhydroxamate	POH
	Tetra-butylbenzylhydroxamate	TBBZ
Phosphonic Acid	Styrene Phosphonic Acid	$C_8H_9O_3P$
	Alkyl phosphate	RH_2PO_4
	Phosphoric acid ester, Alkyl succinamate	F-1682, A845
	Phosphoric acid ester, Alkyl sulfate sodium, Alkyl succinamate	KBX36
Carboxylate	Oleic acid	$C_{18}H_{34}O_2$
	Phthalate	$C_6H_4(COOCH_3)_2$
	Sodium oleate, Parafine oxide soap, Tall Oils, Fatty acid	
Modifying agent	Na silicate	(Water Glass) $Na_2O.SiO_2$ (mass ratio 2:3) 38-40% Solution

Table 2.7: Depressants agents used with bastnaesite Ore [12].

Classification		Components	Depression
Depressants	Sodium Silicate	Na2SiO3 or Na2O3Si	Silicate gangue, salt minerals (fluorite, barite, calcite and dolomite), iron minerals
	Lignin sulfonate		Barite and calcite
	Sodium fluorosilicate	Na2[SiF6]	Barite, calcite and fluorite (activator for REM flotation)
	Sodium fluoride	NaF	Silicate and oxide minerals,
	Sodium sulphides	Na_2S	Zircon when using a fatty acid collector
	Sodium hexametaphosphate	$(NaPO_3)_6$	Calcite
	Starches		Rutile, ilmenite and zircon
	Amylopectin	$(C_6H_{10}O_5)$ n	Zircon
	Quebracho		Xenotime and zircon
	Guar gum	$C_{10}H_{14}N_5Na_2O_{12}P_3$	Naturally hydrophobic gangue (talc) and silicates
	Silica gel	SiO_2	Barite, fluorite and calcite

Hydroxamate and carboxylic collectors are two types of collectors that are frequently used for REM flotation. Hydroxamates are N-Alkyl derivatives of hydroxylamine, through which a complex metallic reaction occurs. The weaker hydroxamic complexes are formed by alkali metal ions, such as Ba^{2+} and Ca^{2+} ions, while the more complex ones are formed by highly charged multivalent RE cations. Following this, complex hydroxides in the system are reabsorbed by the surface mineral. Due to these interactions, hydroxamates form a stable REM surface complex [48][44].

There are two options that these collectors may interact with the surface: chemical absorption and/or surface reactions. They also have the ability to form powerful chelates with REM, which often interact with RE hydroxylated species at the surface or species found in the bulk system, subsequently reabsorbing to the mineral surface. As a consequence, the valuable mineral bastnasite exhibits hydrophobic properties [47][49]. The hydrophilic character of the RE and its inherent solubility in water, as well as the carbonates in the complex solution, lead to the conclusion that these processes are not straightforward [43]. On the other hand, Marion et al. [12] emphasize the possibility of unwanted precipitates in the bulk solution, which could have an adverse effect on the

collector effects. Therefore, these type collectors are highly effective for the flotation of the bastnaesite mineral and general summary of principal findings are presented:

- According to Espiritu et al. [43], using benzo hydroxamate collector shows that the zeta potential of bastnasite tends to become less negative and suggests a significant adsorption for high pH values. This collector was effective between pH 8-9. pH 9 proved to be most successful due to the formation of complex species that absorb on the mineral surface, improving the flotation. This also shows that the supernatant species decrease the recovery of valuables. Jorden et al. [11], who also work with benzo hydroxamate, showed optimal selection at a pH of 9 in the presence of quartz as gangue. Additionally, it is concluded that optimal recovery is strongly dependent on the frother agent used.

- Pradip and Fuerstenau [48], who utilized potassium octyl hydroxamate as a collector, concluded that the presence of this causes a negative charge on the zeta potential of bastnaesite. The absorption occurs through a metal hydroxy complex on the mineral surface, and the maximum recovery is achieved at pH of 9. However, for the same pH value, a high recovery of the gangue minerals (barite and calcite) was also obtained. Therefore, selective flotation could occur at a pH value equal to 8.2.
- Ren et al. [45] tested a modified hydroxyamide acid called MOHA, which was more selective compared to the group of hydroxamates. The results of the zeta potential in the presence of MOHA tend to change towards the negative part. The maximum absorption occurs between pH value of 8 - 10.

Another group of collectors, namely fatty acids belonging to carboxylates, are also among the most preferred agents used in fluorite, barite, and REM flotation. They are collectors which have the characteristic of not being selective. However, due to accessibility, these were one of the first and main collectors for the bastnasite flotation process [48]. Generally, the carboxylate collectors have ions such as $RCOO^{-}$ and $(RCOO)_2^{-2}$, which react with the metal cation, forming Me (OOCR)n. Due to this reaction, the valuable mineral remains with a hydrophobic characteristic. Selectivity is highly dependent on cationic metals exposed on the mineral surface [43].

In this group of collectors, the most commonly used are oleic acids, sodium oleate, and tall oils (mixtures of oleic, linoleic, palmitic, and stearic acids), considering that the oil

part could generate positive results [12]. On the other hand, Pradip and Fuerstenau [48] suggest that the selectivity can be increased by increasing the temperature of the system and adding large amounts of other agents, commonly depressants. Table 2.8 lists the many additional chemicals in conjunction with the carboxylates examined in various studies.

Table 2.8: The Reported summary presented by Marion et al. [12].

Mineral	Collector	Other Agents	Gangue	pH	Research
Bastnasite	Sodium Oleate		- Dolomite Quartz	9 4-8 9	Pavez et al. Espiritu et al. Jordens et al.
	Oleic Acid Linoleic Acid Linolenic Acid	Lignin Sulfonates *(d)* Sodium Fluoride *(d)* Sodium Fluorosilicate *(d)*	Calcite Barite Celestine	10	Morrice and Wong, 1982
	Oleic Acid	Sodium Silicate *(d)*	Barite	8 - 8.5	Chi et al
	Oleic Acid	Sulphonate *(d)*	Pyrite	7-9	

Some of the key research findings on this type of agents can be summarized as follows:

- Bulatovic [53][20] experimenting with sodium oleate as a collector showed that a maximum floatability was reached at pH = 9. In the tests carried out, the IEP of the mineral bastnasite was situated for a pH = 4.9. At this point, the absorption of the collector occurs under conditions of strong electrostatic repulsion, leaving a negative surface charge. It suggested a chemical absorption mechanism. These reactions occur mainly between the oleate and the REE (Ce^{3+} and La^{3+}) of the bastnaesite.
- According to the investigations by Espiritu et al. [43], who also worked with sodium oleate as a carboxylic collector, a significant change was observed in the zeta potential, decreasing to higher negative values.

These findings, along with many other attempts, show mixed results when flotation of REMs (especially bastnaesite) is considered. As mentioned in Section 2.1.2, reported IEP values of bastnaesite in previous research pool tends to vary between pH 4.6 and 9.5 [34] [38], even with the same ore batches studied by different researchers. This volatility and uncertainty in zeta measurements also affect the flotation findings that have been put forward. When considering the additional difficulties in obtaining trusted pure REM crystals and the probability of low reliability, this thesis study focused on zeta

measurements of fluorite and barite, and relevant flotation behavior of fluorite, barite, and REM species with two different fatty acids, sulfonate, and succinamate type collectors.

2.3. Flotation of Fluorite and Barite

2.3.1. Fluorite Flotation

Fluorite flotation normally tends to be quite selective. Due to this challenge, a large number of different chemical agents have been investigated to promote a better flotation process, especially collectors. These collectors have been classified according to their composition as anionic, cationic, and ampharetid collectors.

Anionic collectors are the most commonly used, despite their disadvantage of lower selectivity**.** They can be classified as; fatty acids, oxidized paraffin soup, hydroxamic acids, alkyl sulfonates and alkyl aminates, oleoyl sarcosine, and organic phosphonic acid [34][47][61][36][62]. ***Fatty acids*** are the most popular and inexpensive non-sulfide collectors. Several modifications have been presented to this type of collector to improve their action. Miller and Hiskey and Miller et al. [32][50] demonstrate that the variation of both temperature and concentration has a positive impact on recovery. Moreover, it may be improved by emulsions, halogenations, sulfonations, and the inclusion of nitrogen atoms. ***Oxidized paraffin soups*** are generally used in the presence of gangue minerals such as quartz, calcite, and barite. They have a good characteristic of selectivity, and additionally, they do not require frother agents. However, their collecting characteristics are less selective. ***Hydroxamic acids*** are normally used in the presence of calcite and fluorite due to their selectivity, even without the use of depressant agents. ***Alkyl sulfonates and alkyl aminates*** group cover the most frequently used sodium alkyl sulfonate. According to the number of carbons, their collecting capacity may be increased. Selectivity depends on the control of pH and the free ions of the bulk solution. ***Oleoyl Sarcosine*** stands out with its influence on calcium minerals. Finally, ***Organic phosphonic acid*** is a chelating collector with a high selectivity for calcite, and pH control is the key parameter for its efficiency.

Cationic collectors, on the other hand, perform through physical absorption. The amine belonging to this group is characterized by a fast reaction in favor of the collection, but a positive charge will not be favorable on benefaction. And **ampharetid collectors** have

both anionic and cationic electrical groups and their action is highly dependent on the variation in pH [47].

Tall oil fatty acids (TOFA) collectors are anionic collectors and a subgroup of fatty acids, which are of special interest for this research. TOFA is an unsaturated compound of fatty acids with no or little rosin, long saturated carbon chains (C_{18}), and a carboxylic group that serves as the functional acid part (-COOH). TOFA alone and with surfactants were investigated within this study. The light tone is one of their physical features. They have the advantage of emitting strong energy at the surface of targeted mineral [63][64][65][66].

Fatty acids are successfully applied in fluorite mineral flotation. Some studies indicate interesting results on the absorption mechanisms of fatty acids on mineral surfaces, which eventually affect flotation recovery. Predali and Cases [67] consider that crushing and grinding may be a critical step in the beneficiation process and have an impact on the absorption and effectiveness of collectors since fluorite has many incomplete substances and free ions remain on the mineral surface. Uçar and Özdag [68], whose research was based on infrared spectroscopy studies, came to the conclusion that higher pH levels are associated with higher absorption peaks, and lower pH levels are associated with smaller collector absorption peaks. It would imply that fluorite absorbs less in an alkyl medium, but the existence of insoluble oleates from this collector could result in the medium becoming an acid. It would be advantageous to the system. The study of Quast [69] suggests that the principal ion species involved in absorption are dissociated in the acidic pH. In addition, it supports the idea that the acidic region could cause superior absorption processes in the system. Mielczarski et al. [61] suggest that growth mechanisms may be responsible for the intensity of the oleate layer produced by absorption of the oleic acid type fatty acid collector. According to Mielczarski et.al [70], the presence of oleates also causes a decrease in zeta potential, implying that the collector's absorption would be primarily chemical.

These collectors can be improved, and their selectiveness can be manipulated. Thus, a modified oil fatty acid with sulfonation was the second used collector in the study. This combination of tall oil fatty acid-containing surfactants is also thought to be more efficient. The explanation is that the presence of surfactants may reduce surface tension, improve mineral absorption and change hydrophobicity. Hence, they are expected to

enhance bubble attachment. When these qualities are combined with TOFA, the aforementioned action should be further increased [22][60]. On the other hand, depressing gangue minerals such as barite, calcite, and silicates while floating fluorite is critical. In the case of Beylikova ore, barite is the third mineral of interest. Due to the similar surface properties of fluorite with the gangue minerals, especially barite, depressing agents should also be used. The most common agents for this purpose are quebracho, dextrin, and lignosulfonate. ***Quebracho*** generates a cleaning action, improving grade and reducing recovery. Its efficiency depends on the balance between the concentration of the collector and the depressant. According to the study by Bulatovic [53], increasing quebracho dosage gradually (0 to 440 g/t) leads to an increase in the final fluorite grade in the concentrate (from 87.25 to 96.86). However, recovery was also reported to decrease significantly. Hence, it has to be used cautiously in order to maintain a recovery-grade balance in the final product. ***Dextrin*** depressants work well on mineral gangues such as barite, sulfides, and calcites, and they are also regarded as effective depressants for oxide-containing minerals. Its preparation would be key to efficiency [71]. Finally, ***lignosulfonates*** are used for the depression of barite, replacing the use of quebracho [53].

2.3.2. Barite Flotation

As mentioned earlier, Beylikova ore has barite, fluorite, and mixed REOs. The recovery of the barite in this situation can be considered by reverse or direct flotation. When a system is composed of more than one mineral of interest, sequential flotation is normally considered for the beneficiation of all minerals. Barite flotation within a sequential flotation process, when fluorite flotation has priority, generally includes depressing agents such as dextrin and quebracho, and reasonable results can be obtained. But in this case, a large amount of fluorite is also expected to be collected in the barite rougher concentrate. Then, fluorite is considered the main gangue in this process. On the other hand, when barite flotation has priority over fluorite flotation, fluorite does not have the tendency to float with barite collectors. This path shows better results, especially in terms of selectivity [53]. Some of the common agents used in the beneficiation of barite are listed in Table 2.9 [12].

Table 2.9: The reported summary presented by Marion et al. [12].

Reagent	Function
Sodium fatty alcohol sulfate	Collector
Sodium tallow fatty alcohol sulfate	Collector
Sodium coconut alkyl sulfosuccinamate	Collector
Sodium alkyl sulfosuccinamate	Collector
Sodium fatty alcohol ether sulfate	Collector
Petroleum sulfonate	Collector
Alkyl succinamate	Collector
Soda ash (Na2CO3)	pH modifier, quartz depressant
Sodium silicate	Silica depressant, slime dispersant
Aluminum chlorite (AlCl3)	Calcite depressant
Quebracho	Calcite depressant
Citric acid	Fluorite depressant
Tannic acid	Calcite depressant
Oxalic acid	Silica and iron oxides depressant
Sodium fluoride (NaF)	Barite depressant
Barium chloride (BaCl2)	Barite activator

Some of the important findings considering the use of these agents can be summarized as follows [12][60][53][55]:

Fatty acids and tall oils are frequently used collecting agents because of their selectivity for barite. But one significant disadvantage is that they also have a selectivity for gangue minerals (fluorite and calcite), and they could be reported in barite concentrates. ***Soda Ash*** is an agent used to regulate pH. ***Sodium Silicate*** typically has dispersion characteristic and silicate depressant effects. ***Quebracho*** is a depressant agent that affects mainly calcite. Although dosage is crucial in the process, more than 400 g/t was reported to have a negative impact on recovery. ***Citric Acid*** is an agent acting as a depressant for fluorite. When barite is floated before fluorite, this agent is frequently utilized, and for good results, a dosage exceeding 500 g/t is suggested. Finally, ***Sodium Fluorite (NaF)*** usually acts as a depressive agent for barite when the flotation of the fluorite is prioritized before barite.

Petroleum sulfonate and alkyl succinamate are also collectors of interest and were used in this study. Petroleum sulfonate is a highly active anionic collector with a mixture of sodium sulfonate, fuel oil, and water. Due to its strong hydrophilic property, sulfonate is the main working group of this collector. It typically has a high viscosity and can be dissolved in hot water [60]. According to the findings of Chen et al. [59], petroleum sulfonate can be utilized successfully in a wide pH range.According to the analysis of

Kecir and Kecir [72], petroleum sulfonate is an efficient collector for the mineral barite, and increasing the dosage can increase its effectiveness. Thus, suggesting that a dosage around 2000 g/t could present the highest recovery results. Hou et al. [66], demonstrated that sulfonates have a significant, potent, and effective interaction at the moment of absorption, but the outcome is down to the long hydrophobic chains of collector.

On the other hand, alkyl succinamate collector is also an anionic collector. It is characterized by having a long chain of the alkyl group varying in width and composition. It is substantially more soluble than petroleum sulfonates and requires much less dosages [53]. Panzer and Boyer [73] demonstrated that the collector is more liquid and can flow more easily than other normally used collectors. This leads solubility benefits and requires a lower dosage for effective results. In the study by Kecir and Kecir [72], result might be better at an acid-neutral pH, since raising pH increases the likelihood that undesirable minerals may float. Hadjiev et al. [74] presented that barite with high grades could be obtained with the addition of water glass as a depressant agent.

3. MATERIALS AND METHODOLOGY

In this section, methodology and experimental routes for sample collection, sample preparation, mineralogical characterization, zeta potential measurements, and flotation tests were discussed. Initial ore samples used in flotation tests from Beylikova region were delivered to the laboratory by Rare Earth Elements Research Institute (NATEN) of Turkey. For zeta potential measurements prior to flotation tests with Beylikova ore, pure fluorite and barite samples were supplied to test the effect of flotation reagents and dosages at varying pH values. Acquired samples were crushed, ground, and representatively sampled for each experiment described in the following sections.

3.1. Sample Collection and Preparation

Since the physical properties, amount, and content of an ore body may vary randomly, the representativeness and homogeneity of a sample are critical. Sampling and characterization studies prior to test work are usually the least valued because of common misconceptions. But they have the greatest impact on the credibility of the results obtained. Therefore, critical sampling and sample preparation steps were explained in detail in Figure 3.1 and Figure 3.2.

A primary sampling study was performed in Beylikova district of Eskişehir, Turkey. Samples from the mine site were collected by scanning the entire cross-section of the mirror in both width and length. Samples from the mirror were scraped as vertical stripes. Approx. 8 tons of sample were then collected from the mirror base, as given visually in Figure 3.1. Following, sample heap was stacked on a clean area on the field, homogenized and reduced by mixing, then packaged and delivered to the laboratories. In Figure 3.2, step-by-step images of the laboratory sampling studies are presented. Laboratory sampling studies included subsequent steps of coning, flattening, quartering, intermediate sampling, crushing & screening for size reduction, and repeating the process until final sample amounts are obtained.

Figure 3.1: Sampling studies from mirror.

Figure 3.2: Subsequent steps of sampling (***1:*** coning, ***2:*** flattening, ***3:*** quartering, ***4:*** crushing and screening for size reduction, ***5:*** intermediate sampling, ***6:*** packing final sample).

3.2. Mineralogical and Chemical Characterization

For mineralogical analysis studies, representative samples were completely ground under -150 µm with a laboratory scale ball mill. Bulk samples from the ore deposit were crushed in a closed-circuit with a 2 mm sieve. The crushing stage was performed until all particles passed the 2 mm sieve. Then, samples were ground in an open-circuit ball mill to obtain a product passing below 150 µm. The milling conditions required to achieve this product are provided in Table 3.1. The ground samples were wet sieved to discard -25 µm fraction in accordance with MLA (Mineral Liberation Analyzer) instructions. The remaining -150+25 µm fraction was regarded as the potential feed material and further analyzed with MLA.

The experimental flowsheet for MLA sample preparation from feed is also illustrated in Figure 3.3. MLA analyses were performed by using the combination of the techniques of QEMSCAN (Quantitative Evaluation of Materials by Scanning Electron Microscopy), XRD phase ID (X-ray Powder Diffraction Phase Identification), coupled with Backscattered Electron (BSE) Imaging and Energy-Dispersive Spectrometer (EDS). MLA analyzes covered modal mineralogical analyses, size distributions of detected contents, and liberation and association analyses.

Table 3.1: The grinding conditions to prepare the -150 µm feed MLA samples

Conditions	**Parameter**
Grinding time (min)	20
Sample weight (kg)	2
Pulp density (weight %)	60
Mill speed (mill revolution per minute)	60
Ball size	Mixed Size
Volume of the ball bed (% of the mill volume)	35-40 %
Mill diameter (m)	0.2
Mill length to diameter ratio	≈ 1

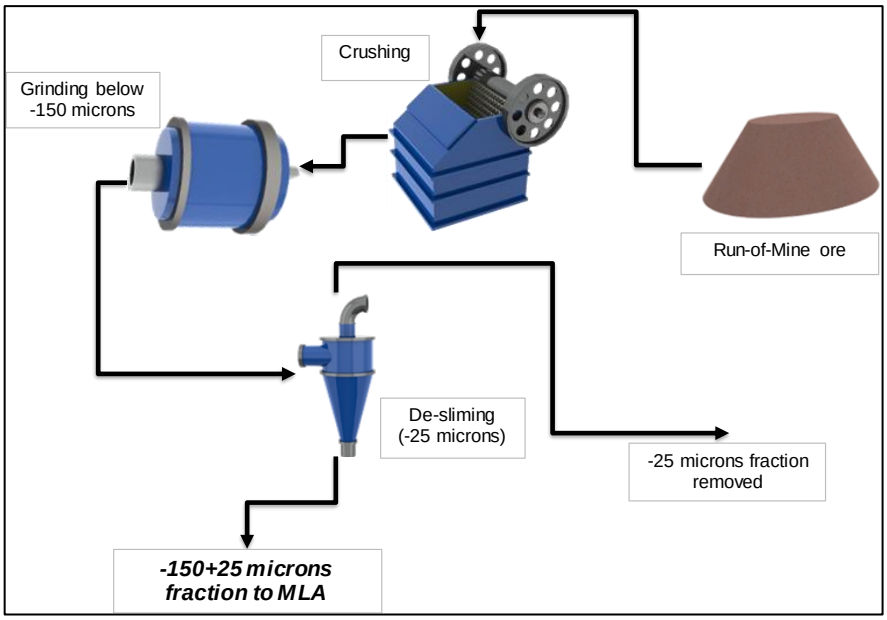

Figure 3.3: MLA sample preparation flowsheet for feed sample

MLA analysis was performed to acquire information about mineral associations and liberation degrees, to determine REMs and principal gangue materials, and to identify gangue minerals generating challenges during flotation.

In addition to MLA analyses, representative feed sample (without removing -25 µm fraction) was also shipped to external laboratories to determine elemental contents. The chemical analysis methods for each critical content were as follows:

- Rare earth elements: ICP-MS with sodium peroxide fusion or XRF with borate fusion.
- Fluorite: EDTA titration.
- Barite: ICP-MS with sodium peroxide fusion.
- Others: ICP-MS with sodium peroxide fusion or XRF with borate fusion.

3.3.Zeta Potential Measurements

Zeta potential is a measure of the repulsion and attraction of the particles in a pulp. Zeta potential analyses were performed with pure fluorite and barite minerals, which are crucial for establishing the flotation conditions and organizing the flotation tests.

In Figure 3.4, the main sample pile of Beylikova ore and a representative mineral rock specimen containing barite, fluorite, and REMs in the clayey and complex matrix are given. Due to the complex mineralogy and altered structure of the ore, it was not possible

to obtain crystals of fluorite, barite, and REE mineral crystals from the Beylikova ore for zeta potential measurements. For these reasons, pure barite and fluorite crystals were separately supplied, and zeta measurement tests were carried out with these samples. These limited number of coarse particles were broken and investigated under the microscope. The free crystals were collected in their purest form with a tweezer. As mentioned in 2nd section, the zeta potential measurement of REMs is very sensitive to ions, and the presence of even a single different ion can change measurements from negative to positive. Since Beylikova ore represents complex mineralogy and multiple formations, it was decided to discuss the zeta data of REMs through a comprehensive review of the literature (Section 2.1). On the other hand, fluorite and barite zeta potentials were individually measured within experimental work.

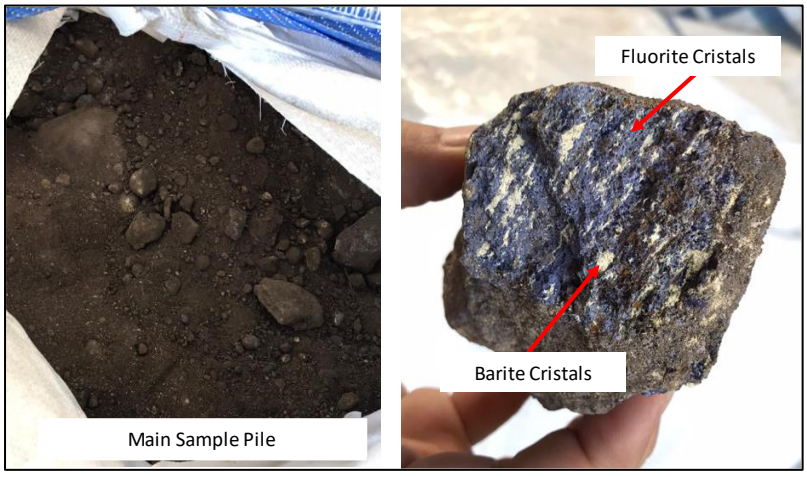

Figure 3.4: Barite and fluorite hand samples selected from the feed sample

Zeta potential measurement studies were carried out with a comprehensive and comparative experimental method. Zeta potential measurements were performed with different types of zeta meters (optical and laser), and results under different reagents and pH values were compared.

Prior to zeta potential measurements, barite and fluorite minerals were manually processed to obtain pure samples by selecting individual crystals. The crystals of barite (Figure 3.5a) and fluorite (Figure 3.6a) were carefully selected and their purities were validated with XRD measurements. Barite and fluorite crystalline samples prepared for testing are given in Figure 3.5b and Figure 3.6b, respectively.

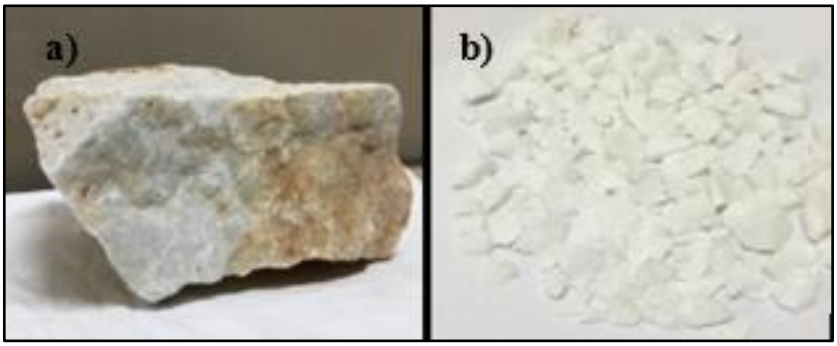

Figure 3.5: Barite for testing process: **a)** seleted barite **b)** crushed and selected pure barite

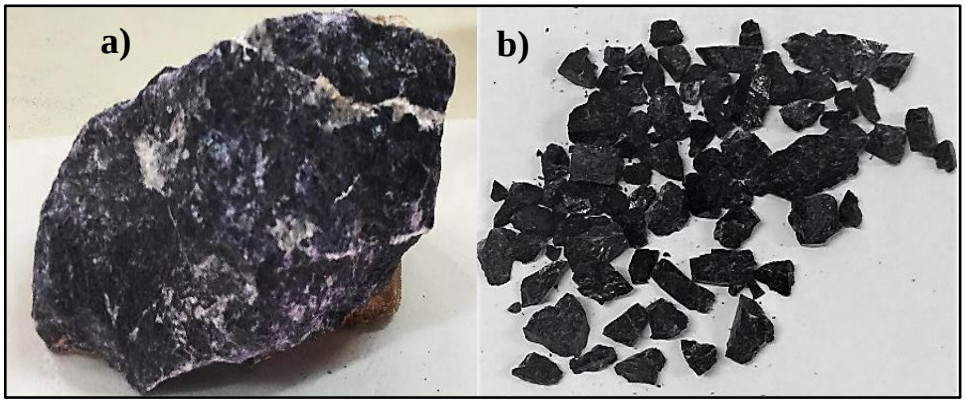

Figure 3.6: Fluorite for testing process: **a)** seleted fluorite **b)** crushed and selected pure flourite

Fluorite and barite samples were then ground using a Retsch RM 100 type mortar mill (Figure 3.7) for up to 1 hour until particle sizes less than -10 µm were reached. -10 µm particle size was selected following the zeta potential measurement instructions described in Section 2.1 for the reliability of bulk solutions. For each new grinding, the mortar was cleaned using quartz and compressed air to avoid contamination between minerals.

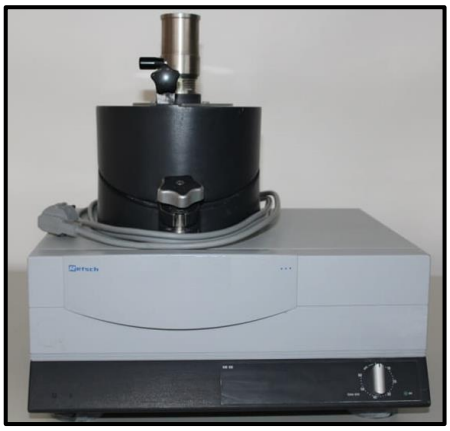

Figure 3.7: Mortar mill grinder – Retsch RM 100.

Ground samples of fluorite and barite were used to prepare the reference bulk samples. All tests were performed with each mineral of interest separately. Reference bulk samples were prepared with NaCl (10 g/L concentration) as the background electrolyte (Figure 3.8) and distilled water [43]. Each mixture was dispersed with a magnetic stirrer for 15 - 30 minutes.

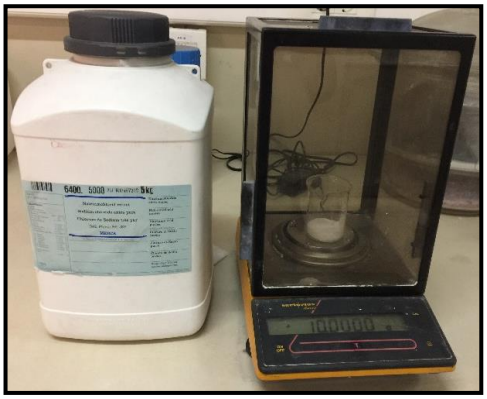

Figure 3.8: Background electrolyte (NaCl) used for bulk solutions

Figure 3.9: Bulk barite sample and bulk fluorite sample prepared for ZP testing

The samples prepared for taking ZP measurements were collected from the bulk samples (Figure 3.9) and adjusted to a new concentration of 0.1 g/L. These new diluted solutions were also used as references to prepare the subsequent samples with different types of collectors and depressants in varying dosages under varying pH values [1].

For barite measurements, samples were prepared with petroleum sulfonate and alkyl succinamate collectors (commercially named AERO 825 and AERO 845) (Figure 3.10a).

AERO 825 is an oil sulfonate collector with high viscosity. It requires special preparation, including vigorous agitation for dispersion and hot water in some cases for better dispersion. On the other hand, AERO 845 is an anionic collector (alkyl succinamate) that contains fatty acids and petroleum sulfonates. They are also soluble in water. For fluorite measurements, samples were prepared with tall oil fatty acid collectors with the commercial names AERO 704 and AERO 726 (Figure 3.10b). AERO 704 is a tall oil fatty acid with a specific acid value and with a rosin acid content. AERO 726 is a tall fatty acid containing surfactants and other chemically complex agents that generate more effective results. All the collectors were prepared with a 1% concentration [60]. The regulators of pH used due to the accessibility and the economic aspect were H_2SO_4 and Na_2CO_3 for acidic and alkaline pH respectively.

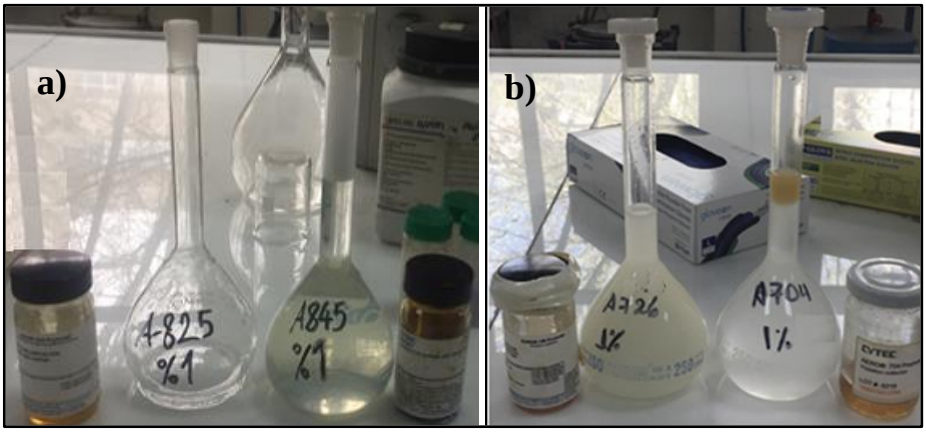

Figure 3.10: Collectors used for **a)** barite and **b)** fluorite

Prior to zeta potential measurements, the particle sizes were determined to verify whether the size was adequate for the specific equipment used. For particle size measurements, the zeta nano dynamic light scattering model (ZN) was used. It basically measures spherical diameter of the particles in a fluid based on the velocity profiles. This measure is used to determine the particle size via *Brownian Motion* principle [33]. For size measurement, firstly, bulk solutions without the addition of chemical agents were prepared. Secondly, an appropriate cell of quartz glass was selected to measure the particle size (Figure 3.11). They are standard square cells suitable for handling low and ultra-low volumes and for registering the particle movements through a period of time. This process was iterative over repeated runs to generate an acceptable collection of data.

Figure 3.11: Quartz glass cell for particle size measuring

Two different zeta potential measurement equipment were used with identical samples namely *Zeta Sizer* and *Zeta Nano*.

3.3.1. Zeta Potential Measurements with Zeta Sizer Equipment

Zeta sizer equipment (ZS) used in the first section of zeta potential measurements is shown in Figure 3.12. The equipment is located in Mining Engineering Department laboratories of Hacettepe University.

Figure 3.12: Zeta sizer machine

The measurements with the ZS instrument require a relatively simple process. It uses the electrophoretic method for measurements. The sample is placed between two different electrodes with a specific voltage. The resulting speed of particles is expected to be proportional to the zeta potential [33]. The steps of the experimental procedure for the ZS instrument are described as follows:

1. Each sample to be measured was placed inside the electrophoretic cell (Figure 3.13a).

2. The cell was sealed by inserting the electrodes, anode and cathode, at their respective ends.
3. The cell was placed under the stereoscopic microscope in the section of the holder with a mirror. It was also connected by the cables to its respective electrodes (Figure 3.13b).
4. The measurement of the specific conductance was taken by means of the energization of the connectors. It measures the appropriate tracking voltage for each sample.
5. The voltage was set, and scanning was initiated by selecting a particle within a configured area of the screen. Tracking data was recorded for measurements of zeta potential (Figure 3.13c – e).
6. At the end of the process, the electrodes were completely disconnected. They were cleaned correctly to remove any layer of oxide, before the next measurement.
7. The subsequent measurements were performed following the same steps, at varying pH values from 3 to 10. For each new measurement, Na_2CO_3 and H_2SO_4 were used as pH controllers. The samples were conditioned for 5 minutes at each pH value prior to each measurement.

Note: Fresh samples were prepared for acidic and basic zeta potential measurements to avoid zeta potential hysteresis. Repeatability in data collection was applied to generate a standard deviation and to ensure data reliability. Each sample was tested 2-3 times, and mean values were obtained.

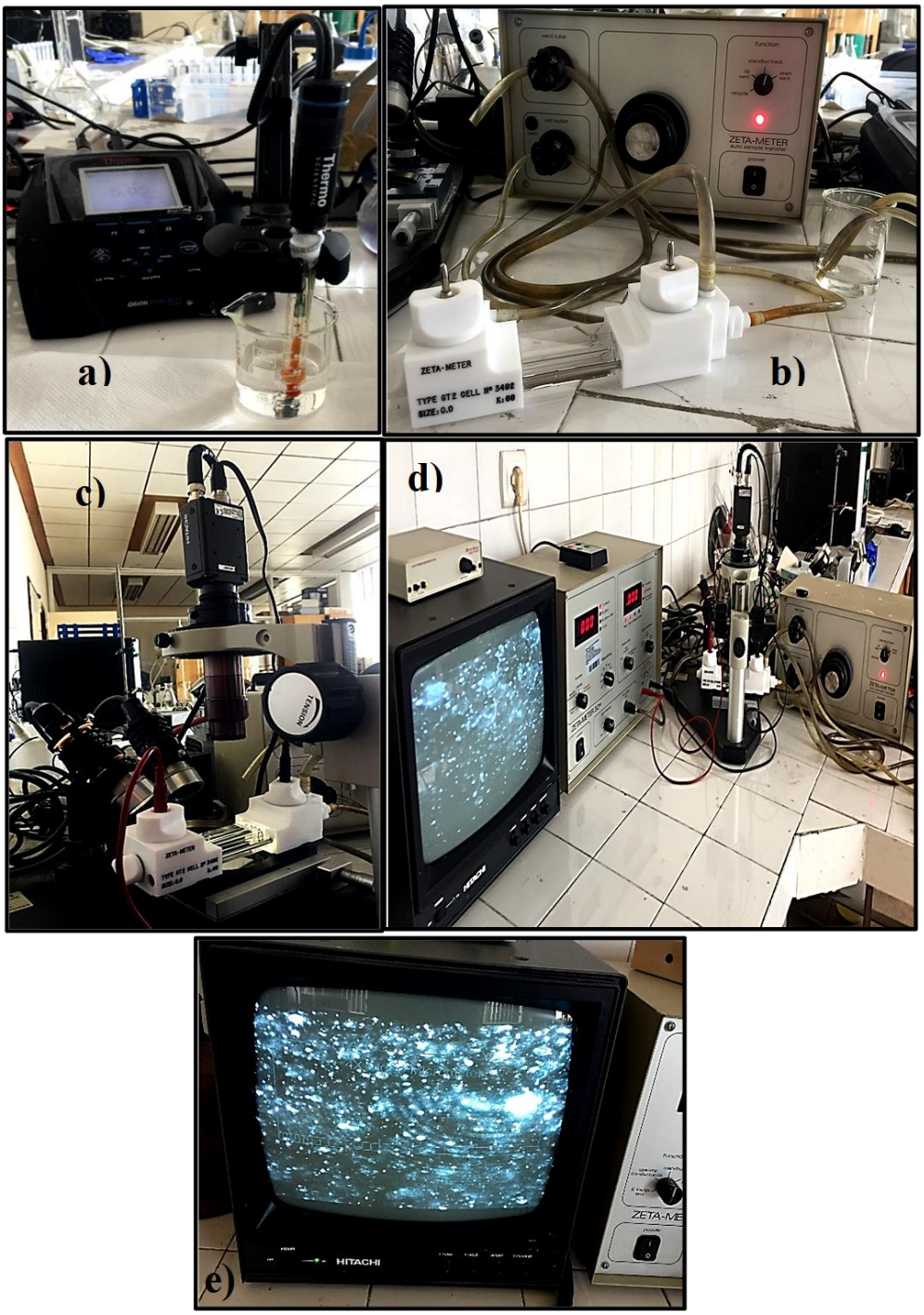

Figure 3.13: Zeta potential measurement process: **a)** the pH measurement **b)** the filling cell with the different samples to be tested **c)** the placement of the filled cell in the stereoscopic **d)** parameter adjustment for zeta potential measurements **e)** particle tracking for zeta potential measurements

3.3.2. Zeta Potential Measurements with Zeta Nano Equipment

Zeta nano (ZN) equipment used in the second section of zeta potential measurements is given in Figure 3.14. Zeta potential measurements are affected by parameters such as pH

variation, chemical agents (collectors, depressants, etc.), and background electrolytes. Additionally, they are highly dependent on the instrument and the technique used. The ZN is an optical-laser instrument incorporated with software and hardware. It uses a red laser to process a size range from 3.8 nm up to 100 µm. This laser is directed through folded capillary cells. The main objective is to measure the zeta potential, but it can also be applied to measure the size of the particles in a liquid medium (Figure 3.15) [33]. The instrument uses a combination of the techniques of ***Electrophoresis*** and ***Laser Doppler Velocimetry*** **(*Doppler Electrophoresis*).** It measures movement and velocity of the particle in an electric field.

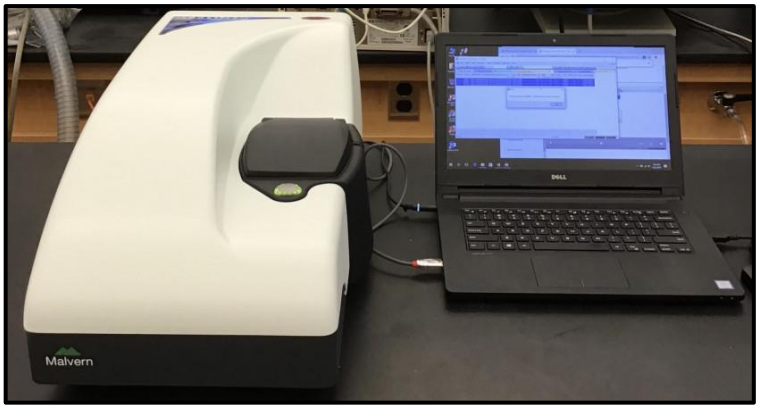

Figure 3.14: Zeta nano machine.

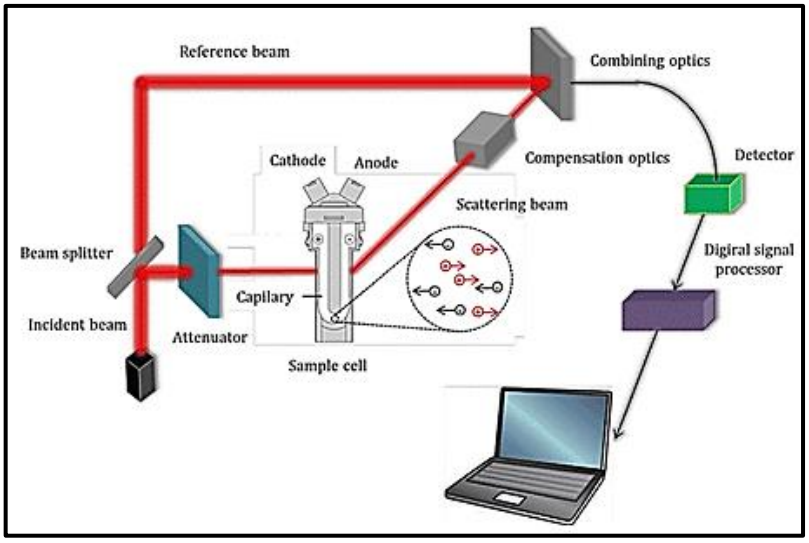

Figure 3.15: Zeta nano operating in a closed loop.

Identical samples and conditions were also tested with ZN. Prior to measurements, the characteristics for optical pre-alignment (Figure 3.16) were stored in the software and

saved to the SOP system (standard operating procedure). In ZN equipment, these characteristics were constantly improved, generating good repeatability and quality data.

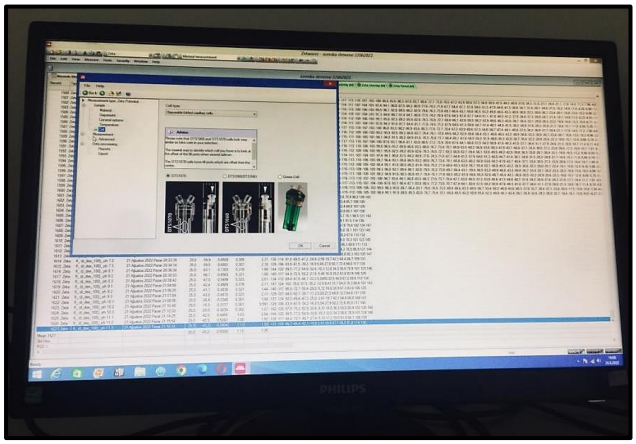

Figure 3.16: Selected parameter to SOP, required process of ZN measurement

Before placing the samples to be measured in ZN, a waiting period of 15 to 30 minutes should be considered to obtain the stabilization of the laser. During the time for laser stabilization, the ZN software was started and setting parameters were entered (Figure 3.17). They were selected optimum for each sample. The repeatability of the tests improved the result of zeta potential measurements.

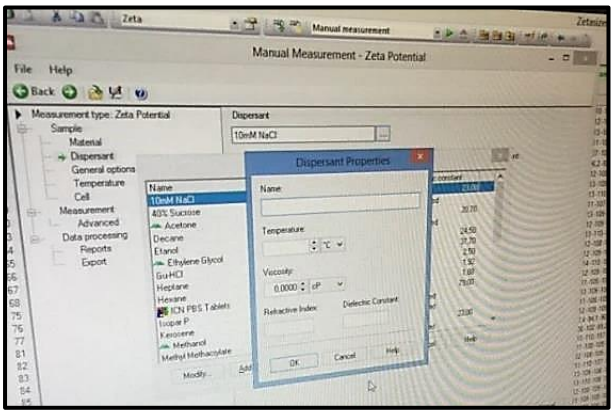

Figure 3.17: The setting parameters to both barite and fluorite measurements

For testing instructions, ZN instrument manual was taken into account. Once the SOP system was prepared, the most appropriate capillary cell was chosen according to the type of measurement (Figure 3.18a). The cell was filled with the sample prepared under the different pH values (from a pH 3 to a pH 11) (Figure 3.18b).

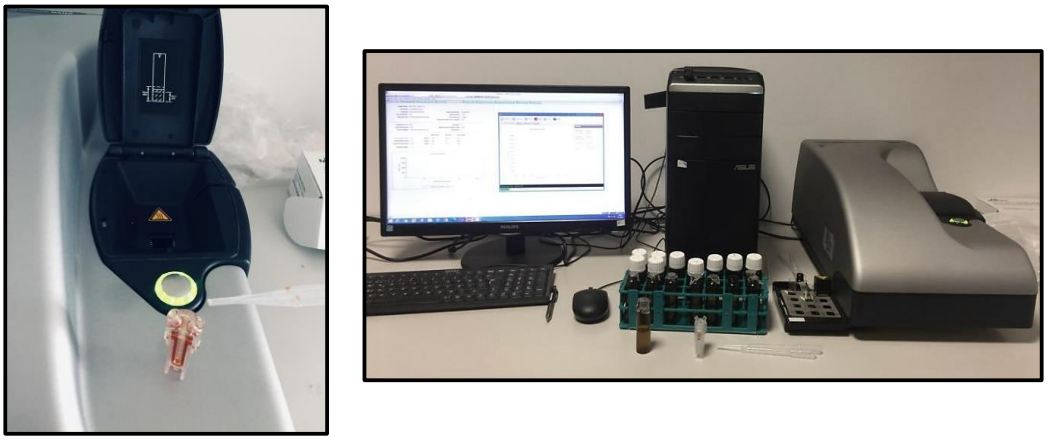

a) Capillary cell filling **b)** Solutions under different pH values

Figure 3.18: Sample preparation for ZN measurement

Finally, the capillary cell was inserted inside the instrument, and waited for the temperature to stabilize at about 25°C. The zeta potential measurement was started simply by activating the software. In the SOP system, 30 runs were established for each measurement and three different measurements were recorded for each pH variation. An important point was the constant review of the capillary cells to avoid corrosion.

3.4. Flotation Tests

In order to examine the flotation behavior of fluorite, barite, and REM in Beylikova, flotation tests were carried out to investigate the pH-dependent recovery and grade changes under different collector and depressant.

The samples used in flotation tests were ground to below -150 µm particle size with a laboratory scale ball mill. Grinding were determined via grinding calibration tests. After grinding, slime fractions below approx. 38 µm were removed by decantation prior to flotation tests.

Within the scope of flotation tests, independent rougher flotation tests were carried out at acidic, natural, and basic pH values with A-825, A-845, A-825 and A-845, A-726, and A-704 type collectors, which are also used in zeta potential measurements. The obtained rougher flotation concentrates and the tailings were directly sent to chemical analysis without being subjected to cleaning steps, and their recoveries were calculated in terms of target fluorite (CaF_2), barite ($BaSO_4$) and total REO (Ce, La, Nd, and Pr oxides) mineral contents.

Independent tests using A825, A845 and a mixture of A825 and A845, which primarily aim at enriching the barite mineral, were carried out at pH 5-5.5, natural pH (8-8.5) and pH 9.5, respectively. The conditions for these tests, which primarily aimed to examine the behavior of the barite mineral in its rougher stage, are presented in Table 3.2. In the specified conditions, the following three distinct collector regimes were investigated:

- The pH-dependent changes in the recovery and grade values of barite rougher flotation products in the tests performed with varying dosages of A825.
- The pH-dependent changes in the recovery and grade values of barite rougher flotation products in the tests performed with varying dosages of A845.
- The pH-dependent changes in the recovery and grade values of barite rougher flotation products in the tests performed with varying dosages of the combination of A825 and A845.

Table 3.2: Barite rougher flotation test conditions

Collector	**A825**	**A825**	**A825**	**A845**	**A845**	**A845**	**A825+ A845**	**A825 + A845**	**A825+ A845**
TEST	**T1**	**T2**	**T3**	**T4**	**T5**	**T6**	**T7**	**T8**	**T9**
Na_2CO_3(%10), g/t	2500	2500	2500	2500	2500	2500	2500	2500	2500
H_2SO_4, g/t	+			+			+		
Na_2SiO_2(%10), g/t	2500	2500	2500	2500	2500	2500	2500	2500	2500
$BaCl_2$(%5), g/t	1000	1000	1000	1000	1000	1000	1000	1000	1000
Queb.(%5), g/t	500	500	500	500	500	500	500	500	500
A825(%5), g/t	400	400	400				300	300	300
A845(%5), g/t				400	400	400	100	100	100
MIBC(µl), g/t	10	10	10	10	10	10	10	10	10
Condition, min	3	3	3	3	3	3	3	3	3
Flotation, sec	350	200		300	300				
pH	5-5.5	Natural (8-8.5)	9.5	5-5.5	Natural (8-8.5)	9.5	5-5.5	Natural (8-8.5)	9.5

Following, independent tests incorporating A726 and A704 for fluorite rougher flotations were performed at pH 5-5.5, natural pH 8-8.5 and pH 9.5, respectively. Barite coarse flotation was performed before each fluorite flotation test. Similar to barite flotation tests, fluorite flotation tests were aimed at examining the behavior of fluorite, barite, and total REO minerals. The greatest rougher tail of barite flotation tests was transferred to fluorite rougher flotation in all fluorite flotation tests. For this purpose, the barite rougher flotation condition in which the greatest results were obtained when A825 and A845 were used together was applied prior to each fluorite flotation test. The conditions applied for fluorite flotations are presented in Table 3.3.

Table 3.3: Fluorite rougher flotation test conditions

	Joint Barite Flotation Test	**Fluorite Rougher**	**Fluorite Rougher**	**Fluorite Rougher**	**Fluorite Rougher**	**Fluorite Rougher**	**Fluorite Rougher**
TEST		T 1	T 2	T 3	T 4	T 5	T 6
Separating Reagent		**A726**	**A726**	**A726**	**A704**	**A704**	**A704**
Na_2CO_3(%10), g/t	2500						
H_2SO_4, g/t		+			+		
Na_2SiO_2(%10), g/t	2500						
$BaCl_2$(%5), g/t	1000						
Queb. (%5), g/t	500						
A825(%5), g/t	300						
A845(%5), g/t	100						
A726(%5), g/t		100	100	100			
A704(%5), g/t					100	100	100
MIBC(µl), g/t	10						
Condition, min	3						
Flotation, sec	200						
Ph	9.5	5-5.5	Natural (8-8.5)	9.5	5-5.5	Natural (8-8.5)	9.5

In the specified conditions, the following two distinct collector regimes were investigated:

- The pH-dependent changes of the recovery and grade values in fluorite rougher flotation products in the tests performed with A726.
- The pH-dependent changes of the recovery and grade values in fluorite rougher flotation products in the tests were performed with A704.

Following the completion of the tests under the specified conditions, all products were sent for chemical analysis, and the results obtained under different conditions were discussed.

4. RESULTS AND DISCUSSION

4.1. Mineralogical Analysis Results

The mineral definitions determined with the modal mineralogical analysis of the -150+25 µm feed sample fraction are given in Table 4.1. According to modal mineralogical analyses, samples used in flotation tests are mainly composed of 37.15% barite, 43.06% fluorite, 6.16% calcite, 0.6% quartz, and 6.97% total REMs. Relatively low percentages of iron oxides, feldspar, hollandite, mica minerals, K-Mg silicates, Si-Al clays, siderite, etc. minerals were also observed. Noteworthy REMs are bastnaesite (3.71%), monazite (2.35%), cerianite (0.32%), and lateritic REMs (0.58%), decayed in clay and barite matrix.

REMs in the lateritic fraction refer to weathered structures mixed with clay and other minerals. It was not possible to identify REMs in this state. The elemental compositions of these structures differ on the surface of the section, and mineral detection is not possible due to the randomly weathered structure. Two exemplary EDS (Energy-dispersive X-ray spectroscopy) spectra regarding the uncertainty of these structures are also given in Figure 4.1 and Figure 4.2. In EDS given in Figure 4.1, approx. 25% Mn, approx. 15% La, and approx. 19% Ce by weight were detected in the lateritic structure. On the other hand, within the EDS example given in Figure 4.2, approx. 14% Fe, 3% Mn, approx. 16% La and approx.18% Ce by weight were detected in the lateritic structure.

Table 4.1: Feed sample modal mineralogical analysis results

Minerals	**%Weight**	**Minerals**	**%Weight**
Pyrite	0.06	K-Mg Silicate (Tainiolite)	1.26
Sphalerite	0.03	Epidote	0.21
Barite	37.15	Si-Al Clays	0.51
Fe Oxi/Hydroxi	0.63	Calcite	6.16
Mn Hydroxide	0.13	Siderite	0.45
Ilmenite	0.03	Bastnaesite (La-Ce)	3.71
Rutile	0.03	Monazite	2.35
Cerianite (inc. Ce hydrox)	0.32	Apatite	0.00
Hollandite	1.68	Fluorite	43.06
Quartz	0.56	Lateritic REE (Altered mixed)	0.39
Feldspar	0.11	Lateritic REE mixed with Mn Hydroxide	0.19
Mica	0.27	Others	0.71
Sum: 100			

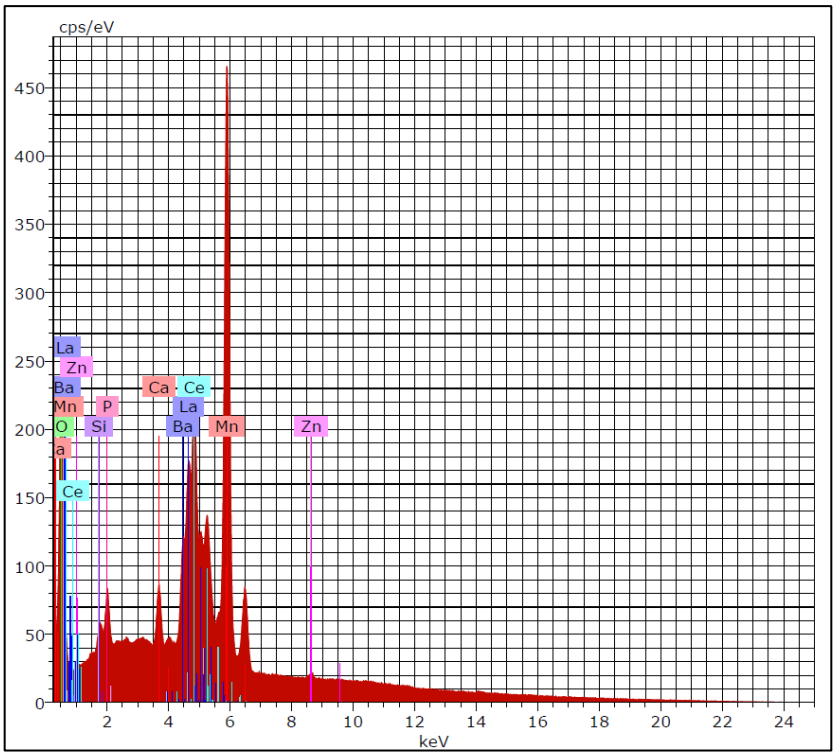

Figure 4.1: Sample EDS spectrum for a lateritic rare earth element composition containing high Mn (manganese).

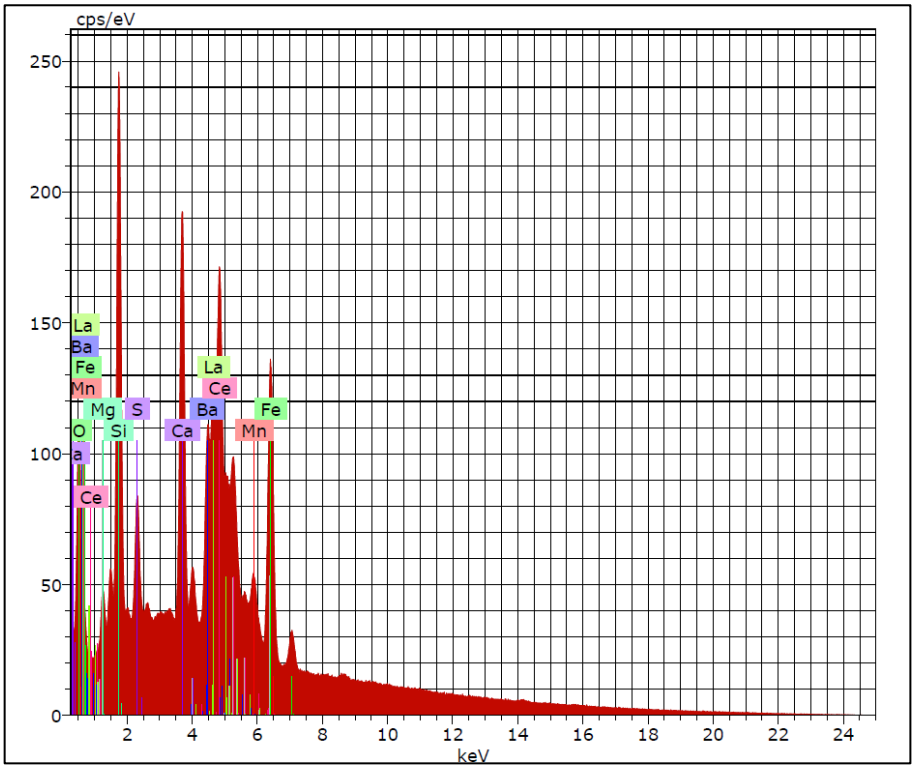

Figure 4.2: A random sample EDS spectrum for a lateritic rare earth element composition containing high Fe and Mn.

The particle size distributions of fluorite, barite, bastnaesite, monazite, and cerianite in the related material were determined separately and presented in Figure 4.3. Fluorite and barite mineral grains were observed in all sizes. While bastnaesite and monazite can be observed even with sizes around 75 µm, they are mostly 20-25 µm in size. Cerianite, on the other hand, consists of grains below 38 µm.

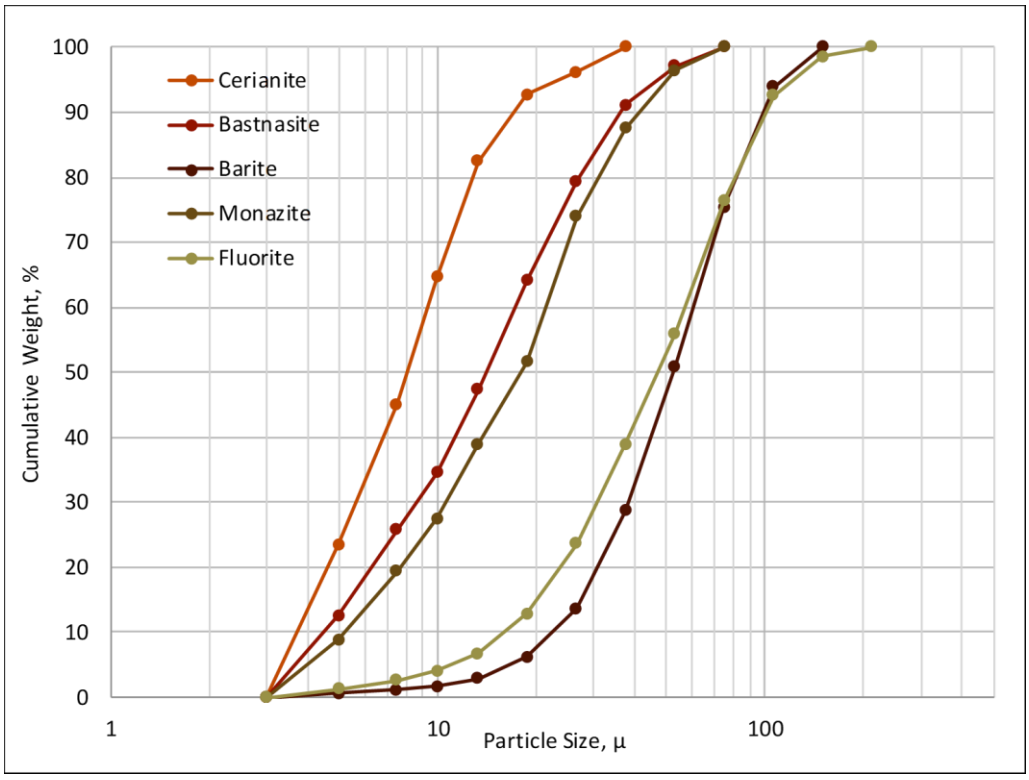

Figure 4.3: Particle size distributions of critical contents in the feed sample.

Liberation and association analysis results of -150+25 µm feed sample are given in Table 4.2. When Table 4.2 was examined, it was seen that barite and fluorite were in the form of free particles at levels of 77.1% and 78.6%, respectively. They also showed binary or ternary locking with other minerals at a level of 20-23% by weight. These liberation rates seem to be sufficient and at the limit value for the first stage fluorite and barite enrichment processes to be carried out with a particle size below 150 µm. Naturally, it is expected that liberation will increase through finer size fractions. REMs, on the other hand, seem to have very low liberation at this size. Free particle amounts of monazite, bastnaesite, and cerianite at -150+25 µm feed remain at the levels of 24.4%, 17% and 1.7%, respectively.

Table 4.2: -150+25 µm feed sample liberation-association analysis results

Barite Liberation, Weight %										
Locked					**Associated**				**Free**	
<= 10%	<= 20%	<= 30%	<=40 %	<=50 %	<=60 %	<=70 %	<=80 %	<=90 %	<100 %	100 %
1.0	0.8	0.9	1.0	0.9	1.5	3.1	4.8	8.8	43.7	33.3
Cerianite Liberation, Weight %										
Locked					**Associated**				**Free**	
<= 10%	<= 20%	<= 30%	<=40 %	<=50 %	<=60 %	<=70 %	<=80 %	<=90 %	<100 %	100 %
22.7	30.8	10.8	4.2	8.6	5.7	6.0	2.5	7.0	1.7	0.0
Bastnaesite Liberation, Weight %										
Locked					**Associated**				**Free**	
<= 10%	<= 20%	<= 30%	<=40 %	<=50 %	<=60 %	<=70 %	<=80 %	<=90 %	<100 %	100 %
14.8	8.0	11.4	8.3	5.9	6.5	8.7	7.9	11.6	13.5	3.5
Monazite Liberation, Weight %										
Locked					**Associated**				**Free**	
<= 10%	<= 20%	<= 30%	<=40 %	<=50 %	<=60 %	<=70 %	<=80 %	<=90 %	<100 %	100 %
14.7	7.9	8.8	6.0	3.6	6.6	8.1	9.6	10.3	22.4	2.0
Fluorite Liberation, Weight %										
Locked					**Associated**				**Free**	
<= 10%	<= 20%	<= 30%	<=40 %	<=50 %	<=60 %	<=70 %	<=80 %	<=90 %	<100 %	100 %
0.8	0.8	0.9	0.9	0.9	1.4	1.8	3.2	10.7	59.3	19.3

Additionally, detailed phase analyses revealed important results. The points that draw attention in phase analyses are that almost 50% of bastnaesite and 33.7% of monazite are in ternary locking structures. Cerianite, on the other hand, is approximately 95% ternary locking. In the feed, it is seen that barite is mainly binary locked with fluorite (9.41%). Similarly, fluorite and barite are seen to be free at a level close to 80% at this size. Barite is locked primarily with fluorite, while fluorite is mostly associated with calcite (12.1%) and cerianite (5.5%). When REMs and barite are examined separately, it is seen that rare earths are mostly locked with barite or have a binary locked with each other. BSE images (backscattered electron images) supporting these findings are also given in Figure 4.4. Figure 4.4 shows the associated of barite and fluorite, and bastnaesite, which is locked to barite in regions where bastnaesite is degraded.

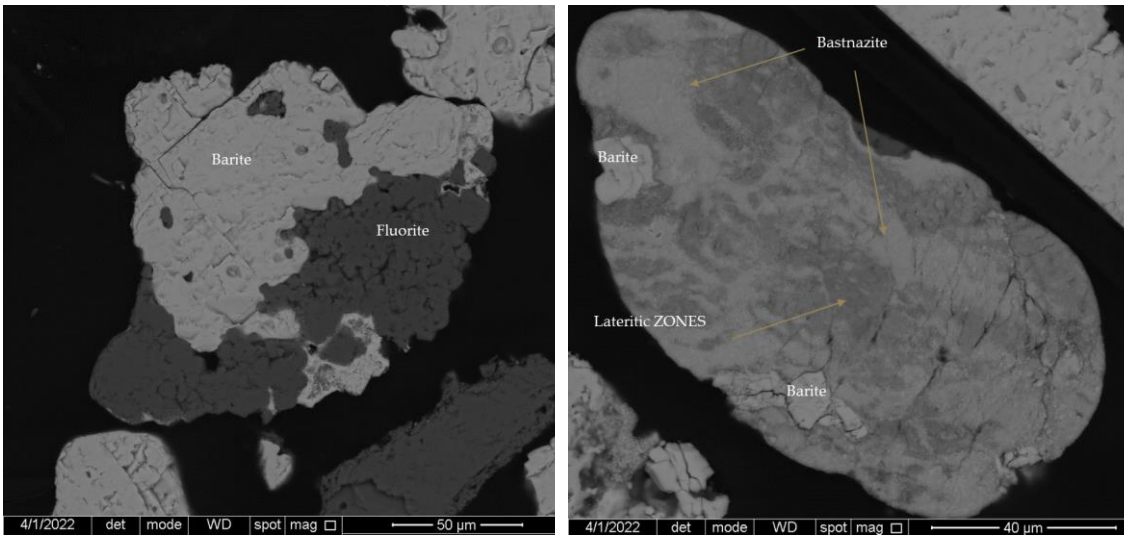

Figure 4.4: BSE images of barite-fluorite associations, and barite-bastnasite association along with lateritic weathering zones in the feed sample

4.2. Chemical Analysis Results of Feed Sample

In addition to MLA analyses, a representative feed sample (without removing -25 µm fraction) was also shipped to external laboratories to determine elemental contents (Table 4.3). It is seen that the Beylikova ore feed contains 53.42% CaF_2, 26.64% $BaSO_4$, 2.62% CeO_2, 2.33% La_2O_3, 0.36% Nd_2O_3 and 560.99 ppm Th.

Table 4.3: Chemical analyses results of feed sample

Ce	**g/t**	**21300**	**CaO**	**%**	**38.6**
Dy	g/t	34	**BaO**	%	17.5
Er	g/t	18.4	**SiO2**	%	2.83
Eu	g/t	37.4	**Fe2O3**	%	2.2
Gd	g/t	84.1	**MnO**	%	1.05
Ho	g/t	6.1	**Al2O3**	%	0.45
La	g/t	19900	**MgO**	%	0.38
Lu	g/t	2	**K2O**	%	0.17
Nd	g/t	3080	**Na2O**	%	0.04
Pr	g/t	1390	**TiO2**	%	0.09
Sm	g/t	187	**P2O5**	%	0.8
Tb	g/t	6.7	**Cr2O3**	%	< 0.01
Th	g/t	493	**V2O5**	%	0.03
Tm	g/t	2.8	**F**	%	26
U	g/t	143	**S**	%	4.36
Yb	g/t	16.5			
LOI	%	3.88			

4.3.Grinding Calibration Tests Prior to Flotation

Within the scope of grinding calibration tests, a laboratory scale ball mill was used in accordance with the Bond mill standards. Grinding tests were carried out with approximately 2 kg of samples at 55-60% solids ratio. Representative feed samples crushed under 3.35 mm were used in grinding calibration tests. The material fill rate was kept between 80-100%, and the ball filling ratio was kept between 40-45%. All tests were carried out at these optimum parameters, and the particle size distributions of the products after 50 min, 30 min, 10 min, 20 min, and 5 min grinding times were measured by sieve analysis.

The product particle size distributions obtained are given in Figure 4.5. When Figure 4.5 is examined, it is seen that 98% of the material can be ground below 150 µm after 20 minutes of grinding. It is not possible to provide sufficient liberation after 10 minutes, at which time the amount of material passing 150 µm size is about 85%. After 30 minutes of grinding, there is no significant increase in cumulative undersize. When the grinding time is increased to 50 minutes, the fraction under 53 µm increases to 95% (overgrinding).

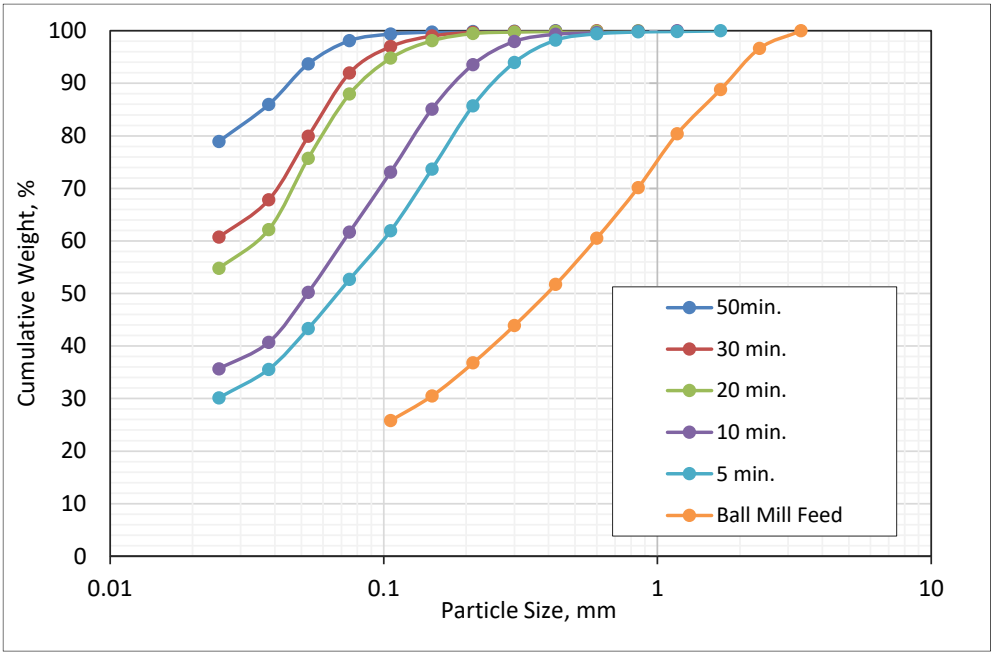

Figure Error! Use the Home tab to apply to the text that you want to appear here.**.5:** Comparison of the particle size distributions obtained after 50 min, 30 min, 10 min, 20 min and 5 min grinding times with -3.35 mm ore.

4.4. Zeta Potential Analysis

4.4.1. XRD Analysis of Zeta Potential Measurement Samples

Prior to taking zeta potential measurements, barite and fluorite minerals were manually processed to obtain pure samples by selecting individual crystals. The purities of these carefully selected crystals of barite and fluorite were validated with XRD measurements. Results of the XRD validation tests for barite and fluorite samples used in zeta potential measurements are given in Figure 4.6 and Figure 4.7, respectively. XRD results of both minerals showed only characteristic peaks for pure barite and fluorite crystals, conforming to the zeta measurement methodology route.

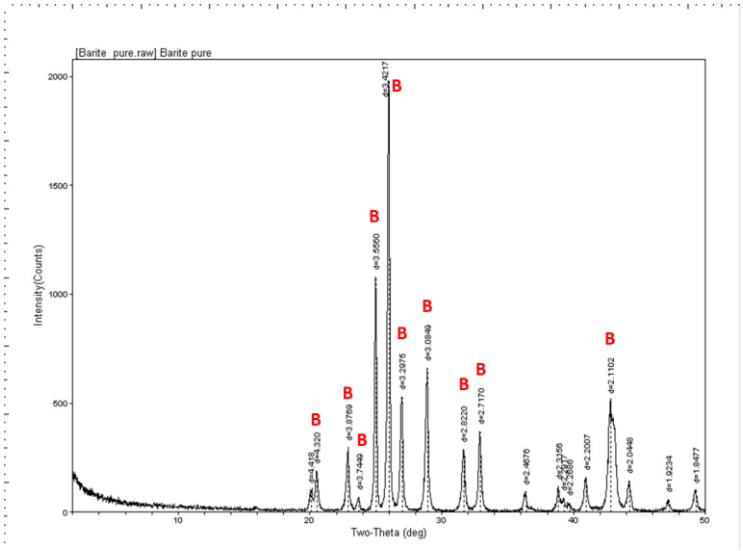

Figure 4.6: Barite sample XRD spectrum (**B**: barite)

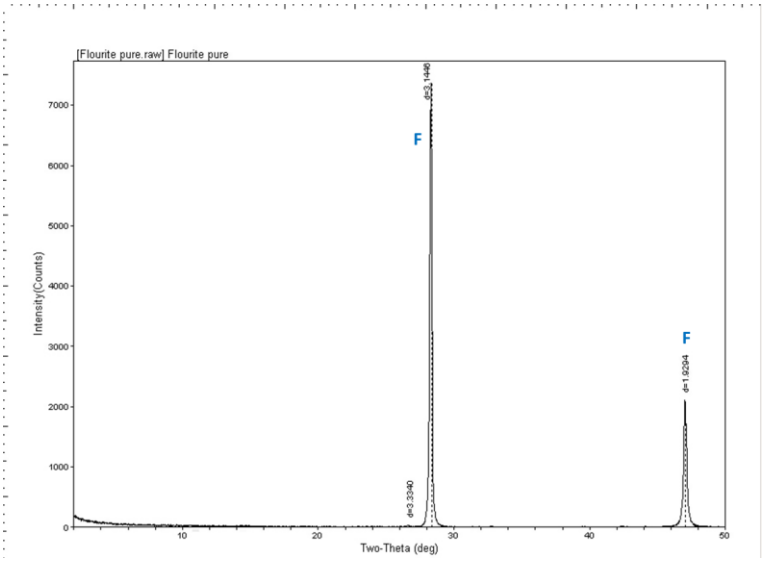

Figure 4.7: Fluorite sample XRD spectrum (**F**: fluorite)

4.4.2. Particle Size Measurements Prior to Zeta Potential Tests

The results of fluorite and barite average sizes measured with zeta-meters are given in Figure 4.8 and Figure 4.9, respectively. The average size measurements were made to ensure that the particles are within the standards required for zeta potential equipment. The results confirming their use in the test procedure are also presented in Table 4.4.

Table 4.4: Particle size of fluorite and barite

Particle Size			
Mineral	**D (nm)**	**D_ avg**	**T (°C)**
Fluorite	924.70	0.88	25.00
	834.80		
Barite	1548.00	1.65	25.00
	1760.00		

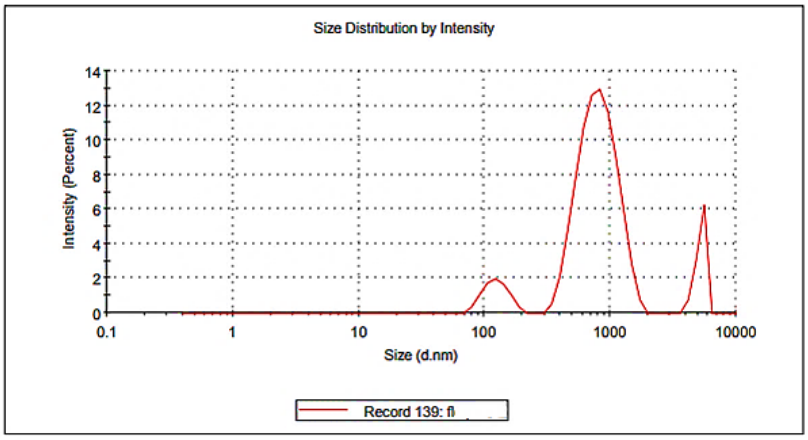

Figure 4.8: Result of fluorite average size particles

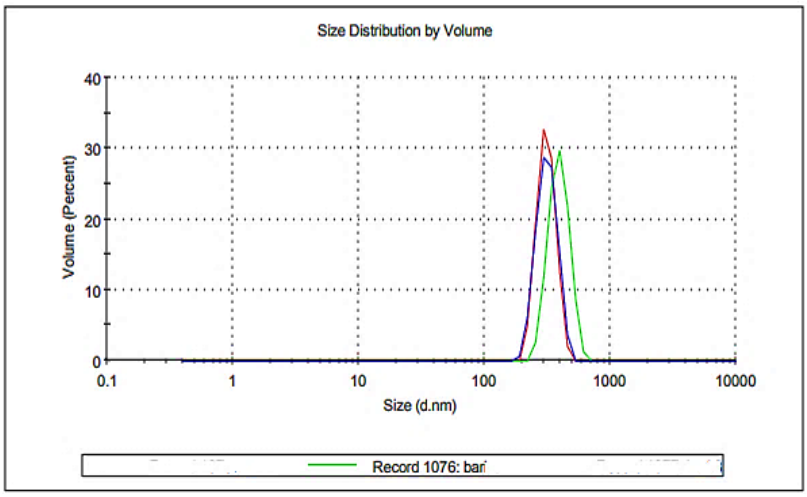

Figure 4.9: Result of barite average size particles

4.4.3. Zeta Potential of Pure Barite

Figure 4.10 illustrates the results of the average measurements of the zeta potential of pure barite as a function of pH. NaCl is used as a background electrolyte in the bulk solution. As described in Section 3.3, zeta measurements were acquired with the two distinct instruments (ZN and ZS) simultaneously. The pH variant was controlled with Na_2CO_3 and H_2SO_4. Barium and sulfate ions are considered the main determining ions in barite due to its composition. However, Anderson and Taylor [1] argue that in both the alkaline and acidic regions, the ions tend to produce subspecies that give a wide range of variation to the ZP response. Also, these results have a wide dependence on the pH value.

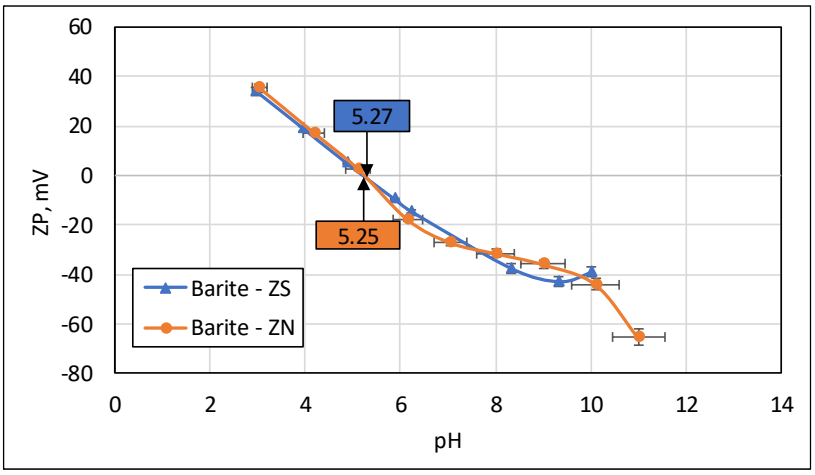

Figure 4.10: Zeta potential of barite in presence NaCl as background electrolyte under different pH values.

In the case of the zeta potential measure of barite with ZN, results exhibit a positive charge response close to 40 mV at low pH values. For the alkaline region, results mostly show low charges exceeding – 60 mV. According to the previous findings of Hang et al. [26], a low charge could be due to the absorption of H^+ on the particle. The importance of size and shape should be noted, considering that with smaller particles, a trend toward a higher potential charge is possible. In terms of the isoelectric point (IEP), ZN presents a pH value equal to 5.25, while ZS shows a pH value of 5.27. The variation between results is very low; they are practically similar. Consequently, the achieved values are consistent with the previously reported values, which are within the range of 4.5 - 7 (Section 2). According to the research presented by Anderson and Taylor [1], if the IEP is found in an acid region, it could be due to a decrement in the barium ion concentration in the

mineral. Additionally, NaCl is considered a good background reagent because it does not produce any absorption properties.

4.4.4. Zeta Potential of Pure Fluorite

Fluorite is one of the highly prevalent minerals associated with REOs. It is important to understand how to change its surface electrical tendency. Due to its composition of calcium and fluorite ions, fluorite is theoretically considered to be slightly dependent on pH values. Figure 4.11 shows the results of the zeta potential of pure purple fluorite as a function of the pH variant, which is controlled by Na_2CO_3 and H_2SO_4. Similar to all zeta potential measurements, the ZS and ZN instruments were used with identical samples for comparison.

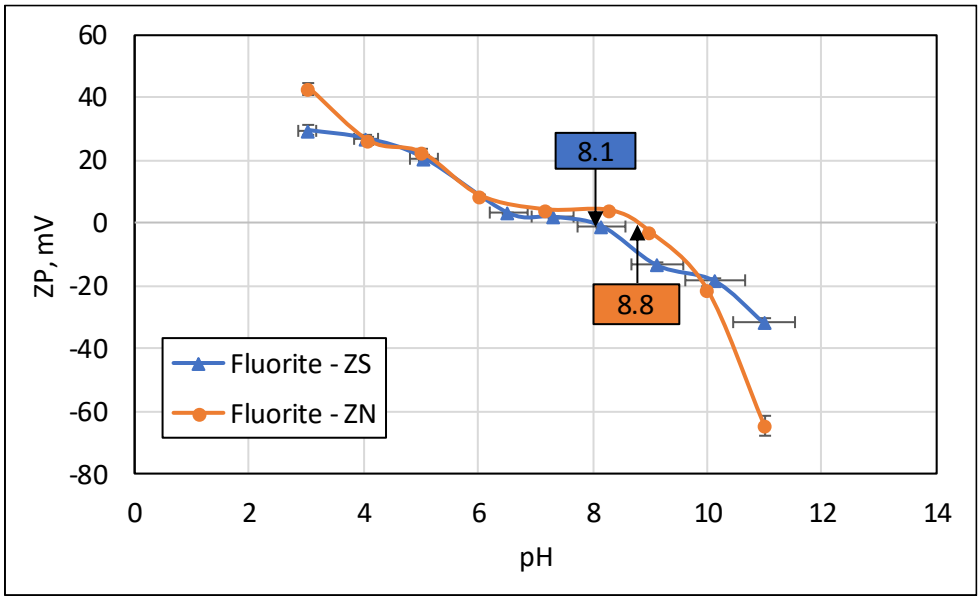

Figure 4.11: Zeta potential of fluorite in presence NaCl as background electrolyte and pH variation.

The result of the measurements with ZN showed that:

- For the most acidic part, it has a positive electrical charge that is close to 40 mV.
- And for the alkaline part with a pH value above 8, it exhibits a negative charge result, reaching a value above -60 mV in the most alkaline pH.

On the other hand, the resulting measurements with the ZS (blue curve) exhibit quite a similar trend, especially for positive charge values. Small differences were observed between the points with the most acidic and alkaline zones. Thus, measurements differ

by a value of 10 mV for ZN with respect to the positive charge, while the negative charge difference is around -30 mV. Additionally, it can be observed that in a pH range of 6 to 8, the electric charge exhibits an almost illegible decrease in electric potential. According to the results presented by Miller et al. and Miller and Hiskey [50][32], the change in pH from the acid region to the alkaline region generates re-modification of the determining ions varying between (1/2 F-, Ca^{++}, HF^{2-}). They also found that fluorite without a carbonatized surface has a tendency to exhibit high values of electrical potential. Figure 4.11 shows how the electric potential tends to decrease above the pH value of 8, considering that the resulting electric potential could be affected by partial superficial carbonatization [71][61][50].

Furthermore, several investigations demonstrate [7][49] that fluorite has distinct surface electrical characteristics according to its origin and its color characteristic, which generate difficulties in controlling the pH in the solution. Zheng et al. [75] presented the effect of fluorite species and their color characteristics on zeta potential. According to them, fluorite with a purple color characteristic tends to generate a low zeta potential, justifying the relatively low zeta potential measurements.

The presented isoelectric points with ZN and ZS equipment are 8.8 and 8.1, respectively, as shown in Figure 4.11. Despite the fact that they have the same base solution, a small variation between these results was observed. The difference in the results is most likely due to the instrument used in the measurements. The point of zero charge for various minerals cannot be explicitly determined, and it is expected to observe a wide range of possible IEPs, considering the fluorite minerals in this group. Thus, IEP results in a minimum pH value of 6.2 and a maximum value of 10.6, as detailed in Section 2.1. Therefore, the two results obtained are considered to be within the acceptable range.

4.4.5. Zeta Potential of Barite Mineral with Agents

Measures of zeta potential under different chemical agents such as collectors and depressors were tested using zeta nano. Due to its accuracy and data quality, these characterizes of the ZN are due to constantly updating its software with every measurement taken.

4.4.5.1. Zeta Potential of Barite Mineral with Collectors

4.4.5.1.1. Barite Zeta Potential with Petroleum Sulfonate (AERO 825) Collector

Figure 4.12 show the results of the zeta potential measurements of barite with the addition of petroleum sulfonate collector under different dosages of 50, 100, and 150 g/t., the petroleum sulfonate collector is known commercially as AERO 825. In the Figure 4.12, a great impact of the collector on the surface of the barite mineral can be observed. Electric charge along all the curves exhibits a decrease in magnitude with the variation of pH. It is especially decreasing in the acid part (pH 3) by around -40 mV at highest dosage of 150 g/t. In the alkyne part, which already showed a negative charge in the absence of a collector, there is also a tendency to decrease, but this decrease becomes less legible.

The AERO 825 is considered an effective collector for barite and an increase in its dosage would increase its effectiveness (Section 2). Nonetheless, this cannot be observed clearly in Figures 4.12. With the low dosage variations, the zeta potential responses differ poorly from each other. It would suggest that to find a true change in the zeta potential, the dosage increment should be quite high as suggested by Kecir and Kecir [72], who suggest that a dose of 2000 g/t would achieve a positive recovery reaching up to 95(%). But considering the complex ore natures, price and selectivity of AERO 825, these extreme dosages are rarely applied.

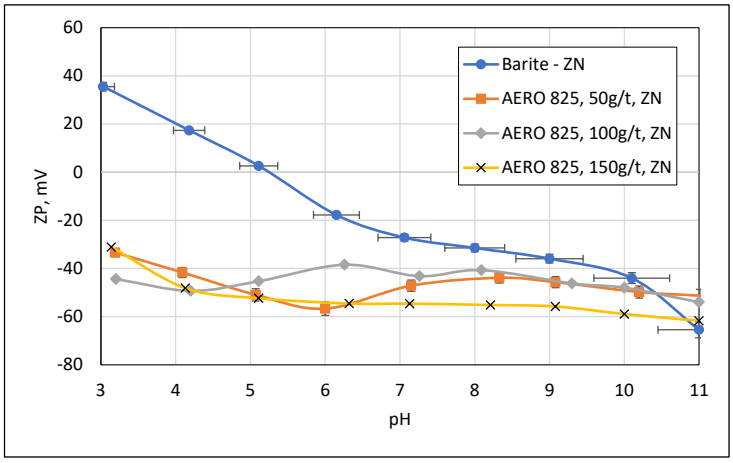

Figure 4.12: Zeta potential of barite measured with ZN in the presence of A825 with variation in dosage

4.4.5.1.2. Barite Zeta Potential with Alkyl Succinamate (AERO 845) Collector

Figure 4.13 shows the results of the zeta potential measurements of barite with the addition of alkyl succinamate collector under different dosages of 50, 100 and 150 g/t.

The alkyl succinamate collector, commercially known as AERO 845, is classified as anionic collector with great solubility, and low dosage requirement characteristics in comparison with petroleum sulfonates collectors, but they are noticeably expensive. In Figure 4.13, a great influence is observed with the addition of the collector. Since, in all the resulting ZP curves, the decrease in electric charges is evident. The resulting curves with the ZN show that the decrease of electrical charge is observed in acidic part, and it becomes more evident with increasing dosages. While for the alkaline part, it is observed that the shifting tendency of the curves is almost imperceptible compared to the curve in the absence of a collector. And for the most alkaline part above a pH of 9, the electric charge has increased.

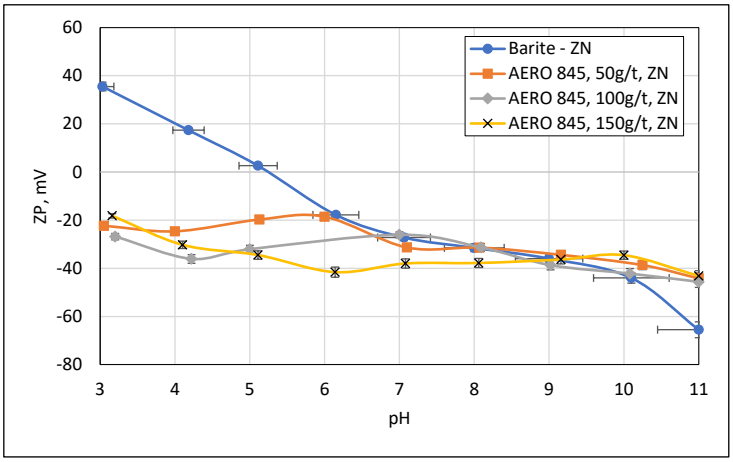

Figure 4.13: Zeta potential of barite measured with ZN in the presence of A845 with variation in dosage.

In general, the ZP measurements are affected by the pH value. AERO845 collector is more effective in the acidic region, especially in the range between 5 and 6. Through the acidic part, there is a possibility that the succinamate molecules do not ionize and cannot adhere effectively to the surface, reducing the collector efficiency. On the other side, at higher pH values, it could be naturally a less efficient.

4.4.5.2. Zeta Potential of Barite Mineral with Depressant Agents

4.4.5.2.1. Barite with Sodium Silicate (Na_2SiO_3) Depressant

Figure 4.14 shows the barite zeta potential curves after adding 1000 g/t and 1500 g/t sodium silicate (Na_2SiO_3) as a depressant using ZN instrument. Sodium silicate is a highly soluble inorganic salt and is made up of metasilicate and disilicate. It is an alkaline material with the possibility of affecting the reagents and raising the alkalinity of the solution. The presence of these metasilicates generally depresses barite, especially in the presence of anionic agents, but exceptions have been found with sulfonating agents. The depressant action is conditioned by pH value and concentration.

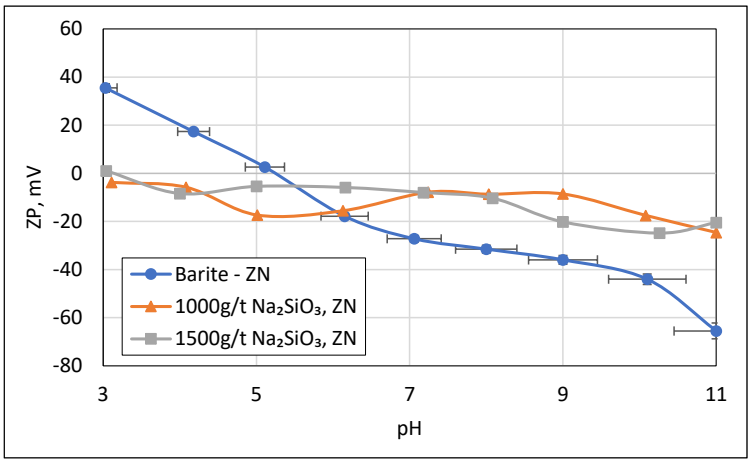

Figure 4.14: Zeta potential of barite measured with ZN in the presence of sodium silicate depressant with variation in dosage.

Figure 4.14 shows a clear effect on the zeta potential and a shift tendency to both increase and decrease in the electric charge depending on the variation of the pH. There is also a variation in response to different dosages. However, some results are discarded because there could have been both internal and external errors during the test, as well as a stability ZP and an ambiguous response trend, particularly at 1000 g/t dose. The resulting curve with a dosage of 1500 g/t shows a better overall trend. The alteration of the electric charge is mainly attributed to reactions of the particles on the surface. This might be due to the agent reacting with the barium ions to generate a more stable and insoluble molecule. In addition, reducing the likelihood of sedimentation, this can also increase their zeta potential.

4.4.5.2.2. Barite with Quebracho Depressant

Figure 4.15 shows the ZP curves after adding 1000 g/t and 1500 g/t quebracho as depressant, using ZN instrument. Quebracho is an organic polymer known for its tannin contents. It would act as depressants by forming bonds on the particles and generating water repellence (hydrophobicity). The dosage should be taken into account as it is likely to have a negative effect on recovery and increase the hardness of the water. Tannins are known to have a high affinity for metals, and they can form complex compounds. So, the tannins bind with the barite and can alter its surface charge. Consequently, they have an eminent effect on the zeta potential curve [53] [72].

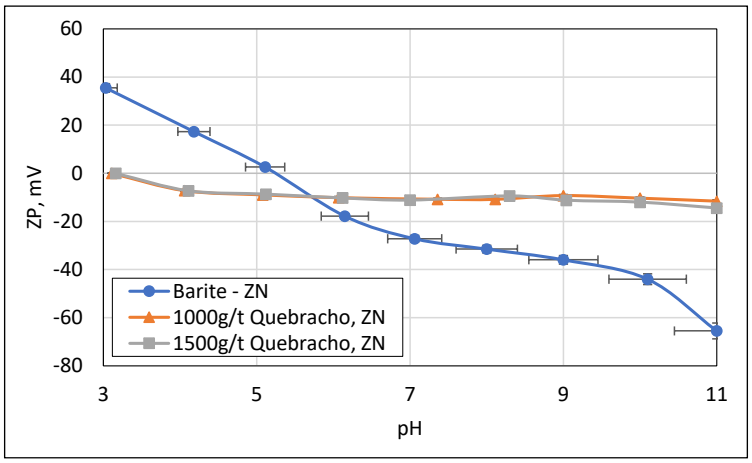

Figure 4.15: Zeta potential of barite measured with ZN in the presence of Quebracho depressant with variation in dosage.

Figure 4.15 shows how curves are affected with quebracho presence. They tend to both increase and decrease the potential charge, taking the IEP as a reference. It has been clearly observed how the pH of the system influences its responses. For high pH values above 5, the barite tends to be charged positively, while for low pH values, it tends to decrease the potential charge. It should be noted that with the two dosages tested, the trend of the curves is similar. Also, according to the previous discussions (Section 2), the solution can be altered by this depressant agent. For example, with the addition of more anionic agents (negative charges), the solution could respond by increasing the negative charge.

4.4.6. Zeta Potential of Fluorite Minerals with Chemical Agents

Measures of zeta potential under different chemical agents such as collectors and depressors were tested using zeta nano. Due to its accuracy and data quality, these characterizes of the ZN are due to constantly updating its software with every measurement taken.

4.4.6.1.Fluorite Minerals with Collectors

4.4.6.1.1. Fluorite Zeta Potential with Tall Oil Fatty Acid (A704) Collector

Figures 4.16 shows the results of the fluorite zeta potential measurements in the presence of 50, 100, and 150 g/t tall oil fatty acid as collector which is commercially called AERO 704 or TOFA.

A great influence of different dosages is observed since the electric charge on all ZP curves under different dosages tends to decrease. The major tendency is observed in more acid pH values, especially with the pH of 3, in this value a decrease of more than 40 mV with respect to ZP of the pure fluorite is exhibited. For the negative charges observed with pure mineral, the trend also decreases at alkaline pH values, but is almost imperceptible at values of 10 and 11. However, this tendency does not continue at higher doses, there is a constant decrease throughout the all curve.

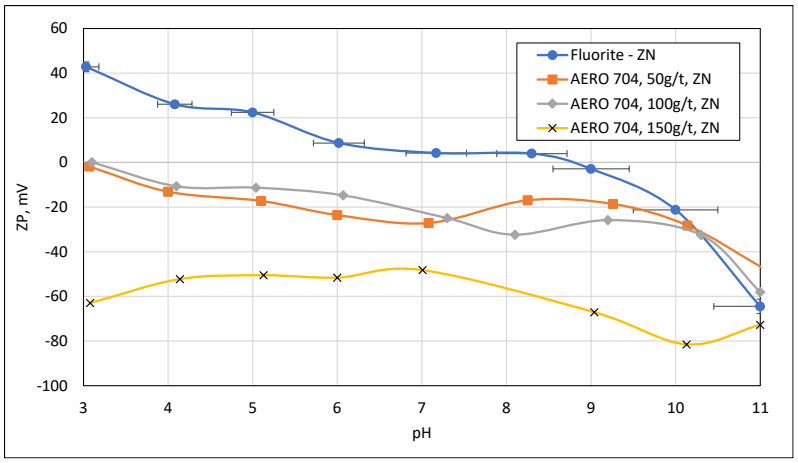

Figure 4.16: Zeta potential of fluorite measured with ZN in the presence of AERO 704 with variation in dosage.

According to the research with TOFA discussed under Section 2, the zeta potential of fluorite should decrease due to absorption mechanisms on the mineral surface

[22][60][64][65][66]. Also, its presence could increase the negative charge of the system and produce an efficient attachment of the particles to the bubbles in the flotation process.

4.4.6.1.2. Fluorite Zeta Potential with Tall Oil Fatty Acid (A726) Collector

Figures 4.17 shows the zeta potential curves with another TOFA type AERO726 (aka A726) collector, with varying dosages of 50 to 100 and 150 g/t. The second TOFA type collector is considered more effective due to improves of the producer (Cytec-Solvay), specially containing surfactants. Surfactants can reduce surface tension, promote mineral absorption, alter hydrophobicity, and improve the ability of bubbles to adhere to surfaces. When these properties are combined with the properties of TOFA, the collection effect of A726 is expected to increase.

Figure 4.17 demonstrated how the ZP curve of pure fluorite is significantly altered by the collector. As the potential charge values drop dramatically along all the resulting curves, this trend is more pronounced in the acidic part. At pH 3, the acidic charge has decreased by more than 80 mV and how the pH gets closer to the neutral zone, this trend becomes weaker. The curves show a similar trend when the dose increment is taken into account. The variation between the resulting curves is not excessive, but it is notorious.

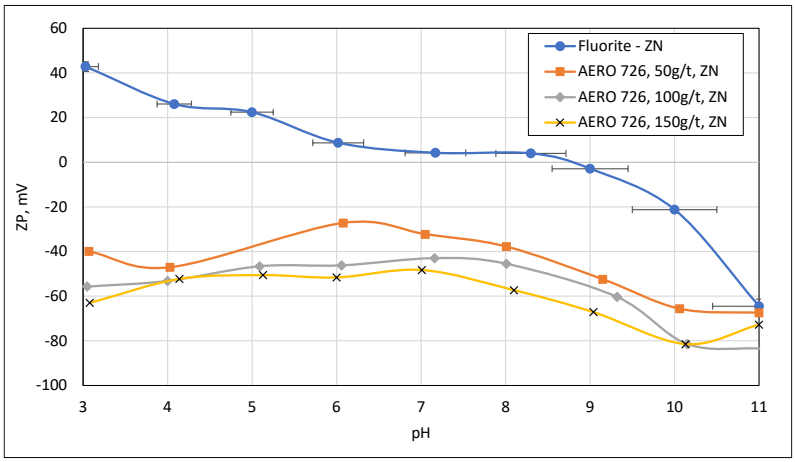

Figure 4.17: Zeta potential of fluorite measured with ZN in the presence of AERO 726 with variation in dosage

4.4.6.2.Zeta Potential of Fluorite Mineral with Depressant Agents

4.4.6.2.1. Fluorite with Sodium Silicate (Na_2SiO_3) Depressant

Figure 4.18 shows the ZP curves of fluorite when 1000 and 1500 g/t sodium silicate are used as depressant. The test was carried out only with ZN. Sodium silicate is an inorganic salt known as water glass. So, Si $(OH)_3$ and Si $(OH)_4$ are mainly responsible for the absorption mechanism, and how they act on the mineral surface depends mainly on the pH value and their concentration. In cases where their concentrations are exceeded, the effect of depression will tend to reduce [76].

The resulting ZP curves were affected by the addition of sodium silicate. The potential charge decrease tendency is obvious especially acidic pH values tested (pH = 3 and pH = 4). At pH 3, the potential charge becomes a negative value, close to -5 mV. It is also the point at which the greatest decrease is exhibited. After this value, the decrement trend is minimal, almost unreadable. This trend continues with very small changes up to pH values close to the IEP point. After that, the results show a greater decline. These results are consistent with previous investigations (Section 2). Because sodium silicate is absorbed by the surface, a decrease in the zeta potential is observed. This can make the mineral less hydrophobic and less likely to attach to bubbles.

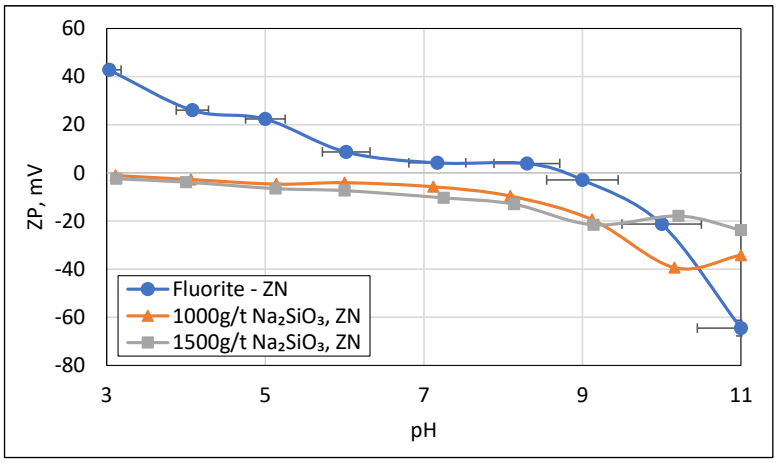

Figure 4.18: Zeta potential of fluorite measured with ZN in the presence of Na_2SiO_3 depressant with variation in dosage.

4.4.6.2.2. Fluorite with Quebracho Depressant

Figure 4.19 shows ZP results when 1000 and 1500 g/t quebracho is as a depressant. Quebracho is a polymer characterized by its deep action on the ZP of fluorite. Figure 4.19

shows that the resulting curves are more negatively charged. In the expected form, but even with an electric decrement charge, they still have a positive charge; for example, at a pH of 3, the resulting values are about 10 mV. The charge measurements start to show a negative potential with an increase in pH.

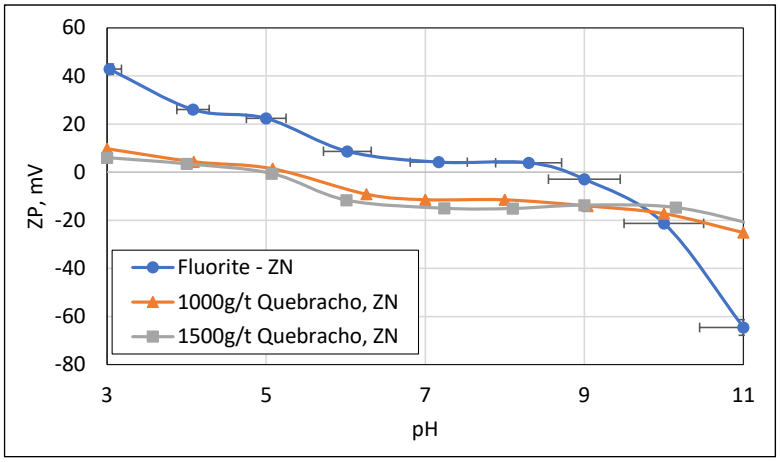

Figure 4.19: Zeta potential of fluorite measured with ZN in the presence of quebracho depressant with variation in dosage.

4.4.6.2.3. Fluorite with Dextrin Depressant

In Figure 4.20, ZP curves of fluorite are shown when 1000 and 1500 g/t dextrin added as a depressant, with ZN equipment. Dextrin is a carbohydrate produced by the partial hydrolysis of starch, which breaks down the long chains into short ones. In many cases, it is considered that the preparation of this depressant plays an important role in its efficiency [72].

Figure 4.20 shows how the effect of dextrin begins with a decrease in the ZP. At the most acidic pH values, the potential charge, although decreasing, still shows positive charge values. At pH 5, the charge values begin to show negative responses, but not with a high effect, as the whole curve does not exceed -20 mV. It should also be noted that as the dosage increases, the charge decreases slightly, but with almost insignificant values that do not exceed -10 mV throughout the curve. Dextrin is known as a polyelectrolyte due to its multiple charged groups. This means that when it is absorbed on the surface of the fluorite, it neutralizes the charge, and with increasing concentration, the neutralization is expected to be greater. It is reflected in the results given in Figure 4.20.

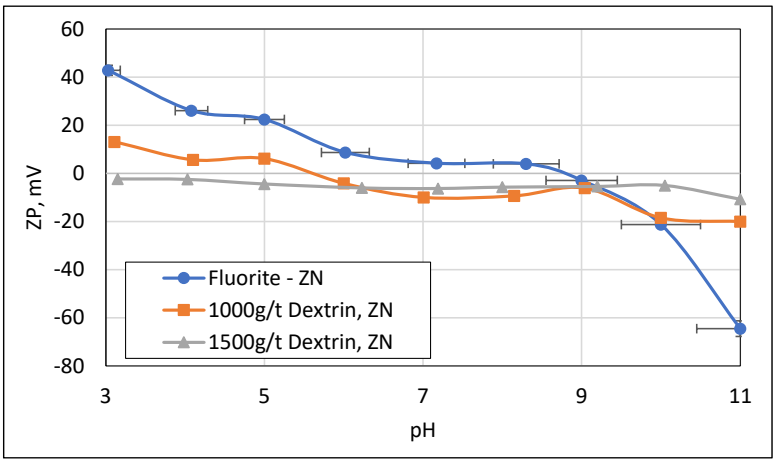

Figure 4.20: Zeta potential of fluorite measured with ZN in the presence of dextrin depressant with variation in dosage

4.5.Flotation Test Results

In order to investigate the flotation behavior of Beylikova ore in terms of target contents, pH-dependent recovery and grade changes in different collector regimes were investigated primarily in line with zeta potential measurement tests. Within the scope of these flotation tests, samples were ground below -150 µm size under specified milling calibration conditions and the fraction below approximately -38 µm was removed by decantation. Accordingly, rougher flotation tests were carried out with A-825, A-845, A-825 and A-845, A-726, and A-704 type collectors at acidic, natural and basic pH values. The rougher flotation concentrates and tailings were sent directly to chemical analyses without cleaning steps and their recoveries in terms of target fluorite (CaF_2), barite ($BaSO_4$) and total REO (Ce, La, Nd and Pr oxides) minerals were examined.

4.5.1. Barite Flotation

4.5.1.1. Barite Flotation with Petroleum Sulfonate (A825) Type Collector

In the flotation tests performed with A825, where 15.06%, 47.38% and 51.10% by weight of the material floated at increasing pH values, respectively. When the tests performed with A825 are evaluated (Figure 4.21 and Figure 4.22), it is seen that a product containing 63.61% $BaSO_4$ can be obtained with a recovery of 88.57% at pH=9.5. At pH=5, a product containing 72% $BaSO_4$ can be obtained, but the recovery of this product remains at 29.55%. In addition, high amounts of CaF_2 and REO are present in this product. CaF_2 reaches the highest recovery and grade values at natural pH. In all tests, no increase in the grade of REO minerals was observed in any product.

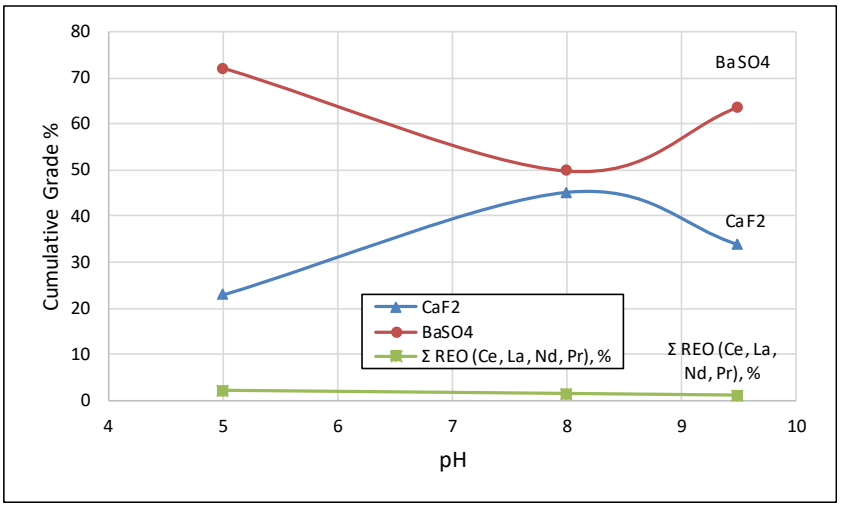

Figure 4.21: Cumulative grade curve results of barite flotation with A825

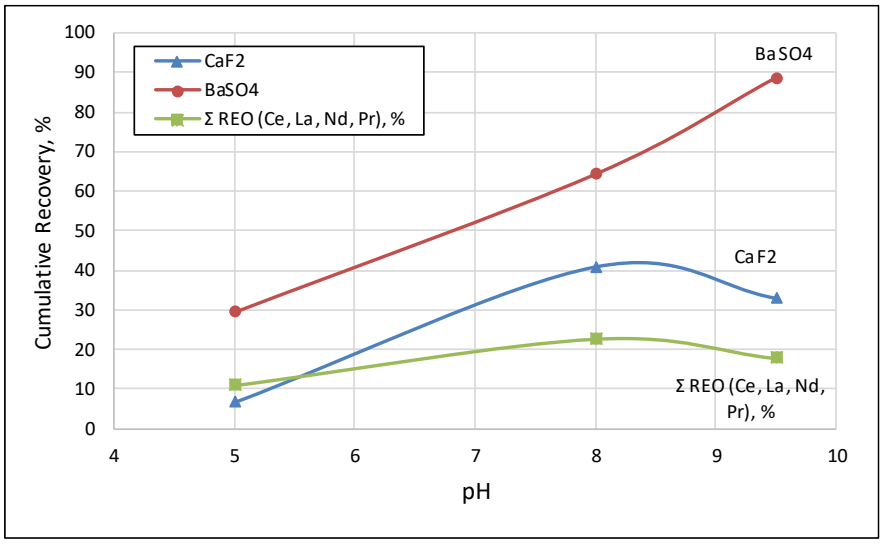

Figure 4.22: Cumulative recovery curve results of barite flotation with A825

Petroleum sulfonate is known to work well with barite. As it is an anionic collector, it adheres to positively charged barite. This may explain why the barite grade and recoveries give the best results (over 72%), since it has a higher electrical charge. In terms of recovery, the tendency is to increase with all pH variations for barite. Due to the fact that the electrical properties of barite are quite comparable to those of fluorite (another major mineral present in this system), fluorite can also benefit the flotation effect when this collector is used. This mineral is therefore considered to be a useful by-product. It is therefore necessary to find a balance between collectors and other agents for the benefit of all the valuable contents. Depressants can also be modified to improve the flotation conditions of valuable minerals. Sodium silicate and quebracho were the depressants used in the test. In the case of quebracho, it has a stronger effect on fluorite, resulting in greater

variations in potential charge. Sodium silicate, on the other hand, is absorbed onto the mineral surface and increases the negative zeta potential. It helps to repel other negatively charged particles and improves the stability of the suspension in the system.

Taking into account all the effects of collectors and depressants, an alkaline pH (8 to 9) may provide the optimum conditions for both recovery and grade for all minerals in the system.

4.5.1.2. Barite Flotation with Alkyl Succinamate (A845) Type Collector

In the flotation tests performed with A845, where 53.90%, 91.74% and 28.99% by weight of the material floated at increasing pH values, respectively. When the tests performed with A845 are evaluated (Figure 4.23 and Figure 4.24), it is seen that almost all of the material (91.74%) floated at natural pH. In this respect, the 97.74% $BaSO_4$ recovery obtained in this test and the REO recovery calculated as 69.85% cannot be considered a success. At other pH conditions, significant grade and recovery values could not be obtained and total REO minerals were dispersed in the products.

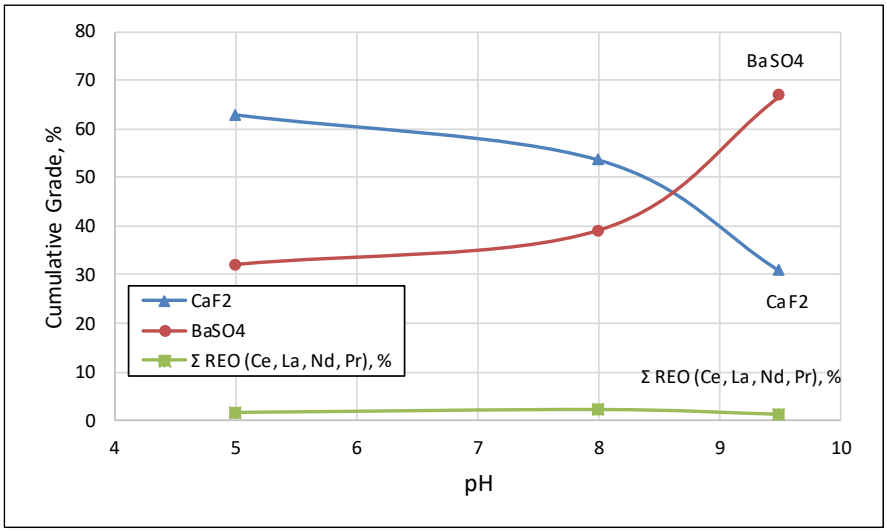

Figure 4.23: Cumulative grade curve results of barite flotation with A845

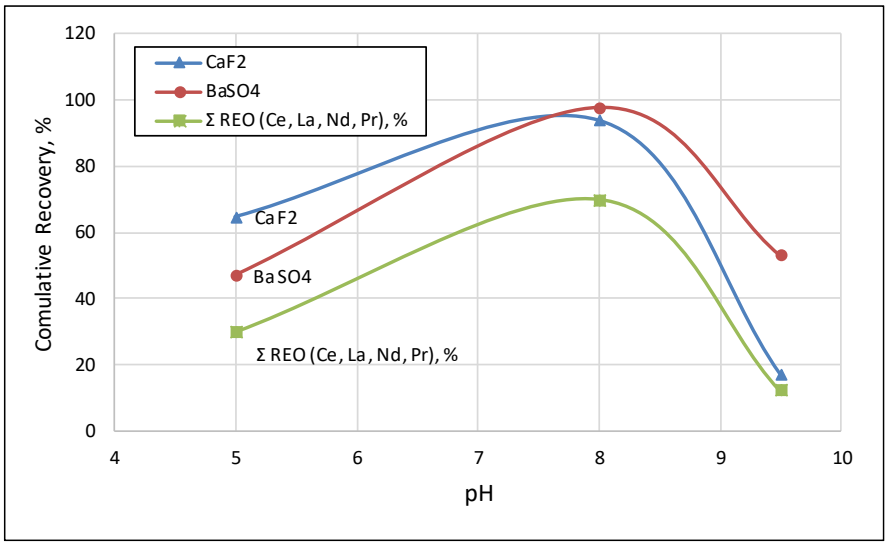

Figure 4.24: Cumulative recovery curve results of barite flotation with A845

Figure 4.24 shows that the barite recovery has a low tendency to increase in the lower pH range (5-7.5) and a high tendency to increase after pH 8, with a percentage of over 60%. These results can be explained by the modification of the zeta potential caused by A845 collector. The barite forms a layer that modifies its electrical charge, which tends to make the particles more stable and less prone to agglomeration. Also, at pH 8, the electrical charge has been stabilized and this could increase the grade, as well as some research suggesting (Section 2) that an increase in hydrophobicity can promote selective flotation and separation of the mineral gangue.

On the other hand, fluorite can have a significant effect on this system due to its properties besides barite. It affects the absorption of the collector, reducing the effectiveness of barite absorption. According to some theories, fluorite alters the zeta potential of barite as well as the absorption competitiveness. The effect of reducing barite flotation efficiency is therefore obvious (Figure 4.24). In contrast to the trend for barite, Figures 4.23 and 4.24 show that fluorite has a higher reaction with this collector in terms of grade and recovery at the highest acidic pH tested.

4.5.1.3. Barite Flotation with Petroleum Sulfonate and Alkyl Succinamate Mixture (A825+A845)

In the flotation tests performed with A825+A845, where 42.11%, 67.40% and 45.42% of the material by weight floated at increasing pH values, respectively. When tests performed with A825+A845 are evaluated (Figure 4.25 and Figure 4.26), it is seen that a

product containing 77.51% $BaSO_4$ with 95.93% recovery at pH=9.5 can be obtained. However, approx. 20% of the REOs and fluorite float within this product. In all conditions, REOs are distributed to the products and no significant grade increase is observed. It is seen that the use of A825+A845 gives better results compared to the conditions where A825 and A845 are tested separately.

According to the previous findings, it was noted that the petroleum sulfonate collector improved the grade and recovery of the barite. On the other hand, the presence of the alkyl succinamate collector decreased barite recovery a bit but improved fluorite recovery. Therefore, according to these results, a system combining these collectors (petroleum sulfonate at a concentration of 300 g/t and alkyl succinamate at a concentration of 100 g/t) was proved to give relatively better results in terms of barite flotation.

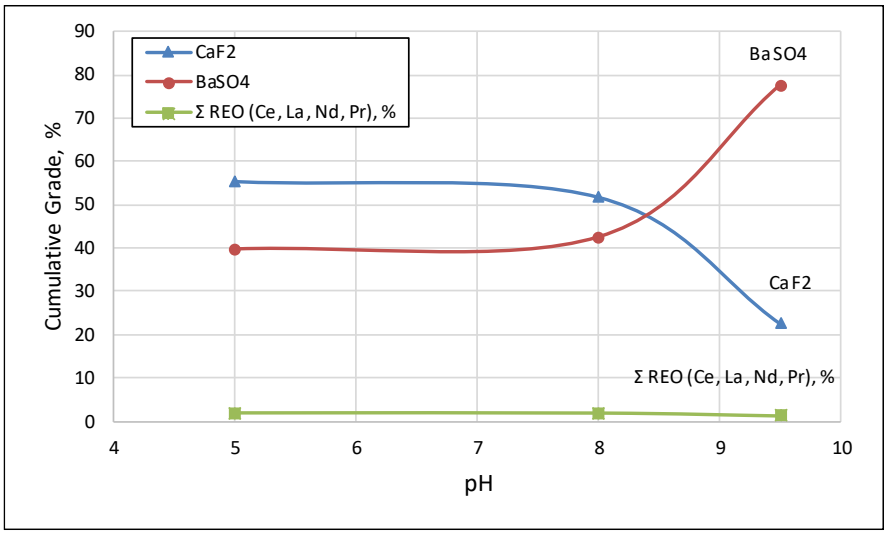

Figure 4.25: Cumulative grade curve results of barite flotation with A825+A845

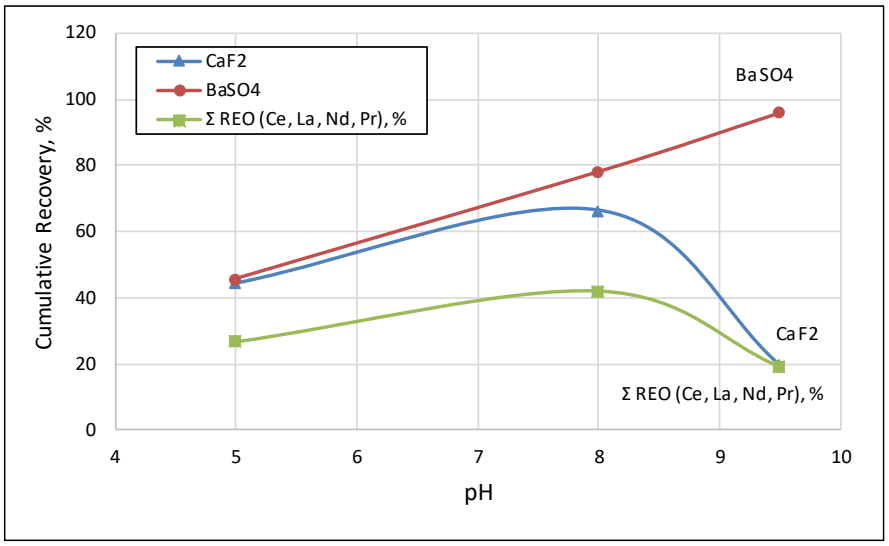

Figure 4.26: Cumulative recovery curve results of barite flotation with A825+A845

4.5.2. Fluorite Flotation

4.5.2.1. Fluorite Flotation with Tall oil Fatty Acid (A704)

In the flotation tests performed with A704, where 21.67%, 16.33% and 40.22% by weight of the material floated at increasing pH values, following the barite coarse flotation stage where approximately 50% of the material floated. When the tests performed with A704 are evaluated (Figure 4.27 and Figure 4.28), it is seen that A704 does not show any selectivity at all pH values and floats almost everything. In terms of REOs, no increase was observed in the products.

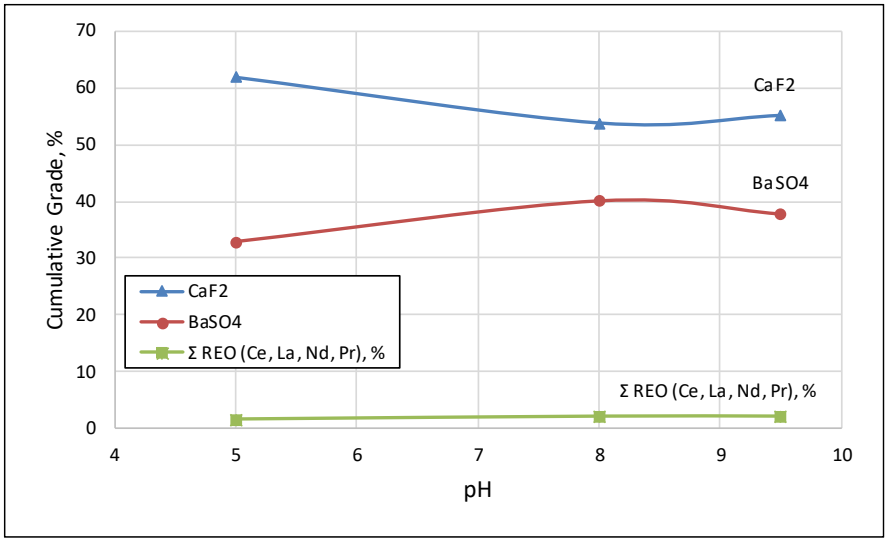

Figure 4.27: Cumulative grade curve results of fluorite flotation with A704

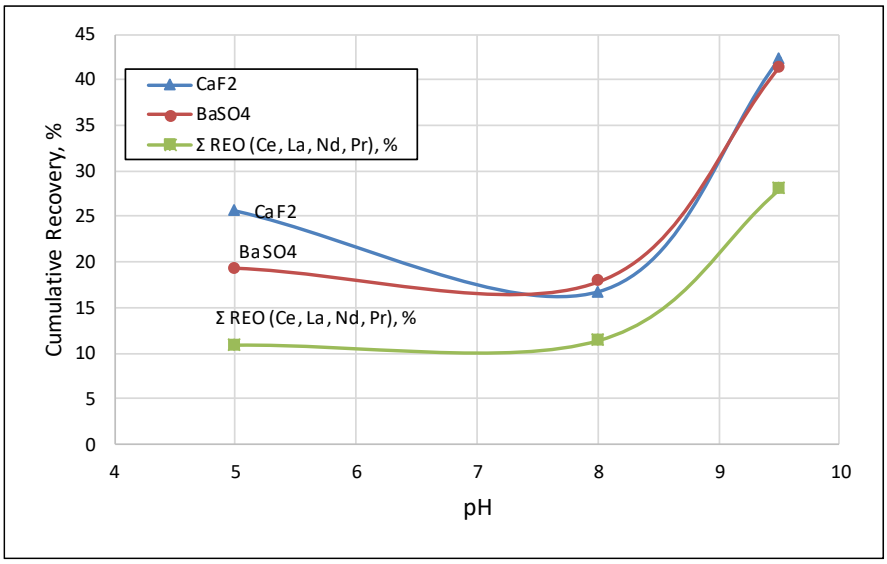

Figure 4.28: Cumulative recovery curve results of fluorite flotation with A704

At pH 5, the grade value is over 60%. The grade decreases as the pH moves towards the alkaline range. After a pH of 8, the change in grade is essentially imperceptible, remaining at a value of around 50%. On the contrary, fluorite shows the greatest recovery at pH 8 and above (Figure 4.28). These results can be explained by the fact that the A704 collector has good absorption on fluorite, so it increases its hydrophobicity and attaches well to the air bubbles. Unfortunately, its low selectivity requires more improvements on this complex flotation exercise.

4.5.2.2. Fluorite Flotation with Tall oil Fatty Acid (A726)

In the flotation tests performed with A726 where 25.96%, 23.19%, and 39.84% of the remaining material can be floated at increasing pH values, respectively, following the barite coarse flotation stage where approximately 50% of the material was floated. When the tests performed with A726 are evaluated (Figure 4.29 and Figure 4.30), it is seen that a product containing 79.80% CaF_2, 7.81% $BaSO_4$ and 2.92% total REO can be obtained at natural pH. However, the CaF_2 recovery of this product remains at a low level (35.28%). At pH=5, the amount of $BaSO_4$ in the product obtained increases to 20.11%. At pH=9.5, it is seen that everything floats without selectivity. In terms of REOs, no significant increase was observed in the products. The fluorite grade (Figure 4.29) shows good results at pH=5. After this point, it gradually increases with higher pH values, peaking at 80% at a pH of 8. Afterwards, this trend reverses, falling by an average of 20% through alkaline regions. Even this little decline can be made up by the recovery because

it performs well in the alkaline pH range, reaching a maximum of close to 47%. The absorption of this collector on the surface creates a protective layer from reactions with the mineral gangue, as well as enhancing flotation of fluorite.

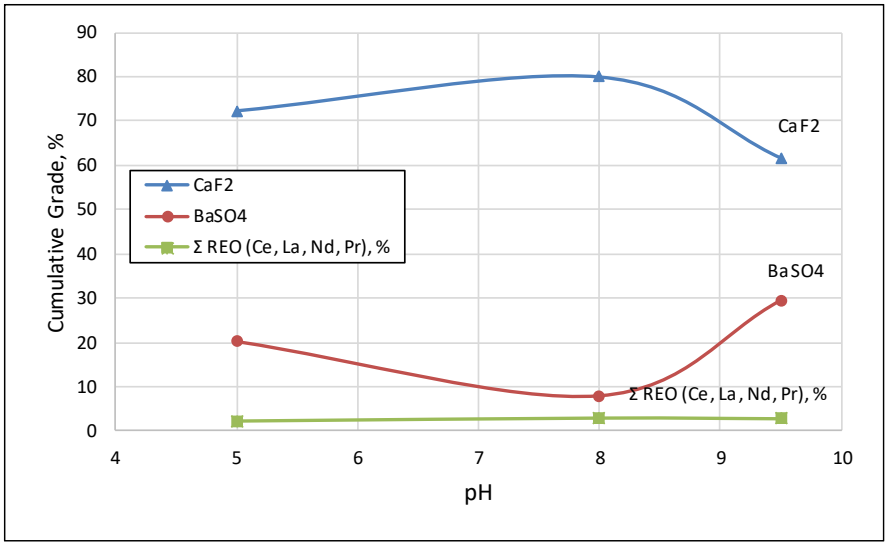

Figure 4.29: Cumulative grade curve results of fluorite flotation with A726

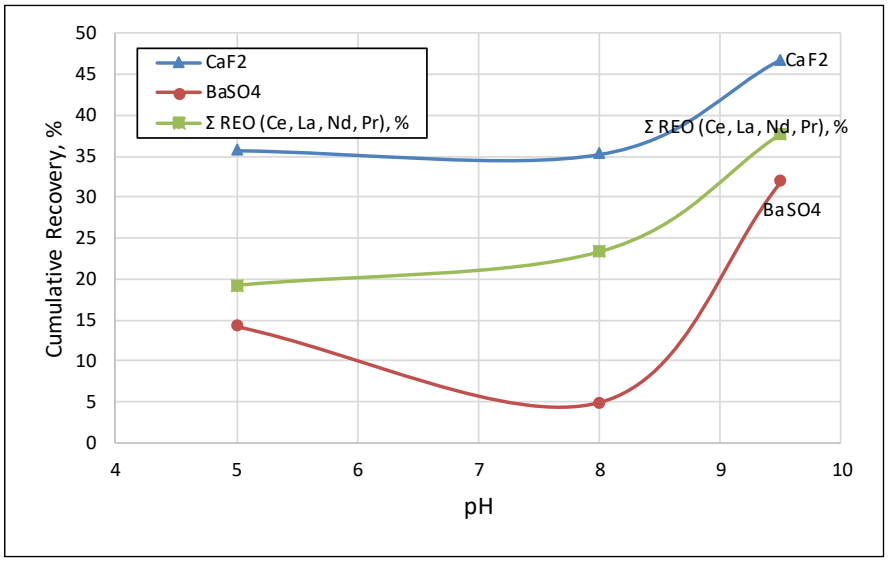

Figure 4.30: Cumulative recovery curve results of fluorite flotation with A726

5. CONCLUSIONS

This thesis study was focused on the flotation behavior of fluorite, barite and REM ore from the Eskişehir-Beylikova region. For this, mineral characterization studies were initiated to determine the mineralogy of the Beylikova deposit. Within experimental studies, pure barite and fluorite minerals were obtained. Pure mineral samples were subjected to zeta potential measurements using the electrophoresis technique under different types of zeta meters (ZS and ZN). Zeta potential measurements were carried out with different conditions and using ZN for occurrent, including different chemical agents such as collectors and depressants. Using the information obtained from the zeta potential measurement tests, a series of flotation tests were then carried out under different conditions for validation and evaluation.

Zeta potential measurements demonstrated that petroleum sulfonate and alkyl succinamate type collectors can be adsorbed on the barite surface while sodium silicate and quebracho have depressing effect and collectors cannot possibly interact with the barite in the presence of these depressants. Similarly, tall oil fatty acid type collectors can be adsorbed on the fluorite surface while sodium silicate and quebracho have only depressing effect at high pH values.

It is important to note that X-ray photoelectron spectroscopy (XPS) was not used within this study to further investigate the adsorption mechanisms of collectors and depressants on the fluorite and barite surface. Instead, detailed flotation tests at varying pH values were performed and obtained recoveries were used to interpret the effects of pH and collector type on flotation performance.

Eskişehir - Beylikova region, which is one of the most important fluorite-barite-rare earth deposits in Turkey, is known as a "Complex Ore" since it consists of a wide variety of minerals. Characterization studies of this ore showed that;

- Fluorite, barite, REMs (bastnasite, monazite, cerianite, and lateritic), calcite, and silicates were the main constituent minerals of the ore. Noteworthy REMs were bastnasite (3.71%), monazite (2.35%), cerianite (0.32%) and lateritic REMs (0.58%) decayed in clay and barite.

- MLA results showed that barite and fluorite were in the form of free particles at levels of 77.1% and 78.6%, respectively. They also showed binary and ternary locking with other minerals at a level of 20-23% by weight. REMs, on the other hand, seemed to have very low liberation. Monazite, bastnaesite, and cerianite free particle remained at levels of 24.4%, 17%, and 1.7%, respectively.

Detailed results of zeta potential measurements tests are listed as follows;

- The ZP measurements with pure barite showed a positive charge in the acidic pH, with the highest electrical charge at around 40 (mV), and a reduction of charge in the alkaline pH, with the lowest charge over -60. (mV). The zeta potential results were fairly similar to measurements with ZS and ZP. IEP, a crucial measurement in the study, showed a value of 5.25 with ZN, whereas with ZS was 5.27. These values lie within the range of 4.5 – 7 previously documented values and these results could suggest a lower concentration of barium ions.
- The ZP of pure fluorite with ZN showed positive electrical charges in the acidic pH range (40 (mV) highest value) and changed to a negative at an alkaline pH value. While the results with the ZS exhibited similarity in the general results, especially in the alkaline pH results. For the IEP measures, the results with ZN and ZS were 8.8 and 8.1, respectively. They were acceptable findings due to the fact that the previous IEP was in the range of 6.2 to 10.6. The carbonatization of the mineral surface could be occurring in the study material and for ratification of this hypothesis more tests should be generated.
- The zeta potential of the barite was analyzed using collectors as petroleum sulfonate and alkyl succinamate in varying dosages with ZN equipment. ***For measurements with petroleum sulfonate collector.*** The measurements showed a significant overall electrical charge decrement, particularly under acidic pH with a decrease of more than -60 (mV). Also, the dosage increment would be necessary to produce a discernible shift. ***For measurements with alkyl succinamate collector.*** The results showed a significant influence of the collector, leading to a drop in charge in all of the resulting curves; a distinctive decrement was in the most acidic region. For variations in dosage, this pattern became more pronounced.

- The zeta potential of the barite was analyzed using depressants as sodium silicate and quebracho, in varying dosages. ***For measurements with sodium silicate depressant.*** The measurements showed an impact of charge decrement, in the acid part, but they tended to increase charge when negative charges were presented. This trend was attributed to surface reactions, especially reactions with barium ions. For variations in dosages, it showed the same and more stable trend. ***For measurements with quebracho depressant.*** The tendency showed to be positively charged with pH values above 7, while for values below pH 7, the tendency was a decrement of the charges. For the dosage variation, the responses were highly similar.
- The zeta potential of the fluorite was analyzed using collectors as tall oil fatty acid and TOFA containing surfactants varying dosages. ***For measurements with tall oil fatty acid collector.*** All measurements had large effects throughout the electric charge, mostly a decrease in positive electric charge. For the variation in dosage, it continued with the same trend, but the decrease was more evident with the increment in dosage. ***For measurements with TOFA containing surfactants acid collector.*** The results showed that the drop in electric charges was significant, being more evident at an acidic pH. While the pH was inching toward the neutral value, this tendency was weaker. Furthermore, this trend was more visible with increasing dosage.
- The zeta potential of the fluorite was analyzed using depressants as sodium silicate, quebracho and dextrin in varying dosages. ***For measurements with sodium silicate depressant.*** The measurements displayed a negative trend, especially at the acid pH levels evaluated; thus, for the point of pH = 3, the charge dropped to values close to -5 (mV). For the variation in dose, the trend did not differ significantly. ***For measurements with quebracho depressant***. As expected, the resulting curves were negatively charged. This was a depressant that acted deeply on the particles, resulting in the highest decrement of the charge. ***For measurements with dextrin depressant.*** The zeta potential measurement showed a decreasing trend, but not as evident as with the previous depressants tested, since it continued with a positive charge in the most acidic part.

Flotation test results showed that;

- The behavior of barite was the main analysis with petroleum sulfonate and alkyl succinamate as main collectors in flotation test. ***Flotation with Petroleum Sulfonate as main collector.*** The barite grade results exhibited better results with acidic pH exceeding 72%. For the recovery, the barite had a permanent tendency to increase throughout the all pHs test. ***Flotation with alkyl succinamate as main collector.*** For the measurements of the recovery, barite showed a tendency to increase, but from a pH of 8, the tendency changed and began to decrease. This collector is characterized by promoting a more stable system with fewer agglomerations. On the other hand, the fluorite could be competing with barite in the process of absorption in the system. ***Flotation with a mix of collectors.*** A system combining these collectors (petroleum sulfonate at a concentration of 300 g/t and alkyl succinamate at a concentration of 100 g/t) was proved to give relatively better results in terms of barite flotation., reaching up to 80 (%) in grade. The recovery exhibited a constant increment.
- The behavior of fluorite was the main analysis with tall oil fatty acid and alkyl and TOFA containing surfactants in flotation test. ***Flotation with TOFA as main collector.*** Fluorite grade curves showed the highest values in the acid part; a pH of 5 showed a grade of over 60 (%), but then it decreased. while for the alkaline part, the grades had a slight rise. Recovery curves showed a constant increase proportional to the increase in pH, especially in the alkaline part. ***Flotation with TOFA containing surfactants as main collector.*** The grade curves showed the highest results, starting with 70 (%) for a pH of 5 and gradually increasing until reaching their maximum at a pH of 8 with 80 (%). For the recovery, they showed great results, reaching a maximum recovery of 47(%) in the alkaline part.

For future studies, performing X-ray photoelectron spectroscopy (XPS) in addition to zeta potential measurements will help better understanding the absorption mechanisms of the flotation reagents.

5. REFERENCES

[1]. Anderson, C., & Taylor, P. (2017). Rare Earth Flotation Fundaments: A Review. American Journal of Engineering Research (AJER), Volume 6, İssue -1.

[2]. Zhang, X., Du, H., Wang, X., & Miller, J. D. (2013). Surface chemistry considerations in the flotation of rare-earth and other semisoluble salt minerals. Mining, Metallurgy & Exploration, 24–37.

[3]. Panda, R., Kumari, A., Jha, M., Rejesh , K., & Lee, J. (2014). Leaching of rare earth metals (REMs) from Korean monazite concentrate. Journal of Industrial and Engineering Chemistry,, 2035–2042.(55)

[4]. Pate, K., & Safier, P. (2016). Chemical metrology methods for CMP quality.Advances in Chemical Mechanical Planarization (CMP). Intel Corporation- Hillsboro , 299 -325.

[5]. King , R. P., & Schneider, C. L. (1998). Mineral liberation and the batch communition equation. Mining Engineering, 1143-1160 .

[6]. Yeşilören Görmüş, N., Gürtekin, G., Erdem, A., & Gülmez, A. (2021). Kizilcaoren (Sivrihisar) Bolgesi Nadir Toprak Element NTE Iceren Minerallerin MIneral Serbestlesme Analiz (MLA) Yontemi Kullanilarak Tayini (Turkish). Int. J. Pure Appl Sci. , 251-264.

[7]. Özbaş, K. E. (1993). Concentration of Barite and Fluorite Minerals of Eskişehir-Beylikahır District. Middle East Technical University.

[8]. Dolak, I. (2020). Eskişehir Bastnasit Cevherinde Bulunan Seryumun Zenginleştirilmesi. DÜMF Mühendislik Derg, 12. https://doi.org/10.24012/dumf.837091.

[9]. Ciccu, R., Curreli, L., Ghiani, A., & Fuganti, A. (1993). Beneficiation of a Turkish Bastnaesite Ore with Associated Fluospar and Barite. Proc. 15th Int. Miner. Process. Congr., Sydney, 23-28.

[10]. C.K. Gupta, N. Krishnamurthy. (2004). Extractive Metallurgy of Rare Earths . CRC Press.

[11]. Jordens, A., Marion, C., Kuzmina, O., & Waters, K. E. (2014). Surface chemistry considerations in the flotation of bastnäsite. Minerals Engineering, 119–129.

[12]. Marion, C., Li, R., & Waters, K. E. (2020). A review of reagents applied to rare-earth mineral flotation. Advances in Colloid and Interface Science, 102-142.

[13]. Tatang, & Wahyndi. (2015). Reviewing the properties of rare earth element-bearing minerals, rare earth elements and cerium oxide compound. İndonesian Mining Jornal, 92-108.

[14]. Wills, B. A., & Finch, J. A. (2016). Chapter 12 – Froth flotation. Boston: Finch J. A. editors.

[15]. Houot, R., Cuif, J. P., Mottot, Y., & Samama, J. C. (1991). Recovery of rare earth minerals with emphasis on flotation process. International Conference on Rare Earth Minerals and Minerals for Electronic Uses. , 301-324.

[16]. White , J., & Megaw, P. (2007). Minerals Forum. Obtenido de https://www.mineral-forum.com/.

[17]. Klinger, J. M. (2015). A historical geography of rare earth elements: From discovery to the atomic age. The Extractive Industries and Society, 572–580.

[18]. Graham, A. (s.f.). CERIANITE CeO2: A NEW RARE-EARTH OXIDE MINERAL. Dominion Gulf Company.

[19]. Chakrabarty, A., Mitchell, R. H., Ren, M., Sen, A. K., & Pruseth, K. L. (2013). Rinkite, cerianite-(Ce), and hingganite-(Ce) in syenite gneisses from the Sushina Hill Complex. Mineralogical Magazine, 3137–3153.

[20]. Bulatovic, S. (2015). Flotation of REO Minerals. En Handbook of Flotation Reagents: Chemistry, Theory and Practice (págs. Chapter 24, 151-173). Elsevier B.V.

[21]. Mark, D. (2014). Lateritic, Supergene Rare Earth Element (REE) Deposits. Arizona Geological Survey, 1-18.

[22]. Kilinc, E., Akarj, A., Kaya, E., & Cocen, I. (2009). Influence of Fatty Acid Based Collector on The Flotation of Heavy Minerals from Alkali Feldspar Ores. Asian Journal of Chemistry, 2263-2269.

[23]. Balaram, V. (2019). Rare earth elements: A review of applications, occurrence, exploration, analysis, recycling, and environmental impact. Geoscience Frontiers, 10(4), 1285–1303.

[24]. Goodenugh, K., Wall, F., & Merriman, D. (2017). The Rare Earth Elements: Demand, Global Resources and Challenges for Resourcing Future Generation. Natural Resources Research.

[25]. Habashi, F. (2013). Extractive metallurgy of rare earths. Canadian Metallurgical Quarterly, 224–233.

[26]. Hang , J., Shi, L., Feng, X., & Xiao, L. (2009). Electrostatic and electrosteric stabilization of aqueous suspensions of barite nanoparticles. Powder Technology, 166-170.

[27]. Huang, J., Zhang, Q., Hongchao, L., & Chao , W. (2022). Difficulties and Recent Achievements in Flotation Separation of Fluorite from Calcite . Minerals , 957.

[28]. Guichard, F., Church, T. M., Trevil, M., & Jaffrezic, H. (1979). Rare earths in barites: distribution and effects on aqueous partitioning. Geochimica et Cosmochimica, 983–997.

[29]. Owens, C. L., Nash, G. R., Hadler, K., Fitzpatrick, R. S., Anderson, C. G., & Wall, F. (2018). Zeta potentials of the rare earth element fluor carbonate minerals focusing on bastnäsite and parisite. Advances in Colloid and Interface Science, 152–162.

[30]. Flotasyon Deneyi. (April de 2022). Obtenido de Metalurji ve Malzeme Muhendisligi: https://www.metalurjik.com/.

[31]. Salopek, B., Krasic, D., & Filipovic, S. (1992). Measurement and Application of Zeta Potential. Zabreb, 147-151.

[32]. Miller, J., & Hiskey, J. (1972). Electrokinetic behavior of fluorite as influenced by surface carbonation. Journal of Colloid and Interface Science, 567–573.

[33]. Mervem Instruments Limited. (2015). Zeta Potential Introduction .

[34]. Pradip. (1981). The Surface Properties and Flotation of Rare-Earth Minerals. Doctoral Thesis, University of California, Berkeley.

[35]. Jordens, A., Cheng, Y. p., & Waters, K. E. (2013). A review of the beneficiation of rare earth element bearing minerals. Minerals Engineering, 97–114.

[36]. Herrera - Urbina, R., Pradip, & Fuerstenau, D. W. (2013). Electrophoretic mobility and computations of solid-aqueous solution equilibria for the bastnaesite-H2O system. Mining, Metallurgy & Exploration, 18–23.

[37]. Pope, M. I., & Sutton, D. I. (1973). The correlation between froth flotation response and collector adsorption from aqueous solution. Powder Technol , 271–279.

[38]. Smith, R. W., & Shomard, D. (1986). Electrokinetic study of the role of modifying agents in flotation of salt-type minerals. AICHE Journal, 865–868.

[39]. Fuerstenau, D. W., & Shibata, J. (1999). On using electrokinetics to interpret the flotation and interfacial behavior of manganese dioxide. International Journal of Mineral Processing, 205–217.

[40]. Fuerstenau, D., Pradip, & Herrera -Urbina . (1992). The surface chemistry of bastnaesite, barite and calcite in aqueous carbonate solutions . Colloids and Surfaces, 95-102.

[41]. Fuerstenau, D. W., & Pradid. (2005). Zeta potentials in the flotation of oxide and silicate minerals. Adv Colloid Interface Sci, 114-115.

[42]. Karatas, D., Salih, M., Ethem, I., & Celik, M. (2017). Flotation Chemistry of a Rare Earth Mineral: Bastnasite. Research Gate.

[43]. Espiritu, E. R., Da Silva, G. R., Azizi, D., Larachi, F., & Waters, K. E. (2018). The effect of dissolved mineral species on bastnäsite, monazite and dolomite flotation using benzohydroxamate collector. Colloids and Surfaces: Physicochemical and Engineering Aspects, 319–334.

[44]. Zhang, X., Du, H., Wang, X., & Miller, J. D. (2014). Surface chemistry aspects of bastnaesite flotation with octyl hydroxamate. International Journal of Mineral Processing.

[45]. Ren, J., Lu, S., Song, S., & Nin, J. (1997). A new collector for rare earth mineral flotation. Minerals Engineering, 1395–1404.

[46]. Cheng, T. (2000). The point of zero charge of monazite and xenotime. Minerals Engineering, 13(1), 105–109.

[47]. Pradip, & Fuerstenau, D. W. (1984). Mineral flotation with hydroxamate collectors. The Institution of Mining and Metallurgy, 161-168.

[48]. Pradip, & Fuerstenau, D. W. (1991). The role of inorganic and organic reagents in the flotation separation of rare-earth ores. International Journal of Mineral Processing, 1–22.

[49]. Pradip, & Fuerstenaun, D. W. (1985). Adsorption of hydroxamate collectors on semisoluble minerals Part II: Effect of temperature on adsorption. Colloids and Surfaces, 137–146.

[50]. Miller, J. D., Calara, J. V., & Paruchurri, V. K. (2004). The surface charge of fluorite in the absence of surface carbonation. Colloids and Surfaces: Physicochemical and Engineering Aspects, 91–97.

[51]. Wang , J., Zhou, Z., Gao, Y., Sun, W., Hu, Y., & Gao, Z. (2018). Reverse Flotation Separation of Fluorite from Calcite: A Novel Reagent Scheme. Minerals, 8(8), 313.

[52]. Wang , R., Wei, Z., Han, H., Hu, Y., & Wang, J. (2019). Fluorite particles as a novel calcite recovery depressant in scheelite flotation using Pb-BHA complexes as collectors. Minerals Engineering, 132, 84–91.

[53]. Bulatovic, S. (2015). Beneficiation of Barite Ores. En Handbook of Flotation Reagents: Chemistry, Theory and Practice (págs. Chapter 34, 129-141). Elsevier B. V.

[54]. Marinakis, K. I., & Shergold, H. L. (1985). The mechanism of fatty acid adsorption in the presence of fluorite, calcite and barite. International Journal of Mineral Processing, 161–176.

[55]. Chen , X., Gu, G., Liu, D., & Zhu, R. (2019). The Flotation Separation of Barite -Calcite Using Sodium Silicate as Depressant in the presence of Sodium Dodecyl Sulfate. Physicochemical Problems of Mineral Processing, 55(2).

[56]. Azizi, D., Larachi, F., & Latifi, M. (2016). Ionic-liquid collectors for rare-earth minerals flotation Case of tetrabutylammonium bis(2-ethylhexyl)-phosphate for monazite and bastnäsite recovery. Colloids and Surfaces A: Physicochemical and Engineering Aspects, 74–86.

[57]. Azizi, D., Sarvaramini, A., & Larachi, F. (2017). Liquid-liquid mineral separation via ionic-liquid complexation of monazite and bastnäsite—an alternate route for rare-earth mineral beneficiation. Colloids Surf, 1-23.

[58]. Ren, J., Song, S., Lopez, A., & Lu, S. (2000). Selective flotation of bastnaesite from monazite in rare earth concentrates using potassium alum as depressant. International Journal of Mineral Processing, 59(3), 237-245.

[59]. Chen, Z., Ren, Z., Gao, H., Zheng, R., Jin, Y., & Niu, C. (2018). Flotation studies of fluorite and barite with sodium petroleum sulfonate and sodium hexametaphosphate. Journal of Materials Research and Technology.

[60]. CYTEC. (2010). Mining Chemicals Hand Book.

[61]. Mielczarski, E., Mielczarski, J., & Cases, J. (2002). Influence of solution conditions and mineral surface structure on the formation of oleate adsorption layers on fluorite. Colloids and Surfaces A: Physicochemical and Engineering Aspects, (205), 79-84.

[62]. Abeidu, A. M. (1972). The separation of monazite from zircon by flotation. Journal of the Less Common Metals, 113-119.

[63]. Villieras, F. (s.f.). Thermodynamic model of ionic and non-ionic surfactant adsorption abstraction on heterogeneous surfaces. Environ. Minéralogie (Langmuir).

[64]. Yue, X. (2005). Study on the composition characterization and interface properties of petroleum sulfonate. Research Institute of Petroleum Exploration and Development.

[65]. Liu , C., Zhou , M., Xia , L., Fu, W., & Yang, S. (2020). The utilization of citric acid as a depressant forthe flotation separation of barite from fluorite. Miner Eng, 156, 106-491.

[66]. Hou , Z., Li , Z., & Wang , H. (2000). T interaction of sodium dodecyl sulfonate and petroleum sulfonate with surfactants. Colloid Surface, 166, 243 -249.

[67]. Predali, J., & Cases , J. (1973). Zeta-potential of magnesian carbonates in inorganic electrolytes. Colloid Interface , (45), 449-458.

[68]. Uçar, A., & Özdag, H. (2002). Mechanism of collector adsorption in fluorite flotation. Mineral Processing and Extractive Metallurgy, 111(2), 100–105.

[69]. Quast, K. (2016). Literature review on the interaction of oleate with non-sulphide minerals using zeta potential. Minerals Engineering , (94), 10-20.

[70]. Mielczarski, E., Donato, P., & Mielczarski, J. (2000). Solution Chemistry in Adsorption Layer Formation of Oleate on Fluorite. Journal of Colloid and Interface Science, 226(2), 269-276.

[71]. Gao, Z., Wang, C., Sun, W., Gao, Y., & Kowalczuk, P. (2021). Froth flotation of fluorite: A review. Advances in Colloid and Interface Science , 290, 102-382.

[72]. Kecir, M., & Kecir, A. (2016). Efficiency of Barite Flotation Reagents a Comparative Study. Journal of the Polish Mineral Engineering Society.

[73]. Panzer, G., & Boyer, W. (1980). Use of C8-34 Alpha olefin Sulfonates to Improve And Enhance The Flotation And Collection Process Used For Barite. Alcolac, Inc., Baltimore, Md., 181,658. /56

[74]. Hadjiev, A., Hadjiev, P., & Georgiev, R. (2000). Flotation of barite from complex iron ore. Geological Institute -Processing of fines, 222-230.

[75]. Zheng, R., Ren, Z., Gao, H., & Qian, Y. (2017). Flotation Behavior of Different Colored Fluorites Using Sodium Oleate as a Collector. Minerals, 159.

[76]. Deng , J., Liu, C., Yang, S., Li, H., & Liu, Y. (2019). Flotation separation of barite from calcite using acidified water glass as the depressant

7. APPENDIX

APPX 1–Zeta Measurements Raw Data-Summary

Fluorite - ZN		Avg pH	Avg Zp (m	Barite - ZN			
Ph	Zp (mV)	3.03	42.83	pH	Zp (mV)	Avg pH	Avg Zp (m
3.03	42.17	4.08	26.05	3.03	37.7	3.03	35.5
3.03	43.49	5	22.4	3.03	33.3	4.18	17.35
4.08	26.1	6.02	8.7	4.18	12.5	5.11	2.6
4.08	26	7.17	4.2	4.18	22.2	6.15	-17.8
5	22.4	8.3	3.95	5.11	1.9	7.06	-27.2
5	22.4	9	-2.9	5.11	3.3	8	-31.5
6.02	9.4	10	-21.25	6.15	-17.5	9	-35.95
6.02	8	11	-64.5	6.15	-18.1	10.1	-44
7.17	4.2			7.06	-27.3	11	-65.5
7.17	4.2			7.06	-27.1		
8.3	2.1			8	-30.7		
8.3	5.8			8	-32.3		
9	1.9			9	-36.8		
9	-7.7			9	-35.1		
10	-18.3			10.1	-44		
10	-24.2			10.1	-44		
11	-61			11	-66		
11	-68			11	-65		
AERO 704, 50g/t, ZN		AERO 825, 50g/t, ZN		AERO 704, 100g/t, ZN		AERO 825, 100g/t, ZN	
Avg pH	Avg Zp (m	Avg pH	Avg Zp (m	Avg pH	Avg Zp (m	Avg pH	Avg Zp (m
3.07	-1.805	3.19	-33.4	3.1	0.12	3.2	-44.4
4	-13.1	4.09	-41.7	4.1	-10.67	4.2	-49.3
5.1	-17.25	5.07	-50.95	5.04	-11.289	5.11	-45.3
6	-23.55	6	-56.7	6.07	-14.73	6.26	-38.45
7.08	-27.15	7.15	-47.15	7.3	-24.95	7.26	-43.2
8.25	-16.95	8.33	-43.9	8.1	-32.35	8.09	-40.7
9.26	-18.6	9.08	-45.7	9.2	-25.85	9.3	-46.2
10.14	-28.25	10.2	-49.8	10.3	-32.45	10	-48
11.04	-47.5	11.01	-51.3	11	-58.05	11	-54
AERO 704, 150g/t, ZN		AERO 825, 150g/t, ZN		AERO 726, 50g/t, ZN		AERO 845, 50g/t, ZN	
Avg pH	Avg Zp (m	Avg pH	Avg Zp (m	Avg pH	Avg Zp (m	Avg pH	Avg Zp (m
3.08	-63	3.14	-31.1	3.07	-39.95	3.05	-22.35
4.14	-52.25	4.13	-48.2	4.03	-47.05	4	-24.65
5.13	-50.55	5.11	-52.4	6.08	-27.2	5.13	-19.75
6	-51.6	6.32	-54.6	7.05	-32.25	6	-18.6
7.01	-48.25	7.13	-54.65	8.01	-37.8	7.1	-31.35
9.04	-67.15	8.21	-55.2	9.15	-52.4	8.07	-31.4
10.13	-81.5	9.08	-55.8	10.06	-65.6	9.16	-34.4
11	-72.75	10	-58.95	11	-67.45	10.25	-38.65
		11	-61.75			11	-44.15
AERO 726, 100g/t, ZN		AERO 845, 100g/t, ZN		AERO 726, 150g/t, ZN		AERO 845, 150g/t, ZN	
Avg pH	Avg Zp (m	Avg pH	Avg Zp (m	Avg pH	Avg Zp (m	Avg pH	Avg Zp (m
3.05	-55.7	3.2	-26.85	3.08	-63	3.16	-18.2
4	-53.2	4.22	-36.1	4.14	-52.25	4.1	-30.25
5.09	-46.6	5	-32.1	5.13	-50.55	5.11	-34.5
6.06	-46.2	7	-26.1	6	-51.6	6.14	-41.6
7.16	-42.95	8.09	-31.35	7.01	-48.25	7.08	-38
8.01	-45.5	9.02	-38.7	8.1	-57.3	8.06	-37.8
9.32	-60.35	10.08	-42.2	9.04	-67.15	9.16	-36.35
10.15	-81.45	11	-45.6	10.13	-81.5	10	-34.55
11.02	-83.5			11	-72.75	11	-43.15